

Regional Water Balance Study for Kyrenia Range Aquifers

**A Thesis Submitted to
the Graduate School of Applied Sciences**

by

Ahmed Jamal Aldalou

**In partial fulfillment of the requirements
for the degree of Master of Science
in Civil Engineering**

**Near East University
Nicosia, North Cyprus
2012**

Approval of Director of Graduate of School of Applied Sciences

Prof. Dr. İlkey SALİHOĞLU

**We certify this thesis is satisfactory for the award of the degree of Masters of Science
in Civil Engineering**

Examining Committee in Charge:

Prof. Dr. Hüseyin Gökçekuş

**Co-Supervisor,
Civil Engineering Department, NEU**

Assoc. Prof. Dr. Umut Türker

**Co-Supervisor,
Civil Engineering Department, NEU,
(Currently working in EMU, Civil
Engineering Department.)**

Assoc. Prof. Dr. Çetin Mazharoğlu

Civil Engineering Department, NEU

Asst. Prof. Dr. Mustafa Ergil

Civil Engineering Department, EMU

Asst. Prof. Dr. Pınar Akpınar

Civil Engineering Department, NEU

ABSTRACT

In this thesis, a brief summary on fundamentals of groundwater engineering, subsurface water and aquifers are reviewed, and a regional water budget estimate of the Kyrenia Range Aquifer, based on hydrologic information is carried out. During the analyses, the Kyrenia Range Aquifer is subdivided into 11 main regions. In this study the spatial distribution, the depth, and the daily abstraction from the available wells were surveyed. The springs existing within the study region are also listed and coordinated. The hydrologic balance studies of the Kyrenia Range Aquifer show that the aquifer has a lifespan of 5 years, unless the pumping rates and depths from the aquifer do not alter in the close future. The available volume of water at the present situation in the sub region aquifers are calculated individually and finally the total volume of water stored in the aquifers is estimated to be 53,56 MCM whereas data analyses show that approximately 12 MCM water is extracted from the 11 regions per year.

Keywords: Water budget, Groundwater, Aquifers, Wells, Evapotranspiration (ETo), Infiltration, Kyrenia Range

ÖZET

Bu tezde, yeraltı suyu mühendisliği, yüzeyaltı suyu ve akiferlerin temelleri üzerine kısa bir bilgi ve Girne Bölgesi Akiferlerinin hidrolojik bilgilerine dayanarak bu bölgenin bölgesel su bütçesi tahmini yapılmıştır.

Analizler süresince çalışma alanı olan Girne Bölgesi Akiferleri 11 ana bölgeye ayrılmıştır.

Bu çalışmada mekansal dağılım, derinlik, ve kuyulardan günlük çekim miktarı gözlemlendi. Ayrıca çalışma bölgesindeki mevcut pınarlar da listelenmiş ve koordinatları belirlenmiştir. Girne Bölgesi akiferinin bu tezde yapılan hidrolojik denge çalışmaları gösteriyor ki, akiferdeki kuyu pompaj miktarları ve kuyu derinlikleri değiştirilmezse, akiferin 5 yıllık ömrü kalmıştır. Her bir akiferin ayrı ayrı mevcut derinliklerde ne kadar su ihtiva ettiği hesaplanmış ve bunun sonucunda ise tüm akiferlerin ihtiva ettiği toplam su hacmi 53.56 milyon metreküp olduğu tahmin edilmistir. Buradaki veri analizleri göstermektedir ki, 11 bölgeden yıllık yaklaşık olarak 12 milyon metreküp su çekimi yapılmaktadır.

Anahtar Kelimeler: Su bütçesi, yeraltı suyu, akiferler, kuyular, Buharlaşma miktarı (ET_o), infiltrasyon (sızma), Girne Bölgesi.

DEDICATION

This thesis was dedicated to my parents,
my lovely wife, my people and to all my friends specially Majed
for their endless love, support and encouragement. Now I dedicate this work to the spirits of
martyrs of Palestine, especially to the martyrs of my family who were killed unjustly by
Israeli military before a week from the date of my jury.

ACKNOWLEDGEMENT

First of all I would like to thanks to my wife for here encouragement, support and patience. I would like to express gratitude to all those who gave me the possibility to complete this thesis. I am deeply indebted to my supervisor Assoc. Prof. Dr. Umut TÜRKER whose help, stimulating suggestions and encouragement guided me throughout the time of this study. He helped me to improve my contributions, and given me crucial advice what to accept and what not to during this study. His commentaries will obviously help my contributions also in my future research efforts, and may direct me to fruitful avenues of study. The most important is his precious instruction at every step during my thesis. At last it has been so great to know him, and I'm glad to be his student.

I wish to thank to Mr. Mustafa SIDAL, who have given me valuable suggestions on the earlier stages of this thesis. Also great thanks to Water Works Department Central and Girne offices who provide me the data related with the wells and who join me during my field trips to the site, and special thanks for Asst. Prof. Dr. Mustafa Ergil for his encouragement and supporting.

TABLE OF CONTENTS

ABSTRACT	iii
ÖZET	iv
DEDICATION	v
ACKNOWLEDGMENT	vi
LIST OF TABLES	x
LIST OF FIGURES	xii
LIST OF ABBREVIATIONS	xviii
LIST OF SYMBOLS	xix
CHAPTER 1: INTRODUCTION	1
1.1 General	1
1.2 Aim and Scope of the Thesis	2
1.3 Guide to Thesis	2
CHAPTER 2: CONCEPTS OF GROUND WATER	4
2.1 Fundamentals of Groundwater Sustainability	4
2.1.1 Overview	4
2.1.2 Subsurface Water	4
2.1.3 Groundwater	6
2.2 Aquifer and Types of Aquifers	6
2.2.1 Definitions	6
2.2.2 Aquifers	7
2.2.3 Types of Aquifers	7
2.2.4 Carbonate Rocks	9
2.2.4.1 Features of a Karst Landscape	11
2.3 Karst Spring	16
2.4 Geology and Hydrogeology	17
2.4.1 Overview	17
2.4.2 Vegetation and climate	18

CHAPTER 3: LONG TERM AQUIFER MONITORING ANALYSIS	20
3.1 Karşiyaka (Vasillia) Region	21
3.2 Lapta (Lapithos) Region	28
3.3 Alsancak (Karavas) Region	35
3.4 Karaman (Karmi) Region	41
3.5 Dikmen (Dihkomo) Region	46
3.6 Çatalköy and Beylerbeyi Region	52
3.7 Değirmenlik Region	59
3.8 Karaağaç-Alevkayası Region	67
3.9 Tirmen Region	71
3.10 Tatlısu -Kantara Region	79
3.11 Boğaz Region	84
3.12 Chapter Conclusion	88
CHAPTER 4: WATER BUDGET ANALYSIS	89
4.1 Water Budgets Development	89
4.2 Ground Water Budgets	90
4.3 Evapotranspiration (ET _o)	93
4.3.1 FAO Penman-Monteith Equation	95
4.4 Infiltration Estimates	97
4.4.1 Calculation of the Water Budget of Aquifer	97
4.4.2 Volume of water stored in the aquifer	99
CHAPTER 5: WATER BUDGET CALCULATIONS FOR 11 REGIONS	101
5.1 Calculation Procedures for Evapotranspiration	101
5.1.1 The Penman-Monteith Formula	101
5.1.2 The Psychrometric constant (γ)	101
5.1.3 Saturation vapour pressure e° (T)	102
5.1.4 Actual vapour pressure (e_a)	103
5.1.5 Slope of the vapour pressure curve (Δ)	103
5.1.6 The soil heat flux (G)	103
5.1.7 Wind speed u_2	104
5.1.8 Calculation Procedure of the Net Radiation (R_n)	104

5.1.8.1 Extraterrestrial radiation for daily periods (R_a)	104
5.1.8.2 Solar radiation (R_s)	104
5.1.8.2.1 Clear-sky solar radiation (R_{so})	104
5.1.8.2.2 Net solar or net shortwave radiation (R_{ns})	105
5.1.8.2.3 Net longwave radiation (R_{nl})	105
5.1.8.3 Net radiation (R_n)	106
5.2 Calculating the Infiltration of the Kyrenia Range	106
5.2.1 Process of Calculating The Water Budget at Karşıyaka Region	106
5.3 The Result of Water Budget Calculation of Kyernia Region	110
5.3.1 Water Budget of Lapta Region	110
5.3.2 Water Budget of Alsancak Region	111
5.3.3 Water Budget of Karaman Region	112
5.3.4 Water Budget of Dikmen Region	113
5.3.5 Water Budget of Çatalköy and Beylerbeyi Region	114
5.3.6 Water Budget of Değirmenlik Region	115
5.3.7 Water Budget of Karaağaç Alevkayası (Alevga) Region	117
5.3.8 Water Budget of Tirmen Region	118
5.3.9 Water Budget of Kantara Region	119
5.3.10 Water Budget of Boğaz Region	120
5.4 Overall capacity of the Kyrenia Range Aquifers	121
CHAPTER 6: CONCLUSION	122
REFERENCES	124
APPENDIX A	129
APPENDIX B	132

LIST OF TABLES

Table 3.1 Classification of 11 sub regions of Kyrenia Range Aquifers	21
Table 4.1 Possible sources of water entering and leaving a ground-water system under natural conditions	91
Table 5.1 Minimum Monthly Temperature Averages for Lapta, Boğaz, Alevkayasi and Esentepe regions (Meteorology Department, 2010)	102
Table 5.2 Maximum Monthly Temperature Averages for Lapta, Boğaz, Alevkayasi and Esentepe region (Meteorology department, 2010)	102
Table 5.3 Result of Infiltration and Evapotranspiration	106
Table 5.4 Results of Calculation for aquifer of Karşıyaka Region	109
Table 5.5 Results of Infiltration and Evapotranspiration of Karşıyaka Region.	109
Table 5.6 Result of Infiltration and Evapotranspiration of Lapta Region.	110
Table 5.7 Calculation Result of the Aquifer of Lapta Region.	111
Table 5.8 The Result of Infiltration and Evapotranspiration of Alsancak Region.	111
Table 5.9 The Calculation Result of the Aquifer of Alsancak Region	112
Table 5.10 The Result of Infiltration and Evapotranspiration of Karaman Region.	112
Table 5.11 The calculation result of the aquifer of Karaman region	113
Table 5.12 The Result of Infiltration and Evapotranspiration of Dikmen Region.	113
Table 5.13 The Calculation Result of the Aquifer of Dikmen Region	114
Table 5.14 The Result of Infiltration and Evapotranspiration of Çatalköy and Beylerbeyi Region.	114
Table 5.15 The Calculation Result of the aquifer of Çatalköy and Beylerbeyi Region.	115
Table 5.16 The Result of Infiltration and evapotranspiration of Değirmenlik Region.	116
Table 5.17 The Calculation Result of the aquifer at Değirmenlik Region.	116
Table 5.18 The result of Infiltration and Evapotranspiration of Karaağaç Alevkayası	

Region	117
Table 5.19 The Calculation Result of the aquifer at Karaağaç Alevkayası Region	117
Table 5.20 The result of Infiltration and evapotranspiration of Tirmen Region.	118
Table 5.21 The Calculation Result of the aquifer of Tirmen Region.	119
Table 5.22 The Result of Infiltration and Evapotranspiration of Kantara Region.	119
Table 5.23 The Calculation Result of the aquifer of Kantara Region	120
Table 5.24 The Result of Infiltration and Evapotranspiration of Boğaz Region.	120
Table 5.25 The Calculation Result of the aquifer of Boğaz Region	121
Table 5.26 Water Stored Areas and Volume of Aquifer of 11 regions	121

LIST OF FIGURES

Figure 2.1 The unsaturated zone, capillary fringe, water table, and saturated zone	5
Figure 2.2 A cross section of the subsurface, depicting several hydrologic situations including types of aquifers (Kansas, 1993).	8
Figure 2.3 Cross-section of confined and unconfined aquifers	10
Figure 2.4 Cross section of Karst Features (Monroe, 1970).	11
Figure 2.5 Solution rate vs. degree of saturation. Instead of decreasing linearly (A.N Palmer, 1984).	12
Figure 2.6 Schematic representative of the growth of a carbonate aquifer drainage system Starting in the recharge area and growing toward the discharge area	13
Figure 2.7 Effects of fissure density and orientation on the development of caverns.	15
Figure 3.1 Areal picture showing the locations of boreholes (from top view) at Karşiyaka Region (scale, 1:45,000).	22
Figure 3.2 Wells depth details and Spring elevations at Karşiyaka Region.	23
Figure 3.3 Drawdown of dynamic water level of MTA-14.	25
Figure 3.4 Drawdown of dynamic water level of MTA-15.	25
Figure 3.5 Average daily discharge of different years for Karşiyaka Pigaoulla Spring based on month June 2009.	26
Figure 3.6 Average daily discharge of different years for Karşiyaka Manastri Spring based on month June 2009.	27
Figure 3.7 Average daily discharges of different years for Kozanköy spring based on month June 2009.	27
Figure 3.8 Karşiyaka Pigaoulla Spring	28
Figure 3.9 Kozanköy Spring	28
Figure 3.10 Areal picture showing the locations of boreholes (from top view)	

at Lapta Region (scale 1:33,750).	28
Figure 3.11 Wells depth details and springs elevations of Lapta Region.	30
Figure 3.12 Drawdown of dynamic water level of MTA-8 during years (1998-2002).	31
Figure 3.13 Drawdown of dynamic water level of MTA-12 during years (1998-2010).	31
Figure 3.14 Drawdown of dynamic water level of 9/74 during years (1981-2001).	
Figure 3.15 Average daily discharges at different years for Lapta Başpınar Spring in Lapta based on month June.	33
Figure 3.16 Average daily discharges of different years for Katouries Şht.Ahmet Kemil Sk.Üst Spring of Lapta based on month June 2009.	34
Figure 3.17 Average daily discharges of different years for Dragondas of Lapta Spring based on month June 2009.	34
Figure 3.18 Average daily discharges of different years of Lapta Başpinari Spring at Lapta based on month June 2009.	34
Figure 3.18a Katouries (Şht.Ah.K.Sk.Üst) spring in Lapta.	35
Figure 3.18b Dragondas Spring in Lapta	35
Figure 3.19 Areal picture showing the locations of boreholes (from top view) at Alsancak village Region (scale1:45,000).	36
Figure 3.20 Wells depth details and Springs elevations at Alsancak Region.	37
Figure 3.21a Average daily discharges of different years for Malatya Köy Spring based on month June 2009.	38
Figure 3.21b Malatya Köy Spring.	38
Figure 3.22a Average daily discharges of different years for Çıkarma Eski Manastır Spring based on month June 2009.	38
Figure 3.22b The picture of Çıkarma Eski Manastır spring Karaolanoğlu.	39
Figure 3.23a Average daily discharges of different years for Ilgaz Lower Spring based on month June 2009.	39

Figure 3.23b Ilgaz Lower Spring Ilgaz.	39
Figure 3.24 Drawdown of dynamic water level of well 48/69 in different years.	40
Figure 3.25 Drawdown of dynamic water level of well 1991/55 in different years.	41
Figure 3.26 Areal picture show the locations of boreholes (from top view) in Karaman and Boğaz village Regions (scale 1:26,000).	42
Figure 3.27 Wells depth details and springs elevations at Karaman and Boğaz village Regions.	43
Figure 3.28 Drawdown in dynamic water level of well 26A in different years.	44
Figure 3.29 Drawdown in dynamic water level of well 26B in different years.	44
Figure 3.30 Drawdown in dynamic water level of well MTA-11 in different years.	45
Figure 3.31 Drawdown in dynamic water level of well MTA-1 in different years.	46
Figure 3.32 The location of borehole from top view in Dikmen Region (scale, 1:30,000).	46
Figure 3.33 Areal picture show the locations of boreholes (from top view) in 2009 in Dikmen Region.	48
Figure 3.34 Drawdown in dynamic water level of well 173/62 in different years.	49
Figure 3.35 Drawdown in dynamic water level of well 1994/25 in different years.	50
Figure 3.36 Drawdown in dynamic water level of well 22/74 in different years.	50
Figure 3.37 Drawdown in dynamic water level of well 38/87 in different years.	51
Figure 3.38 Drawdown in dynamic water level of well 45/79 in different years.	51
Figure 3.39 Drawdown in dynamic water level of well 23/46 in different years.	52
Figure 3.40 Drawdown in dynamic water level of well 1-74 in different years.	52
Figure 3.41 Areal picture showing the locations of boreholes (from top view) in Çatalköy and Beylerbeyi Region (scale1:40,000).	53
Figure 3.42 Wells depth details and springs elevations at Çatalköy and Beylerbeyi Region	55
Figure 3.43 Drawdown in dynamic water level of well EB-10 in different years.	56

Figure 3.44 Drawdown in dynamic water level of well MTA-4 in different years.	56
Figure 3.45 Drawdown in dynamic water level of well B-30 in different years.	57
Figure 3.46 Drawdown in dynamic water level of well 14/70 in different years.	57
Figure 3.47 Drawdown in dynamic water level of well MTA-13 in different years.	58
Figure 3.48 Drawdown in dynamic water level of well B-20 in different years.	58
Figure 3.49 Drawdown in dynamic water level of well MTA-2 in different years.	59
Figure 3.50 Average daily discharges at different years for Ozanköy ANI Spring.	59
Figure 3.51 Areal picture showing the locations of boreholes (from top view) at Değirmenlik Region (scale, 1:53,000).	60
Figure 3.52 Wells depth details and springs elevations at Değirmenlik Region.	61
Figure 3.53 Drawdown in dynamic water level of well 1975/37 in different years.	63
Figure 3.54 Drawdown in dynamic water level of well 21/89 in different years.	63
Figure 3.55 Drawdown in dynamic water level of well 13A in different years.	64
Figure 3.56 Drawdown in dynamic water level of well 20/74a in different years.	64
Figure 3.57 Drawdown in dynamic water level of well 20/74 B in different years.	65
Figure 3.58 Drawdown in dynamic water level of well 18-b in different years.	65
Figure 3.59a Average daily discharges at different years for Çatalköy village spring.	66
Figure 3.59b Pictures of Çatalköy village spring.	66
Figure 3.60 Areal picture showing the locations of boreholes (from top view) Karaağaç Alevkayasi Region (scale, 1:44,000).	67
Figure 3.61 Wells depth details and springs elevations at Karaağaç Alevkayasi Region.	68
Figure 3.62 Drawdown in dynamic water level of well MTA-19 in different years.	69
Figure 3.63 Drawdown in dynamic water level of well 44/67 in different years.	70
Figure 3.64 Average daily discharges at different years of Karaağaç Çeşmeler (Viysitou) spring.	70

Figure 3.65 The pictures of Karaağaç Çeşmeler Viysitou spring.	71
Figure 3.66 Areal picture showing the locations of boreholes (from top view) Tirmen Region (scale, 1:43,000).	72
Figure 3.67 Wells depth details and springs elevations at Tirmen Region	74
Figure 3.68 Drawdown in dynamic water level of well 37/76 in different years.	75
Figure 3.69 Drawdown in dynamic water level of well 19/66 in different years.	75
Figure 3.70 Drawdown in dynamic water level of well MTA-3 in different years.	76
Figure 3.71 Drawdown in dynamic water level of well 17/74 in different years.	76
Figure 3.72 Drawdown in dynamic water level of well 6/68 in different years.	77
Figure 3.73 Average daily discharges at different years of Aslanbaşı Spring.	77
Figure 3.74 Pictures of Aslanbaşı Spring at Tirmen Region.	78
Figure 3.75 Discharges in month June of different years for Bahçeli Verysi spring	78
Figure 3.76 The pictures of Bahçeli Virysi spring.	79
Figure 3.77 Areal picture showing the locations of boreholes (from top view) in Tatlısu Kantara Region (scale, 1:125,000).	80
Figure 3.78 Wells depth details and springs elevations at Tatlısu Kantara Region	81
Figure 3.79 Drawdown in dynamic water level of well MTA-21 in different years.	83
Figure 3.80 Drawdown in dynamic water level of well 116/65 in different years.	83
Figure 3.81 Drawdown in dynamic water level of well B-1 in different years.	84
Figure 3.82 The location of borehole from top view in Boğaz Region (scale, 1:25,000).	84
Figure 3.83 Wells depth details and springs elevations at Boğaz Region.	85
Figure 3.84 Drawdown in dynamic water level of 1/65 in different years.	86
Figure 3.85 Drawdown in dynamic water level of well MTA-10 in different years.	87
Figure 3.86 Drawdown in dynamic water level of well 13/74 in different years.	87
Figure 4.1 Diagrams illustrating water budgets for a ground-water system for predevelopment and development conditions.	90

Figure 4.2 Regional ground-water-flow system that comprises subsystems at different scales and a complex hydrogeologic framework .	93
Figure 4.3 Reference evapotranspiration (ET _o)	94
Figure 4.4 Water budget shape.	98
Figure 4.5 Frustum of sphere	99
Figure 4.6 Cross section for water storage in an aquifer.	100
Figure 5.1 Top view of the aquifer at Karşıyaka Region (scale, 1:37,000).	108
Figure 5.2 Top view of the aquifer at Lapta Region (scale, 1:37,000).	110
Figure 5.3 Top view of the aquifer at Alsancak region (scale, 1:46,000).	111
Figure 5.4 Top view of the aquifer at Karaman Region (scale, 1:35,000).	112
Figure 5.5 Top view of the aquifer at Dikmen Region (scale, 1:31,000).	113
Figure 5.6 Top view of the aquifer at Çatalköy and Beylerbeyi region (scale, 1:36,000).	114
Figure 5.7 Top view of the aquifer at Değirmenlik Region (scale, 1:45,000).	115
Figure 5.8 Top view of the aquifer at Karaağaç Alevkayası Region (scale, 1:33,000).	117
Figure 5.9 Top view of the aquifer at Tirmen Region (scale, 1:45,000).	118
Figure 5.10 Top view of the aquifer at Kantara Region (scale, 1:135,000).	119
Figure 5.11 Top view of the aquifer at Boğaz Region (scale, 1:3,000).	120

ABBREVIATIONS

DD	Decreased discharge
DWL	Dynamic Water Level
ET _o	Evapotranspiration
FAO	Food and Agriculture Organization
GMD	Geology and Mining Department
Inf	Infiltration
IRR	Increased recharge rate
MCM	Millions Cubic Meters
M.S.L.	Mean Sea Level
MTA	General Directorate of Mineral Research and Exploration of Turkey
P	Pumpage
ppt	Precipitation
RH	Relative Humidity
WS	Volumetric rate of water removed from the storage
WWD	Water Works Department

LIST OF SYMBOLS WITH SI UNITS

P_h	Power
q	Flow capacity
ρ	Density of fluid
g	Gravity
h	Differential head
Q	Pumping rate
ET_0	Reference Evapotranspiration
G	Soil heat flux density
T	Air temperature
T_{dew}	Dew-point temperature
u_2	Wind speed
e_s	Mean saturation vapour pressure
e_a	Actual vapour pressure
Δ	Slope of the vapour pressure curve
γ	Psychrometric constant
z	Elevation above sea level
R_a	Extraterrestrial radiation
G_{sc}	Solar constant
d_r	Inverse relative distance Earth-Sun
ω_s	Sunset hour angle
ϕ	Latitude
δ	Solar declination
a_s	Regression constant
m_c	Fractional of cloud cover

R_{ns}	Net solar or shortwave radiation
R_s	Incoming solar radiation
R_{nl}	Net outgoing longwave radiation
σ	Stefan-Boltzmann constant
f	Cloudiness adjustment factor expresses the effect of cloudiness
α	Albedo or canopy reflection coefficient
ε'	Net emissivity expressing a correction for air humidity
$\frac{dh}{dt}$	The yearly change in water level by time in meters (m/year).
A	Surface area of water budget.
H	Difference in height between well depth and water level (m).
r	Radius of circular area (m).
V	Volume of water budget (m ³).

CHAPTER 1

INTRODUCTION

1.1 General

Within the hydrologic cycle the excess water available on the earth surface is pulled downward by gravity and the water percolates from the soil surface travels towards deeper layers. The travel of water is conveyed through the pores of the soil or cracks on the rocks until the water meets with the saturated water zone. The water stored in this saturated zone, known as groundwater, then either naturally moves due to energy head differences and discharges via springs, or as a seepage into streams, lakes and rivers or pumped artificially back to earth surface. Depending on the hydraulic flow conditions, the groundwater flow can be classified as laminar or turbulent flow. The groundwater formations dominated by fractures and cracks are likely to have a turbulent flow condition and mostly defined as Karst Aquifers (Hadjicharalambous, 2008).

The heterogeneous structure of the karst systems and the variable recharge regimes of karst systems create complex hydrogeological conditions (Bonacci, 2001). Right after the precipitation occurs the water infiltrates through the covered soils or through fractured zones reaching to the saturation zone. All around the world, karst aquifers are the main groundwater resource where the surface water resources are limited or contaminated (El-Hakim et al, 2007). Various approaches can be used to simulate groundwater flow in karst systems, including equivalent porous media distributed parameter, lumped parameter, and dual porosity approaches, as well as discrete fracture or conduit approaches (Scanlona et al, 2003). Many studies have focused on hydrologic modeling of karst aquifer systems like a multi cell groundwater model. Multi cell model investigates the potential improvement in the modeling of karstic aquifers by using a mixed equation suitable for both the free surface and pressure flow conditions in karstic conduits (Rozos and Koutsoyiannis, 2005).

1.2 Aim and Scope of the Thesis:

1. To carry out a literature survey, assessment and documentation of previous research progress in the area of Kyrenia Range Aquifer.
2. To investigate whether the Kyrenia Range Aquifer can be accepted as a single large unit or can be considered as a spot of regional aquifers.
3. To analyze and understand the data gathered from Water Works Department during the long term aquifer monitoring process.
4. To search for a relationship in terms of hydraulic properties between the southern and northern foothills of the range.
5. To estimate and figure out the time-wise changes in groundwater levels at each sub region.
6. To suggest a schematic representation of subsurface water boundaries of each sub region and establishing their plan and section views.
7. To locate the coordinates of the existing springs and the wells within the regions by the help of GPS and GIS software.
8. To find the evapotranspiration rates of each sub-region by the help of Penman-Monteith equation.
9. To extract the infiltration rates due to precipitation, in order to get the water budget of aquifers.

1.3 Guides to Thesis

The thesis contains the following chapters:

Chapter 1: The introduction that contains a short background identifying the aim and the scope of the main outline of the thesis.

Chapter 2: It highlights the concepts of ground water, with a quick overview of fundamentals of groundwater, aquifers and types of aquifers. Brief information on geologic and hydrogeologic conditions of Kyrenia Range.

Chapter 3: Long term aquifer monitoring analysis, including the detailed plan views and cross-sections.

Chapter 4: Theoretical formulization of water budget based on the conservation of mass theory.

Chapter 5: Analyzes of the infiltration and evapotranspiration rates at each region based on Penman-Monteith Method and calculating the water budget for each sub region.

Chapter 6: Conclusion drawn from the performed outcomes from each chapter were presented. Furthermore, recommendations for future research were also given.

CHAPTER 2

CONCEPTS OF GROUND WATER

2.1 Fundamentals of Groundwater Sustainability

2.1.1 Overview

The following reviews some basic facts and concepts about ground water that serves as background for the discussion of groundwater sustainability. Ground water occurs almost everywhere beneath the land surface. Natural sources of freshwater that become ground water are (1) areal recharge from precipitation that percolates through the unsaturated zone to the water table Figure 2.1, and (2) losses of water from streams and other bodies of surface water such as lakes and wetlands (Aeyll, et al; 2007). Streams and other surface-water bodies may either gain water from ground water or lose water to ground water. Streams commonly are significant source of recharge to ground water downstream from mountain fronts and steep hill slopes in arid and semiarid areas and in karstic terrains. Groundwater is a part of the hydrologic cycle, including surface and atmospheric waters (Todd, 1979).

2.1.2 Subsurface Water

Water beneath the land surface occurs in two principal zones, the unsaturated zone and the saturated zone. In the unsaturated zone, the voids—that is, the spaces between grains of gravel, sand, silt, clay, and cracks within rocks—contain both air and water. Although a considerable amount of water can be present in the unsaturated zone, this water cannot be pumped by wells because it is held too tightly by capillary forces. The upper part of the unsaturated zone is the soil-water zone. The soil zone is crisscrossed by roots, voids left by decayed roots and animal and worm burrows, which enhance the infiltration of precipitation into the soil zone. Soil water is used by plants in life functions and transpiration, but it also can evaporate directly to the

atmosphere (Aeyll, et al; 2007). The endless circulation of water between ocean, atmosphere, and land is called the hydrologic cycle (Freeze and Cherry, 1979).

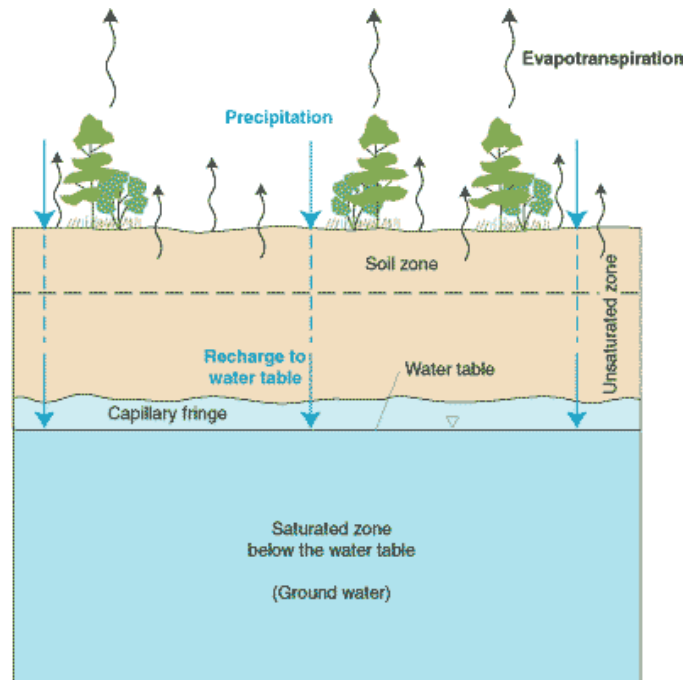


Figure 2.1: The unsaturated zone, capillary fringe, water table, and saturated zone (Aeyll, et al; 2007).

In contrast to the unsaturated zone, the voids in the saturated zone are completely filled with water. Water in the saturated zone is referred to as ground water. The upper surface of the saturated zone is referred to as the water table. Below the water table, the water pressure is high enough to allow water to enter wells, thus permitting ground water to be withdrawn for use. A well is constructed by inserting a pipe into a drilled hole; a screen is attached, generally at its base, to prevent earth materials from entering the pipe along with the water pumped through the screen. The depth to the water table is highly variable and can range from zero, when it is at land surface, to hundreds of meters in some types of landscapes. Usually, the depth to the water table is small near permanent bodies of surface water such as streams, lakes, and wetlands. An important characteristic of the water table is that its configuration varies seasonally and from year to year. According to the Aelly, et al, in 2007, during the recharge of groundwater resources, infiltrated

water reaches to the upper surface of the saturated zone which shows wide variation in the quantity, distribution, and timing of precipitation.

2.1.3 Groundwater

The term groundwater is usually reserved for the subsurface water that occurs beneath the water table in soils and geologic formations that are fully saturated (Freeze and Cherry, 1979). Groundwater flow is a special case of liquid flow in porous media. Groundwater flow or seepage is a movement of water in the voids of the earth's crust. The materials of interest are soils and fractured rocks. Groundwater flow depends on the properties of the medium in which it occurs, on the properties of the liquid and on the hydraulic gradient. The domain of groundwater flow is that part of space, in which the motion takes place. The water body below the ground surface is called subsurface water. The subsurface water system is composed of unsaturated and saturated zones (Batu, 1998). In the unsaturated zone, the spaces between particle grains and the cracks in rocks contain both air and water. Although a considerable amount of water can be present in the unsaturated zone, this water cannot be pumped by wells because capillary forces hold it too tightly. In contrast to the unsaturated zone, the voids in the saturated zone are completely filled with water. The approximate upper surface of the saturated zone is referred to as the water table. Water in the saturated zone below the water table is referred to as ground water. Between the unsaturated zone and the water table is a transition zone; the capillary fringe. In this zone, the voids are saturated or almost saturated with water that is held in place by capillary forces.

2.2 Aquifer and Types of Aquifers

2.2.1 Definitions

A unit of rock or an unconsolidated deposit is called an aquifer when it can yield a usable quantity of water. The boundary between the vadose zone and the zone of saturation is termed the water table. Its location is determined by the elevation to which water rises in un-pumped wells and it is just the top of the zone of saturation. Groundwater is recharged from, and eventually flows to, the

surface naturally; natural discharge often occurs at springs and seeps, and can form oases or wetlands. Groundwater is also often withdrawn for agricultural, municipal and industrial use by constructing and operating extraction wells. The study of the distribution and movement of groundwater is hydrogeology, also called groundwater hydrology (Sophocleous, 2002).

2.2.2 Aquifers

Most aquifers are of large in areal extent and may be visualized as underground storage reservoirs. Water enters a reservoir from natural or artificial recharge; it flows out under the action of gravity or is extracted by wells (Todd, 1979). An aquifer is best defined as a saturated permeable geologic unit that can transmit significant quantities of water under ordinary hydraulic gradients (Freeze and Cherry, 1979). Groundwater occurs in many types of geologic formations; those known as aquifers are of most importance (Todd, 1979). The term aquifer is used for saturated formations. Etymologically, aquifer means “water-bearing formation”. The word aquifer is produced from two Latin words: aqua (water) and ferre (to bear). Aquifer is defined as a single geologic formation or a group of geologic formations that transmits and yields a significant amount of water (Batu, 1998).

2.2.3 Types of Aquifers

There are many types of aquifers that are classified depending on the geological properties of the formation. An aquifer is water bearing capacity which consists of a bed rock, or other an earth material, from which a useable quantities of ground water can be produced by a well or spring. Springs are site where groundwater emerges from an aquifer to become surface water. Springs occur along creeks and rivers where the water table, or the surface at the top of the ground water, meets the land surface. Also spring occur where impermeable rocks, such as shale, underlie or have been faulted against permeable rock. The impermeable rock blocks the flow of the ground water, forcing it to the surface (Figure 2.2.).

Aquiclude Aquifer is defined as a geologic formation that does not have the capability to transmit a significant amount of water (Batu, 1998).

Aquitard Aquifer or a confining layer is defined as a geologic formation that can transmit water at a relatively low rate compared with aquifers (Batu, 1998).

Aquifuge Aquifer is defined as geologic formation neither absorbs nor transmits water (Batu, 1998).

Alluvial Aquifer is formed by the deposition of weathered materials such as sand and silt particles. The water flow in these aquifers is very slow.

Confined Aquifer is also known as artesian aquifer (Todd, 1979), which is an aquifer whose upper and possibly lower boundary is defined by a layer of natural material that does not readily transport water. According to Freeze and Cherry, confined aquifer is an aquifer that is confined between two aquitards. In a confined aquifer, the water level in a well usually rises above the top of the aquifer. If it does, the well is called an artesian well and the aquifer is said to exist under artesian conditions (Freeze and Cherry, 1979).

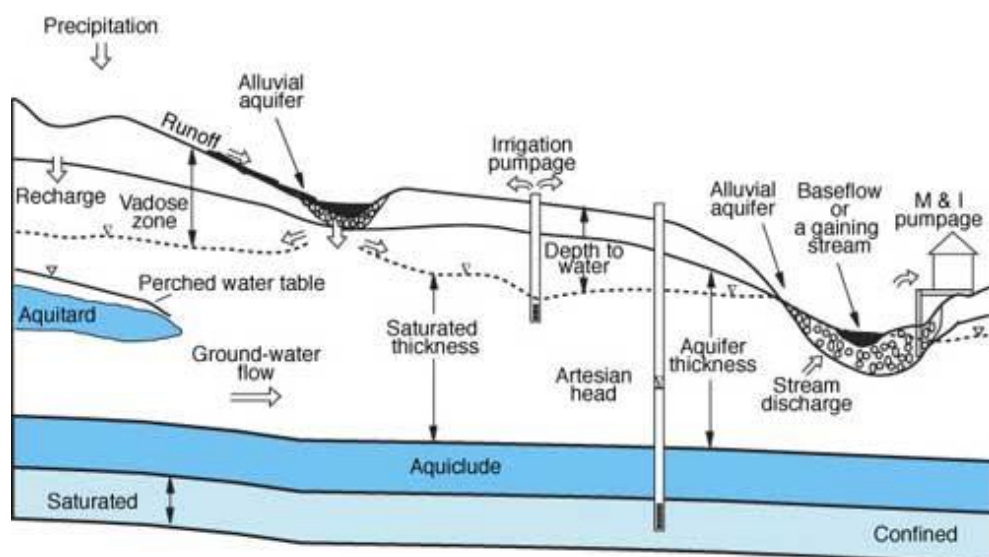


Figure 2.2 A cross section of the subsurface, depicting several hydrologic situations including types of aquifers (Kansas, 1993).

Unconfined Aquifer is an aquifer in which the water table is at or near atmospheric pressure and is the upper boundary of the aquifer. Because the aquifer is not under pressure the water level within a well is the same as the water table outside the well. Figure 2.3.

Karstic Aquifer is an aquifer that is formed in limestone based material through the wearing away process. Karst is a term applied to topography formed over limestone, or gypsum; and characterized by sinkholes as shown in Figure 2.4. (White, 1969).

2.2.4 Carbonate Rocks

Karstic aquifer is generally formed in limestone based material through the wearing away process. Karstic processes result in the creation of surface and underground cavities. Each cavity may have a different shape (circular or linear), size (small or large), depth (shallow or deep) and, of course, genesis type (Fetter, 1942).

The term karst is derived from a Slavic word that means barren, stony ground. It is also the name of a region in Slovenia near the border with Italy that is well known by its sinkholes and springs.

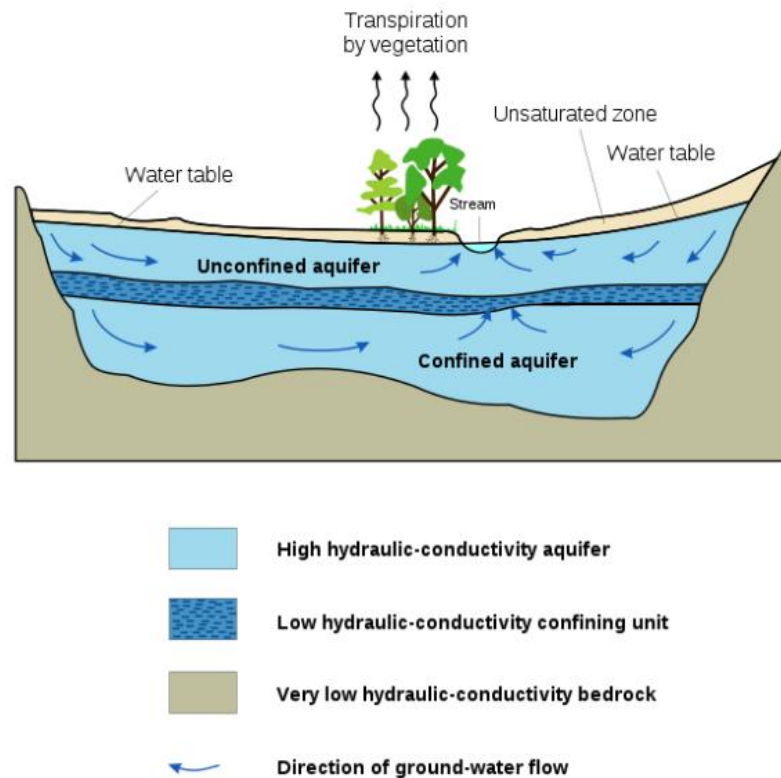


Figure 2.3 Cross-section of Confined and Unconfined Aquifers (U.S. Geological Survey, 1999).

The word has been adopted by geologists worldwide as the term for all such terrain. A karst landscape most commonly develops on limestone but can develop on several other types of rocks, such as dolomite, gypsum, and salt. The primary porosity of limestone and dolomite is variable. If the rock is elastic, the primary porosity can be high. Chemically precipitated rocks can have a very low porosity and permeability if they are crystalline. Bedding planes can be zones of high primary porosity and permeability. Limestone and dolomite are soluble in water that is mildly acidic. In general, if water is unsaturated with respect to calcite or dolomite, it will dissolve the mineral until it reaches about 99+ % saturation with respect to calcite (Plummer, et al., 1978). The rate of solution is linear with respect to increasing solute concentration until somewhere between 65% and 90% saturation, but at some locations the rate decreases dramatically. Figure 2.5 shows

the general nature of solution rate as a function of degree of saturation. As it is observed the line instead of decreasing linearly, the solution rate drops sharply.

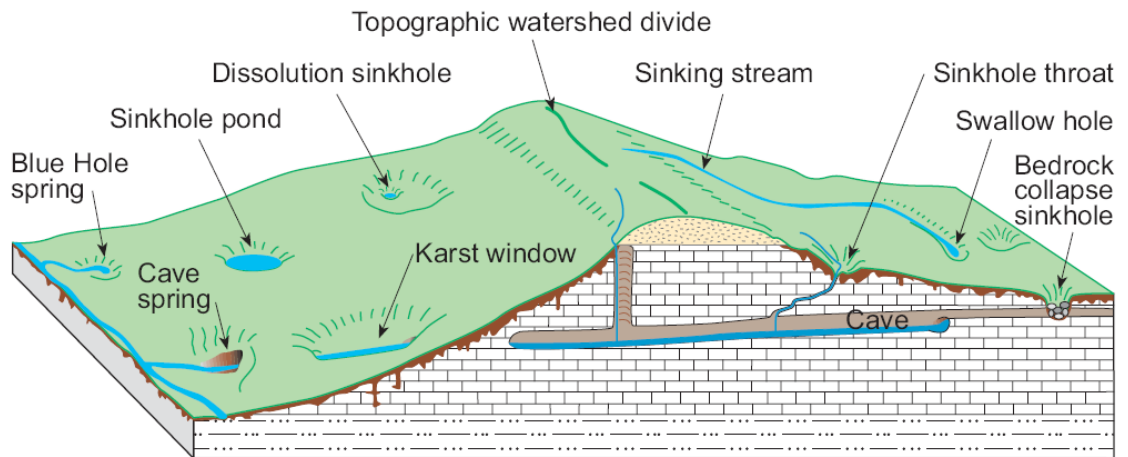


Figure 2.4 Cross section of karst features (Monroe, 1970).

2.2.4.1 Features of a Karstic Landscape

Massive chemically precipitated limestone can have very low primary porosity and permeability. Secondary permeability in carbonate aquifers is due to the solutional enlargement of bedding planes, fractures, and faults (Ford & Ewers, 1978). The rate of solution is a function of the amount of groundwater moving through the system and the degree of saturation (with respect to the particular carbonate rock present) but it is nearly independent of the velocity of flow. The width of the initial fracture is one of the factors controlling how long the flow path is, until the water reaches 99+ % saturation and dissolution cases (Palmer, 1984).

Initially, more ground water flows through the larger fractures and bedding planes, which have a greater hydraulic conductivity. These become enlarged with respect to lesser fractures; hence, even more, water flows through them. Solution mechanism of carbonate rocks favors the development of larger openings at the expense of smaller ones. Carbonate aquifers can be highly anisotropic and non-homogeneous if water moves only through fractures and bedding planes that

have been preferentially enlarged. Water entering the carbonate rock is typically unsaturated. As it flows through the aquifer, it approaches saturation, and dissolution slows and finally ceases.

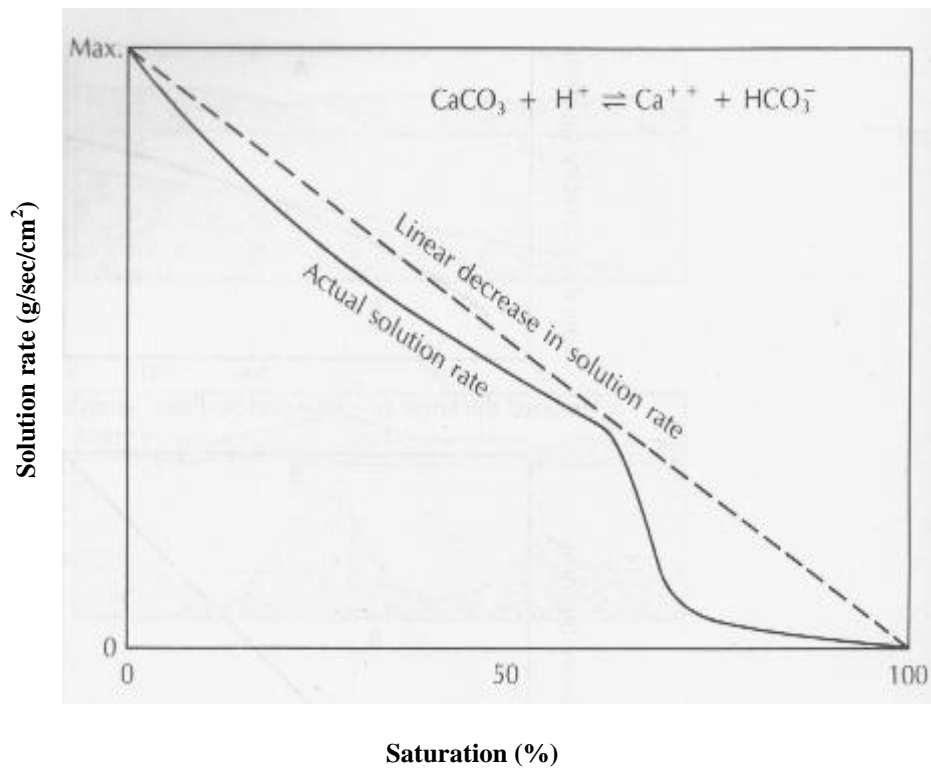


Figure 2.5 Solution rate vs. Degree of Saturation. Instead of decreasing linearly, the solution rate drops sharply to a low level at 65 - 90% saturation (A.N Palmer, 1984).

It has been shown experimentally that solution passages from the recharge area to the discharge area and that, as they follow fracture patterns, many smaller solution openings join to form fewer but larger ones (Ewers et al., 1978). Eventually, many passages join to form one outlet (Figure 2.6). In Figure 2.6, picture A represents that most joints in the recharge area undergo solution enlargement; B shows that as the solution passages grow, they join and become fewer; and at C, eventually, one outlet appears at the discharge zone. Greater ground water movement -hence, solution- takes place along the intersection of the joints or a joint and the strike of intersecting joints. A second mode for the entry of unsaturated water into a carbonate aquifer occurs near valley bottoms. Water tables in many karstic areas are almost flat owing to high hydraulic

conductivity. Floodwaters from surface streams can enter the carbonate aquifers and reverse the normal flow. If the floodwaters are unsaturated with respect to the mineral in aquifer, solution will occur (White, 1969). Shallow holes, or shafts leading from surface streams, can carry surface water underground into caverns. Shallow holes can drain an entire stream or only a small portion of one. Geochemical studies have shown that there are two types of groundwater found in complex carbonate aquifer systems (Shuster and White, 1971). The joints and bedding planes that are not enlarged by solution contain water that is saturated with respect to calcite (or dolomite), because of low hydraulic conductivity of these openings, the water mass moves slowly.

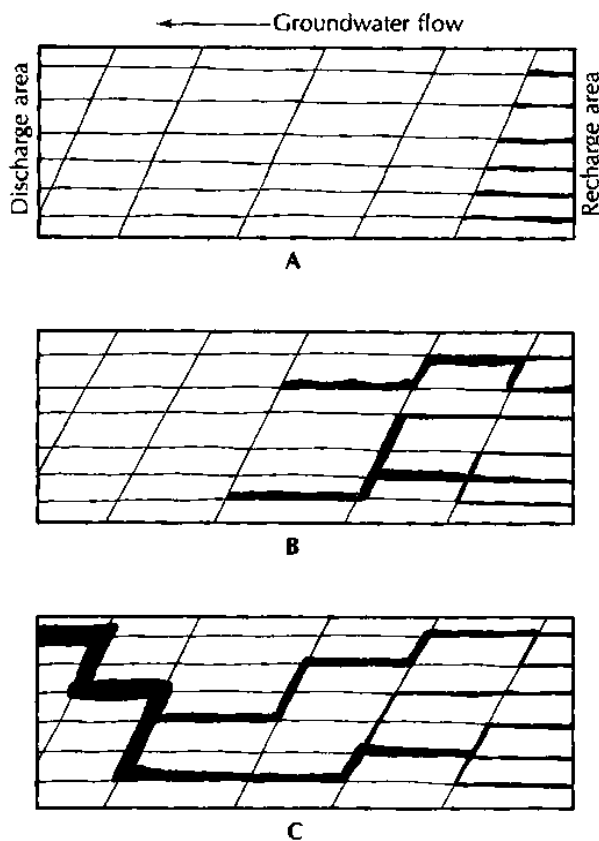


Figure 2.6 Schematic representative of the growth of a carbonate aquifer drainage system starting in the recharge area and growing toward the discharge area (Fetter, 1942).

Another mass of water, generally partially saturated, moves more rapidly through well-defined channels that are close to the water table. It is this second body that forms the passageways. Cave systems can be formed above, at, or below the water table. They form when free-flowing water

enlarges a fracture or bedding plane sufficiently for non-Darcian flow to occur. This can be above the water table if a surface stream enters the ground in the unsaturated zone (vadose cave), below the water table if the joint or bedding plane through which flow is occurring dips below the water table (phreatic cave), or at the water table itself (water-table cave) (Ford and Ewers, 1978).

The pattern of cave passages is controlled by the pattern and density of the joints and/or bedding planes in the carbonate rock (Ford and Ewers, 1978). Figure 2.7 shows the influence of fissure density and orientation on cave formation. With widely spaced fissures, the cave can develop below the potentiometric surface because the fissure pattern is too coarse to allow the cave development to parallel the water table as detailed in Figure 2.7 A and B. If the fissure density is great enough, cave development can occur along the water table as detailed in Figure 2.7 C and D.

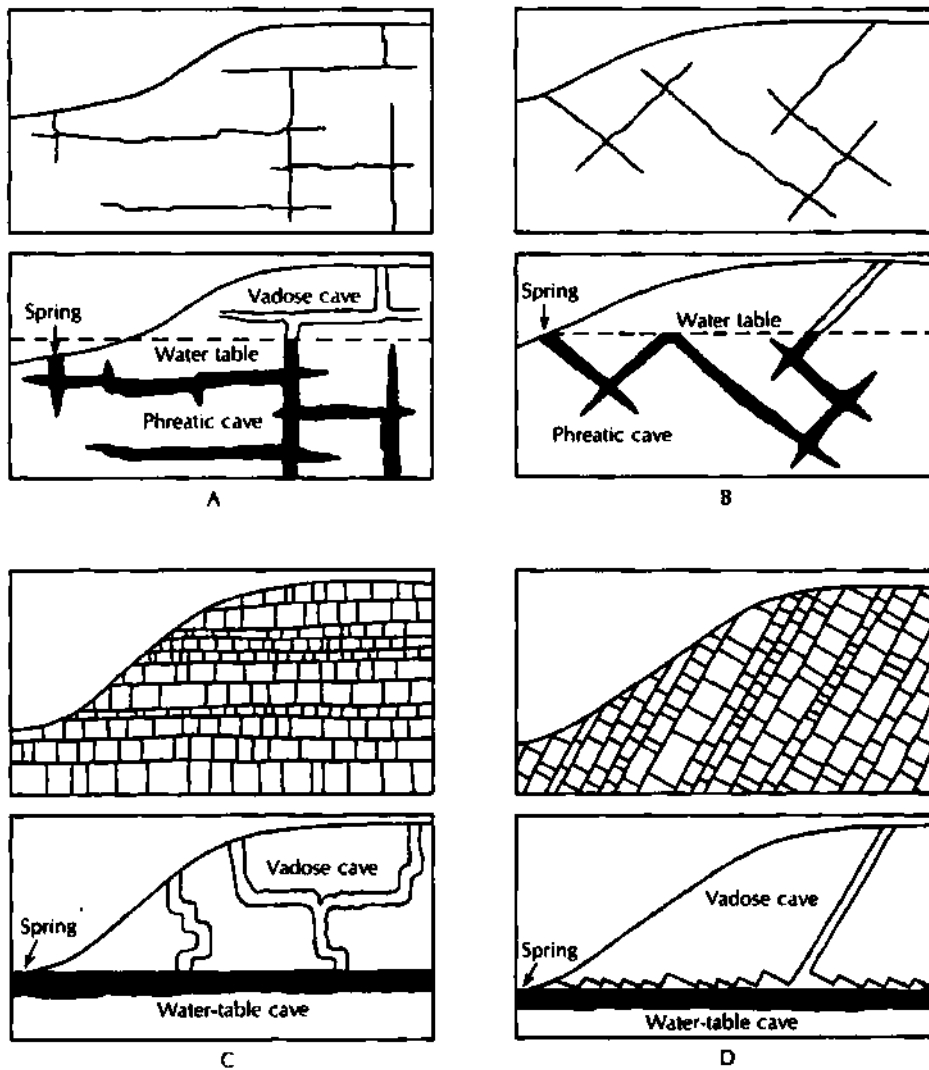


Figure 2.7 Effects of fissure density and orientation on the development of caverns.

Source: (Modified from D.C. Ford and R. O. Ewers).

Vertical shafts can form in the vadose zone by under-saturated infiltrating water, trickling down the rock surface (Brucker, Hess and White, 1972). Some caves that are presently dry were formed at or below the water table when the regional water table was higher. The regional base level of a karstic region is typically a large river. If the river is down cutting, the regional water table will be lowered. The result will be a series of dry caves at different elevations, each formed when the regional water table was at different levels.

Carbonate aquifers show a very wide range of hydrologic characteristics (White, 1969). Diffuse-flow carbonate aquifers have a little solutional activity directed toward opening large channels; these are to some extent homogeneous. Free-flow carbonate aquifers diffused recharge but have well-developed solution channels along which most flow occurs. Ground-water flow in free-flow aquifers is controlled by the orientation of the bedding planes and fractures that determine the locations of solutional conduits, but not by any confining beds.

2.3 Karst Spring

Confined-flow carbonate aquifers have solution openings in the carbonate units, but low-permeability non-carbonated beds exert control over the direction of ground-water movement. Karst springs occur where the groundwater flows within the gas concentrated to dissolve rocks and form a conduit or cave within the soluble rocks. The groundwater basin of a karst spring collects drainage from all the sinkholes and sinking streams in its drainage area. The water flowing from each sinkholes joints together underground to form ever-increasing flow in successively larger passages, which discharge at a spring. Karst springs, or cave spring, can have large opening and discharge very large volumes of water. The soil cover, narrow fractures, small conduits, and larger cave passages collectively from a karst aquifer (Currens, 2002).

A sinkhole is any depression in the surface of the ground from which rainfall is drained underground, karst sinkholes form when a fracture in the limestone bedrock becomes enlarged. Sinkholes form in two ways, in the first way, the roof of cave becomes too thin to support the weight of the bedrock and soil above it. The cave roof then collapse, forming a collapse sinkhole. Bedrock collapse is rare and the least likely way a sinkhole can form, although it is commonly summed to be the way all sinkholes form. The second way sinkholes form is much more common and much less dramatic. As the bedrock under a sinkhole is dissolved and carried away underground, the soil gently slumps or erodes into the sinkhole. Once the underlying conduits become large enough, insoluble soil and rock particles are carried away too. Dissolution sinkholes

from gradually over long periods of time, with occasional episodes of soil or cover collapse (Currens, 2002).

2.4 Geology and Hydrogeology

2.4.1 Overview

Five Finger Mountain Range, formed during the Carboniferous-Permian (350–250 mya) to Middle Miocene (15 mya). The Five Finger range is generally characterized as karst topography (Necdet 2003), and its geologic history has involved episodic rift, passive-margin, active-margin, strike-slip and uplift phases (Robertson and Woodcock 1996). The younger (85–15 mya) autochthonous marine sediments (i.e., lava, sandstone, siltstone, and marl) are named the Lapithos, Belapais, and Kythrea Formations, and thrust into this are a smaller area of older allochthonous carbonate (i.e., limestone) masses are named the Dhikomo, Sykhari, Hilarion, and Kantara Formations.

The calcareous limestone and chalk sedimentary rock formations are considered pervious to highly pervious percolate rainfall. The calcareous formation tilts to the north, and directs the majority of the drainage up to the coast. Interestingly, the range is considered part of Alpine belt connecting the Pyrenees to Himalayan ranges (FAO, 1995).

The Kyrenia region is approximately 80 km in length, has an average width of 4 km, and a total area of 310 km². The Karpas region is approximately 30 km in length, has a width of 0.75 km, and a total area of 60 km² (Endreny and Gokcekus, 2009).

The Five Finger Mountain Range forms the northern boundary of the Mesaoria plain, which, during the Tertiary period was the Athalas Sea and accumulated clayey impervious to slightly pervious deposits. The region was formed by a succession of Upper Cretaceous (70 mya) to Pleistocene (ca. 1 mya) sedimentation (FAO, 1995), and has many schist formed hills bounding the plain. The Yialias and Pedhieos Rivers flow ephemerally east into Famagusta Bay and the Serrahi (Serraghis) River flows ephemerally west into Morphou. South of the Mesaoria is the Troodos Mountain Massif, occupying the southern third of the island. It was formed in the

Triassic period from volcanic activity and subsequent up thrusting of oceanic crust when Africa and Europe converged. These igneous rocks consist of ophiolite, pillow lavas, diabase, gabbro, peridotite, dunite, and serpentine (FAO, 1995), and while they are rich in copper, they cause a poor drinking water supply. Rocks of the Troodos are mostly impervious to slightly pervious, and water that does infiltrate, provides down gradient communities with relatively soft, spring fed, drinking water. Surface waters from the Troodos are vulnerable to pollution originating from the outcrops of copper sulfate mines (FAO, 1995).

2.4.2 Vegetation and Climate

Ground cover above the 250 m contour varies with the aspect of the Five Finger Mountain range, where the northern face is more verdant, and with the degree of exposed rock surfaces. Based on site samples, nearly 15% of the projected surface area of the range is covered by un-vegetated soil and exposed rocks. Cyprus climate is intense Mediterranean type with a cool wet winter extending from November to mid-March and hot dry summers from May to mid-September, separated by rapid seasonal change in springs and autumns. Five-Finger Mountain range mean daily temperature for the high peaks is 7°C in January and 25°C in July based on long year averages respectively, and for comparison mean January and July temperatures along the North Coast are 13° and 28°C, and at the Mesaoria plain are 10° and 29°C. Analysis of temperature at gages within the Mesaoria plane and South Coast revealed 1°C rise within the past 100 years (Price et al. 1999), based largely due to the increase in daily minimum values at both gages due may be global warming.

Climate extremes and isolation from larger land masses have created a wide range and large number of Cypriot indigenous plant taxa (species, subspecies, varieties, hybrids and forms), with 52 trees, 131 shrubs, 88 sub-shrubs and 1,637 herbs recorded in 2005 (MOA, 2005).

Vegetation surveys along the Five Finger Mountains clearly distinguish the moisture at the north side and the rain shadow at the south side. Mediterranean cypress (*Cupressus sempervirens*), which prefers the limestone substrate of the region, grows with Calabrian pine (*pinus brutia*) on

the lower elevations and less steeply sloped north sides. *Cupressus sempervirens* occur as a single stands on the high peaks and steep slopes where the adequate soil has accumulated.

Down slope of the southern mountain peaks, these woodland stands and their accompanying moist environment plant community grade into dry tolerant flora. Dry tolerant forests species (xerophilous, sclerophyllous, evergreen, and thorny) include Garigue, which are low- and sub-shrubs, and Phrygana, which are more sub-shrubs and herbs, that occupy recently burnt and over-grazed areas. Magui forests evolve from the Garigue and Phrygana cover, and are noted for average heights between 2 and 3 m. growing within the small cracks of rock surfaces that are isolated chasmophytic flora, with specific species that are more tolerant to limestone rocks (MOA, 2005).

CHAPTER 3

LONG TERM AQUIFER MONITORING ANALYSIS

Water storage in karst aquifer is classically estimated by the analysis of the spring hydrograph (Mangin, 1975) and by lumped models that simulate the spring discharge (Pinault et al., 2001; Fleury et al., 2007). At the same time, combining spring data and water level fluctuations on deep wells of karst aquifers plays a dominant role in the understanding of the hydrological system as a whole. However, these methods are favorable under the long and precise spring and well monitoring programs.

In this study, the well and spring monitoring data is used to yield spatial and time wise information on the storage and flow conditions on the karst system of Kyrenia Range Aquifers. Based on the assumption that Kyrenia Range aquifer consists of small and regional formations, depending on the gathering of the wells, 11 different sub regions in which intensive pumping operations are carried out on Kyrenia Range Aquifer were studied. All the existing wells serve only for domestic water supply purposes. The urban and rural settlement at the southern and northern foothills of Kyrenia Range benefits from this sub region aquifers. The data is gathered from the archives of Water Works Department. The Department has been regularly monitoring the wells at Kyrenia Range since the beginning of ENVIS database project in 2000. For the case of simplicity, this study assumes that 11 sub-regional aquifers are all independent of each other. As a result, Table 3.1 details the regional names and locations of these 11 sub-regional aquifers.

Table 3.1 Classification of 11 sub regions of Kyrenia Range Aquifers.

Serial No.	Region Name	Location by Foothills
1	Karşiyaka (Vasillia)	Northern face
2	Lapta (Lapithos)	Northern face
3	Alsancak (Karavas)	Northern face
4	Karaman (Karmi)	Northern face
5	Dikmen (Dhikomo)	Southern face
6	Çatalköy (AyiosEpiktitios)	Northern face
7	Değirmenlik (Kythrea)	Southern face
8	Karaağaç Alevkayası (Alevga)	Southern face
9	Tirmen (Trypimeni)	Southern face
10	Kantara (Kantara)	Northern face
11	Boğaz (Boghaz)	Southern face

3.1 Karşiyaka (Vasillia) Region

Karşiyaka (Vasillia) Region is at the north-west part of Kyrenia Range. There are three boreholes, B-35, MTA-14 and MTA-15 within this region. MTA-15 is at the southern foothills of mountains where MTA-14 and B-35 are at the north. There are three main spring within this area, which are known as Karşiyaka Pigaoulla, Karşiyaka Manastır, and Kozan springs. The aerial photograph of the region and a cross-section of the region lined on one section are given in the Figures 3.1 and 3.2.

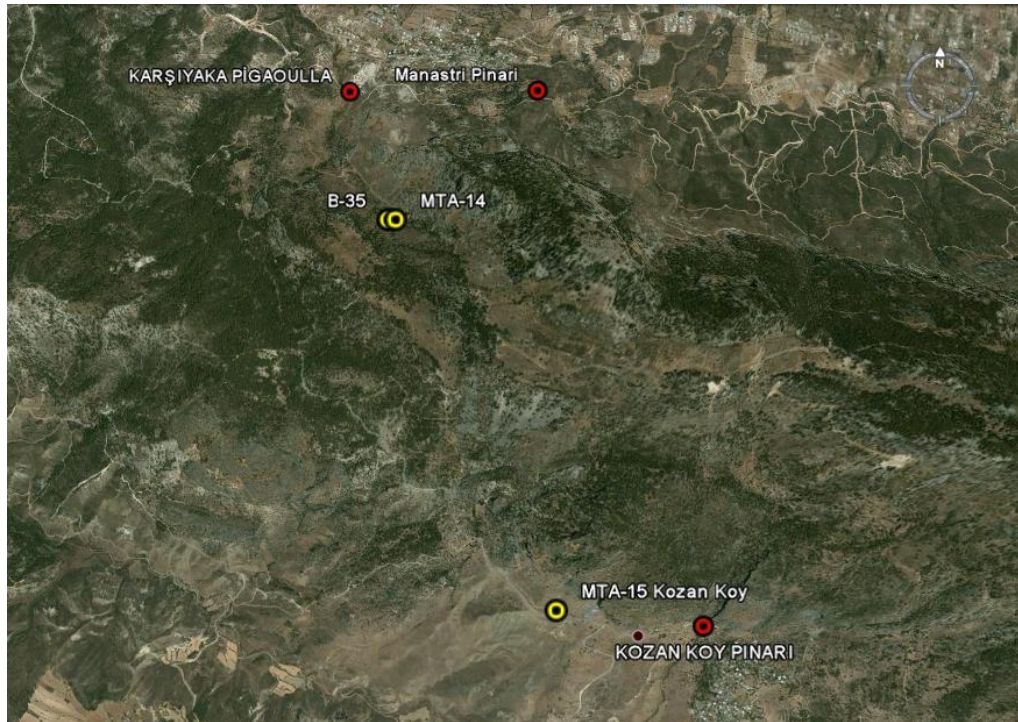


Figure 3.1 Areal picture showing the locations of boreholes (from top view) at Karşıyaka Region (scale, 1:45,000).

B-35 drilled in 1966; the static water level of the well was 255 m at that time (Dixey, 1975). The static water level has increased up to 258 m during 1966-69 periods; the appertaining catchment area of karst limestone has an approximate extent of 1.5 km²; as permanent extraction rate was recommended a quantity of discharge up to 40 m³/h (Mixius et al., 1964).

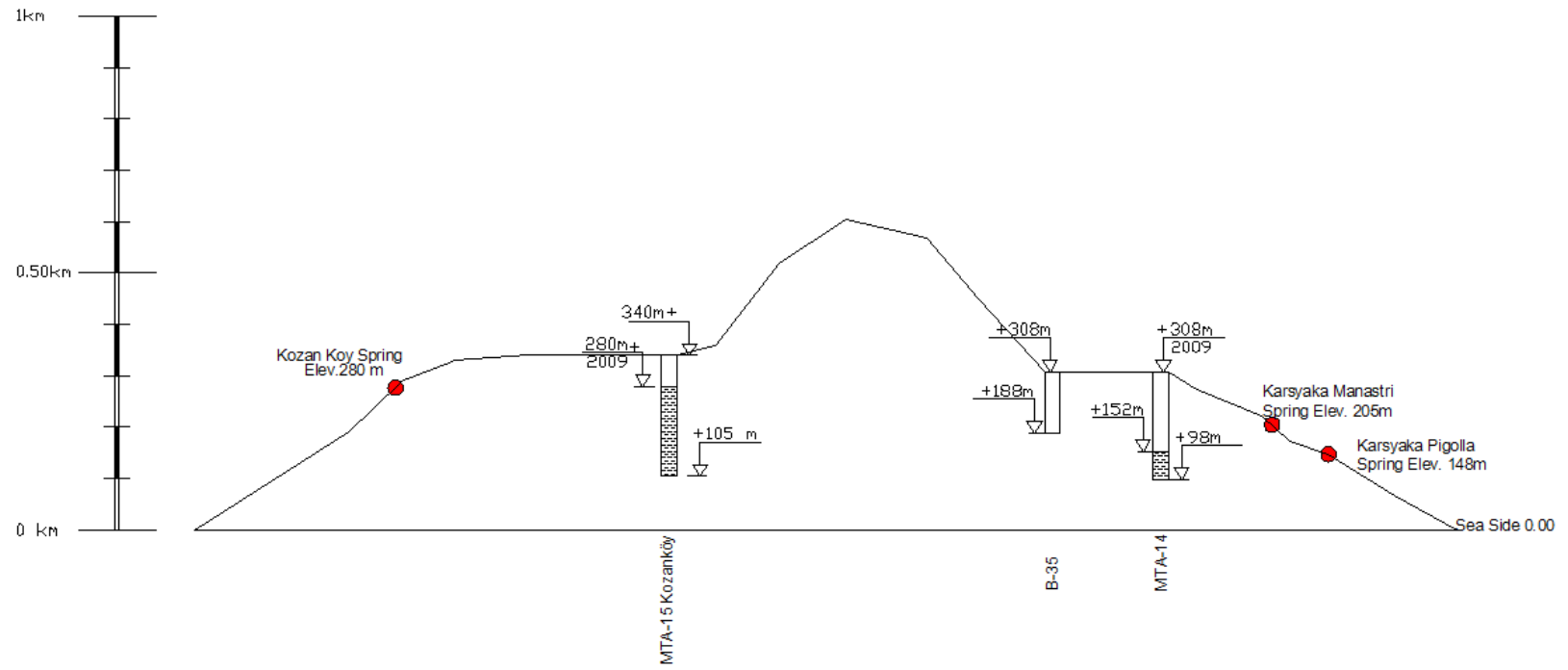


Figure 3.2 Wells depth details and spring elevations at Karşıyaka Region.

The water level had a steep rise of 3 meters in 1966-67 seasons. There was a change in general trend after 1969. The water level in B-35 dropped suddenly to 6.5 m in April 1970, presumably because of the commencement of heavy pumping rate. According to the reports of German Technical Assistant in 1964, the borehole B-35 has been drilled in light-grey calcareous limestone of the Lapithos Formation up to a depth of 30 m. After that, a 25 m fault zone with intensive tectonic mashing of black-grey Hilarion dolomites and brown-grey clay marls mass crossed. Steady drilling progress and all other typical characteristics of drilling in very hard rocks indicate that B-35 remains in karst marble of the Hilarion Formation till down to the final depth (Mixius et al., 1964). The permanent high pumping rates dried up the well later in 1998, during the drilling processes of MTA-14. The authorities then replaced B-35 with MTA-14 which was 90 m deeper than B-35.

The yield of MTA-14 was 52 m³/hr in April 2008. The total drawdown on MTA-14 well is observed to be 72 meters within the last 7 years.

General Directorate of Mineral Research and Exploration of Turkey has drilled MTA-15 in 1998. MTA-15 is located at Southern part of Kyrenia Range closed to Kozan village. The well supplies domestic water requirements of the village. The dynamic water level (dwl) in MTA-15 is 280 meters, which is 152 meters in MTA -14. The head difference between MTA-14 and MTA-15 is 128 meters. This is a good indication that the two wells are not connected to each other. In 2005, water supply project to Şirinevler was completed and 175 m³/day is supplied from MTA-15 to Şirinevler village. Therefore, the pumping rate of the well MTA-15 was increased from 8 m³/day to 18 m³/day. This was the main reason of sudden drop on dynamic water level (dwl) of MTA-15 as shown in Figure 3.4.

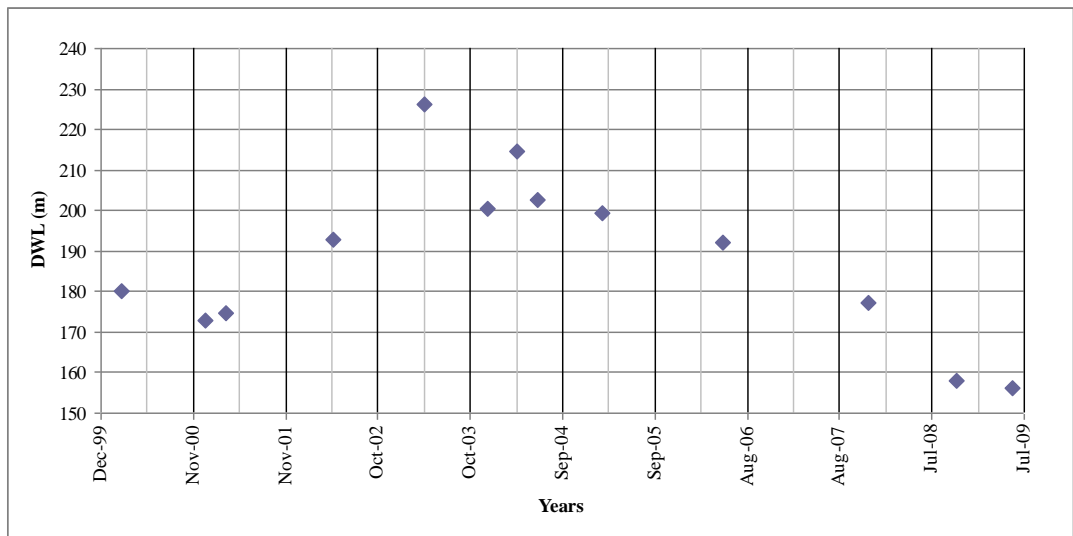


Figure 3.3 Drawdown of dynamic water level of MTA-14.

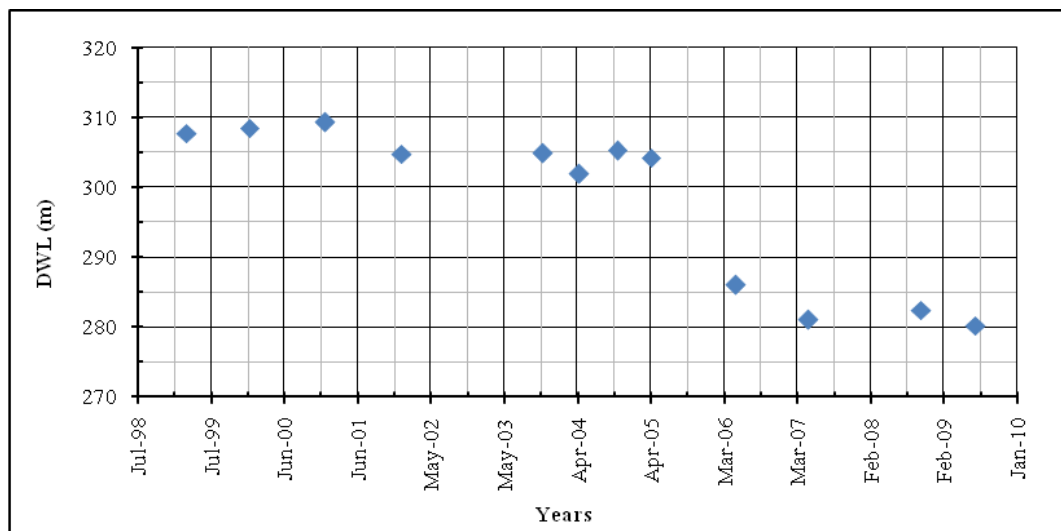


Figure 3.4 Drawdown of dynamic water level of MTA-15.

At Karşıyaka region there were two springs which were once flowing but lately dried. These springs are Karşıyaka Pigaoulla and Karşıyaka Manastır springs. The surface elevations of springs were 148 and 205 meters from mean sea level, respectively. The spring monitoring in 1966-1969 periods resulted in peak discharge of Karşıyaka Pigaoulla spring as 320 m³/day (DSI, 1982). The karstic formation of the region prevents the head connection between the wells and the springs. MTA-14 well is at 1 km south to both of the springs. The dynamic water level at the well is 152

meters which is higher than Piagoulla spring but lower than Manastır spring. Thus, even there were no possibilities to have a flow in Manastır well; at least small amount of discharge was exists in Pigaoulla spring due to the flow gradient of 2.6 % from MTA-14 to Pigaoulla spring. Kozanköy Spring is located at the southern part of Kyrenia Range, opposite of Karşıyaka village. The spring has been used since 1967 and discharging 225 m³/day on an average. Nowadays, the spring is discharging with small difference from the previous years. Together with the workers of Water Works Department, the author performed a site visit to the spring (on 10th of June 2009), and the discharge of spring was measured as 235 m³/day. The discharges of the springs within the region are given in the Figures 3.5, 3.6 and 3.7. The monitoring of the spring flows was held under primitive methods, in which a bucket of 10 liters were let to be fill by the discharging spring. The timer was used to estimate the time pass until the bucket fills with water. By this way the discharge of the spring was evaluated.

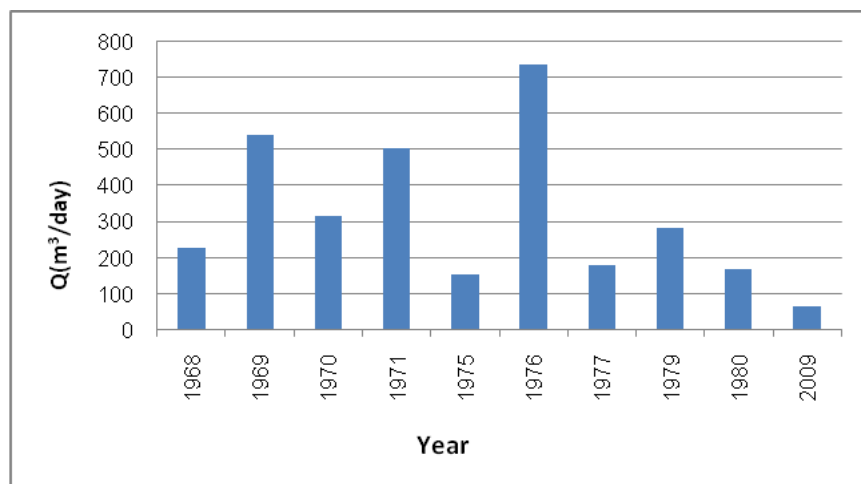


Figure 3.5 Average daily discharge of different years for Karşıyaka Pigaoulla Spring based on month June 2009.

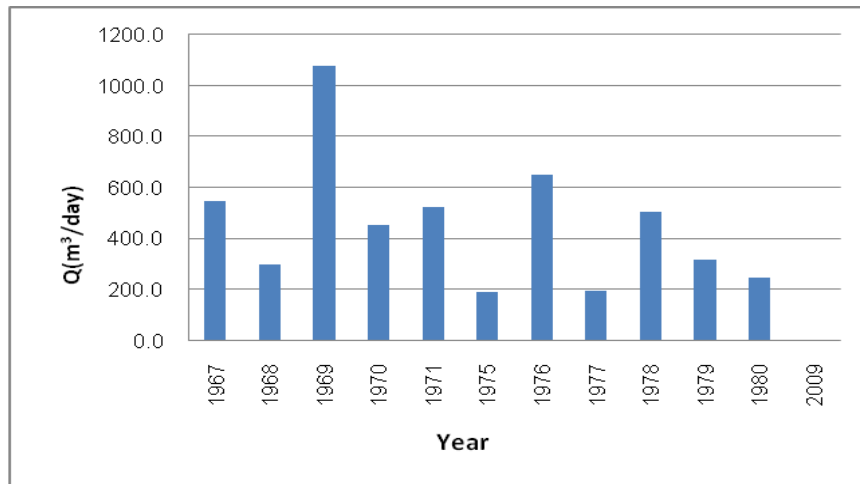


Figure 3.6 Average daily discharge of different years for Karşıyaka Manastri Spring based on month June 2009.

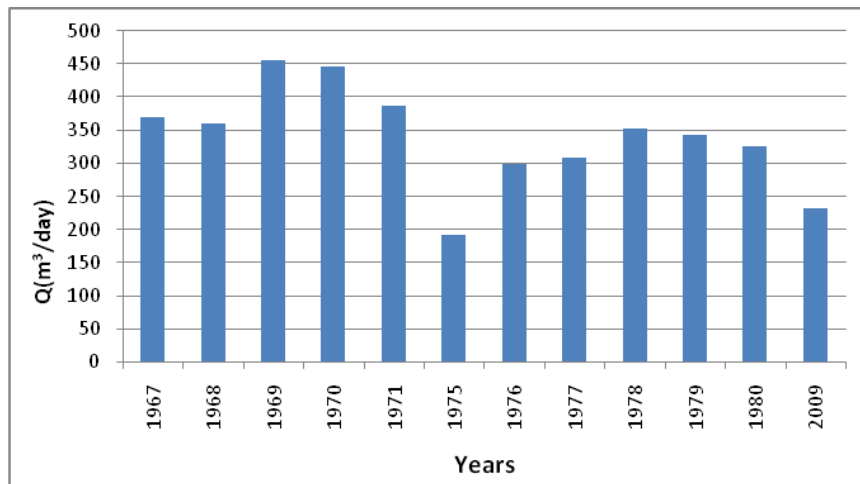


Figure 3.7 Average daily discharges of different years for Kozanköy spring based on month June 2009.

The pictures taken during the site visit to Karşıyaka and Kozanköy areas are given in the Figures 3.8 and 3.9.



Figure 3.8 Karşıyaka Pigaoulla Spring



Figure 3.9 Kozanköy Spring

3.2 Lapta (Lapithos) Region

Lapta Başpınarı (Lapithos), Lapta Dragondas, Lapta Hajietilli and Lapta Katouries springs are the four main springs available at Lapta region. Also, there are five main boreholes in which three of them are drilled, operated and monitored by the General Directorate of Mineral Research & Exploration of Turkey, namely MTA-8, MTA-12 and MTA-9. The other two wells are 9/74 and 53/68. Areal photograph of the area and the cross-section of the region lined on one section are given in the Figures 3.10 and 3.11.



Figure 3.10 Areal picture showing the locations of boreholes (from top view) at Lapta Region (scale, 1:33,750).

The MTA-8 well has been operated since 1995 and lately, abandoned due to extreme drawdown of dynamic water level. The latest discharge measurement from this well has been monitored as 4 m³/hr which is 34,560 m³/year.

The dynamic water level observations regarding to the short drawdown period of MTA-8 is given in Figure 3.12. Since the yield of MTA-8 was limited, the domestic water supply of Lapta village was supplied from MTA-12, which is 32 m³/h. This well was constructed in 1998 during the groundwater investigations of MTA. The dynamic water levels of MTA-8 and MTA-12 was almost same during the years 1999 to 2003. Dynamic water levels of MTA-8 and MTA-12 wells are shown in Figures 3.12 and 3.13.

The well MTA-9 is located at the southern foothills of Kyrenia Range, close to Şirinevler. This well is used for irrigation purposes.

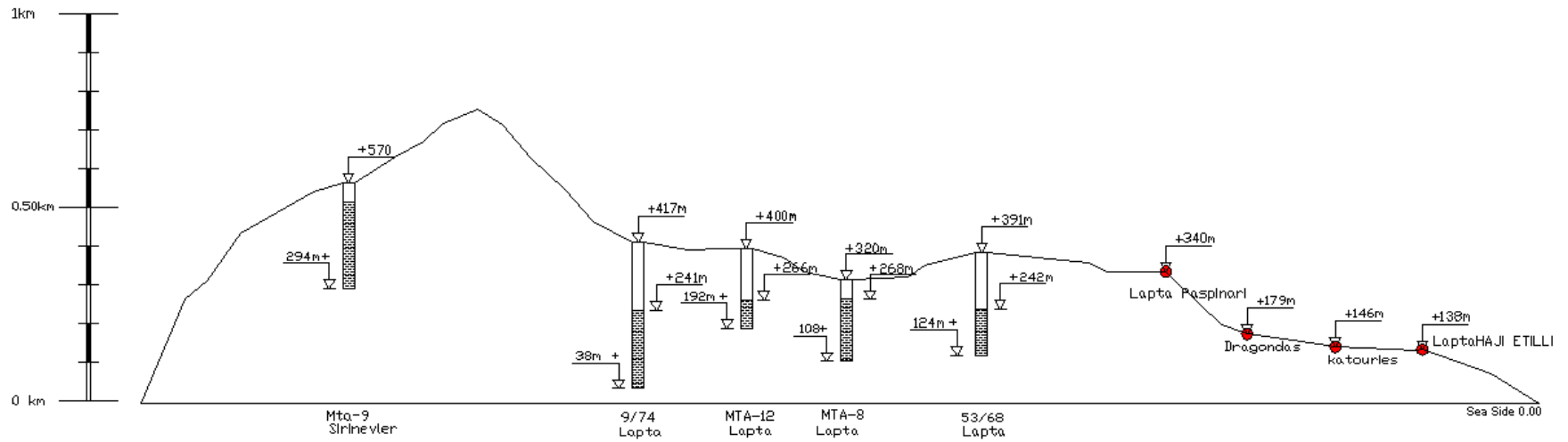


Figure 3.11 Wells depth details and springs elevations of Lapta region.

The water level in MTA-9 is around 255 m from mean sea level, which is approximately same as the Lapta Region wells. This can be a good indication of relationship between the aquifers of Şirinevler and Lapta region.

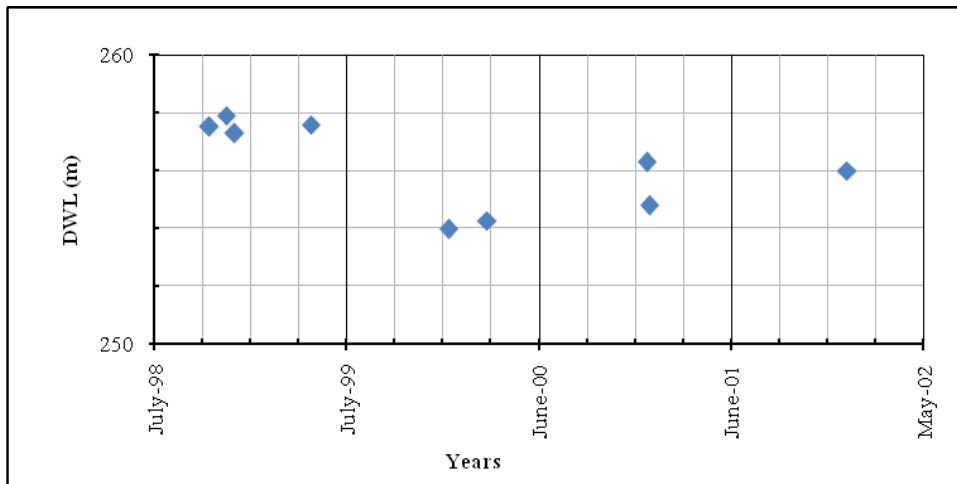


Figure 3.12 Drawdown of dynamic water level of MTA-8 during years (1998-2002).

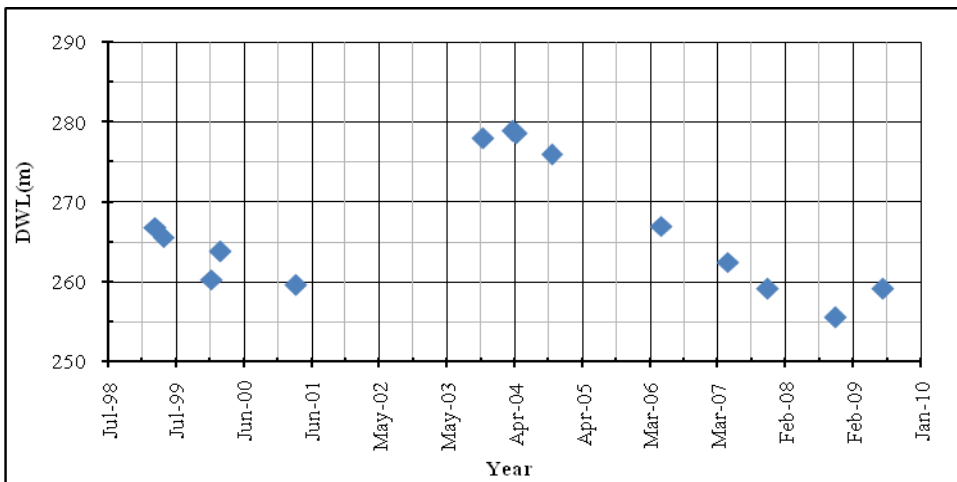


Figure 3.13 Drawdown of dynamic water level of MTA-12 during years (1998-2010).

The springs of Lapta region were supplying considerable amount of water between 1960 to 1980's, flowing throughout the year, an average of $1.7 \times 10^6 \text{ m}^3$ per year. By the beginning of 1960's, the stakeholders of the region have decided to open wells at the region. The aim was to control the discharge of the aquifer by pumping considerable amount of water during winter so as to prevent the loss of water from the springs during winters. For this purpose, the Geology and Mines Department of

Cyprus has drilled the borehole 53/68 in 1968 and the borehole 9/74 in 1974. The borehole 53/68 has been drilled 1 km. southeast of Lapta Başıpınar Spring and was started in operation with a pumping rate of 52 m³/hr. The pumping rate of 53/68 decreased to half by 2002 discharging 28 m³/h; pumping from 53/68 was not a successful trial to decrease the yield of Lapta Başıpınar Spring, which means that the well did not manage to create appreciable effect on Lapta Başıpınar spring. It was clear that extra boreholes would be required with same discharges around Lapta Başıpınar spring so as to control the discharge of this spring. The control of the boreholes would need to be within one or two kilometers around the spring, so that the effect of the pumping could readily be observed due to multiple effects of drawdown. On this purpose, the second borehole 9/74 has been drilled under the supervision of hydro-geologist Frank Dixey, in 1974. However, the operation of this well has been started around 5 years later in 1980, supplying water to Lapta village. The well 9/74, on purpose, was constructed at western part of the Lapta Başıpınar spring. As soon as 9/74 started to operate, the flow rates of Lapta Başıpınarı spring has start to decline Figure 3.14. This was a good indication of the groundwater flow direction at the region proving that the water is moving from western elevations to northeastern foothills.

However, the theory and the theory based future plans of this spring did not match with the realities of the nature. As the years passed, the discharge rate of the spring has declined. The following drought seasons and over pumping from borehole 9/74 has further declined the flow rates of this spring. The inevitable end of the spring has approached by the beginning of 1990's. The flow rate of spring was monitored as "null" by the beginning of summer 1990. The "null" position has been observed for the next 10 years in which strong precipitation in late 2000 has initiated the flow of spring for some years. However, the permanent over pumping from well 9/74 has again dried out the Lapta Başıpınar spring. Nowadays, the 9/74 well is the only water resource that discharging 35 m³/hr and is supplying water to Alsancak Village. Unfortunately, the spring of Alsancak has dried some few years ago Figure3.14.

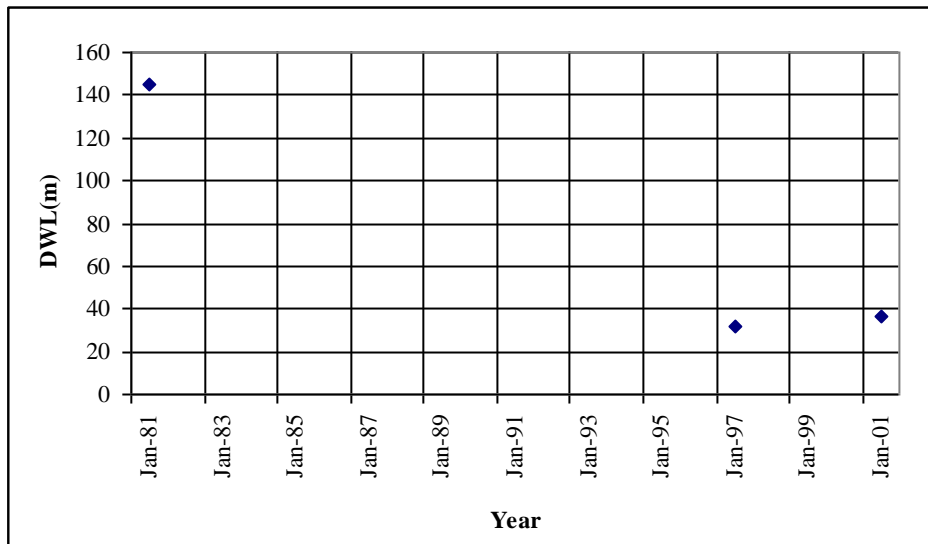


Figure 3.14 Drawdown of dynamic water level of 9/74 during years (1981-2001).

The remaining three springs were Lapta Dragondas, Lapta Hajietilli and Lapta Katouries springs. These springs are still discharging since they are far below the static water level. As it is seen in the Figures 3.15, 3.16 and 3.17 these springs that are around 145 meters above mean sea level are discharging at average rate of 172, 3, and 15 cubic meters per day based on month June respectively. Figures 3.18a. and 3.18b. pictures of these springs in 2009. The discharge values of all the springs are the monthly flow rates for the month June.

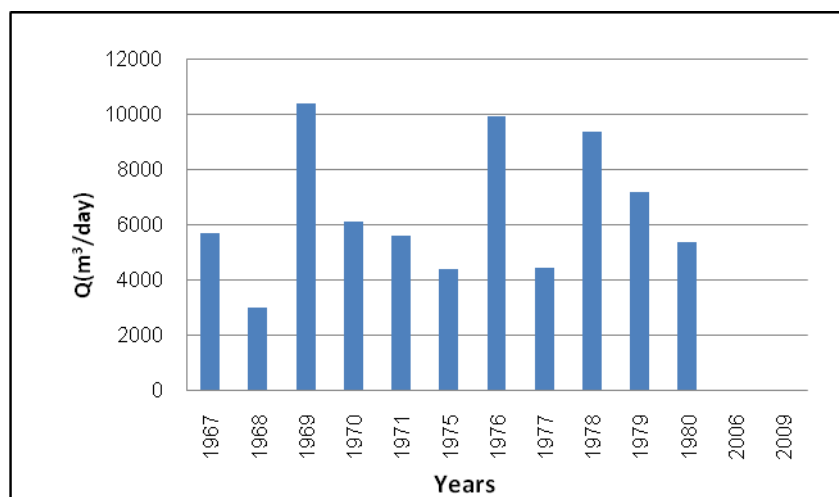


Figure 3.15 Average daily discharges at different years for Lapta Başpınar Spring in Lapta based on month June.

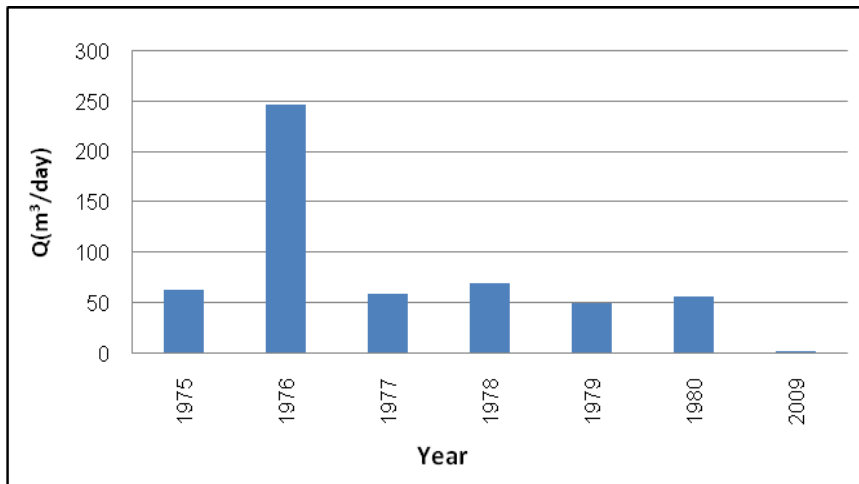


Figure 3.16 Average daily discharges at different years for Şht.Ahmet Kamil Sk.Alt Haji Etilli Spring in Lapta based on month June 2009.

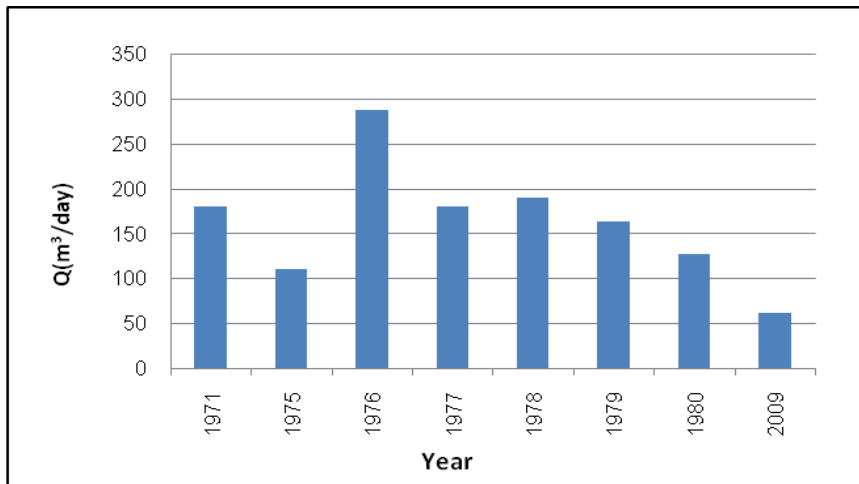


Figure 3.17 Average daily discharges at different years for Katouries Şht.Ahmet Kamil Sk.Üst Spring in Lapta based on month June 2009.

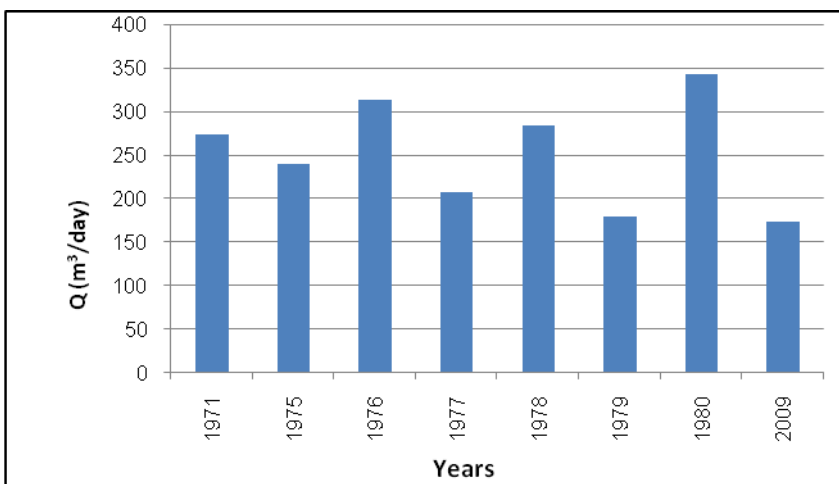


Figure 3.18 Average daily discharges at different years for Dragondas Lapta Spring based on month June 2009.



Figure 3.18a. Katouries (Şht.Ahmet Kamil Sk.) Spring in Lapta.



Figure 3.18b. Dragonas Spring in Lapta

3.3 Alsancak Region

There are five springs and three wells at the considered area. Three of these springs are still flowing. The aerial photo of the area and the cross-section of the region lined on one section are given in the Figures 3.19. and 3.20. The springs, which are still flowing are, Malatya Village Spring (Malatya Köy Pınarı), Ilgaz Lower Spring (Ilgaz Alt Pınarı) and Malatya Upper Spring (Malatya Ust Pınarı).

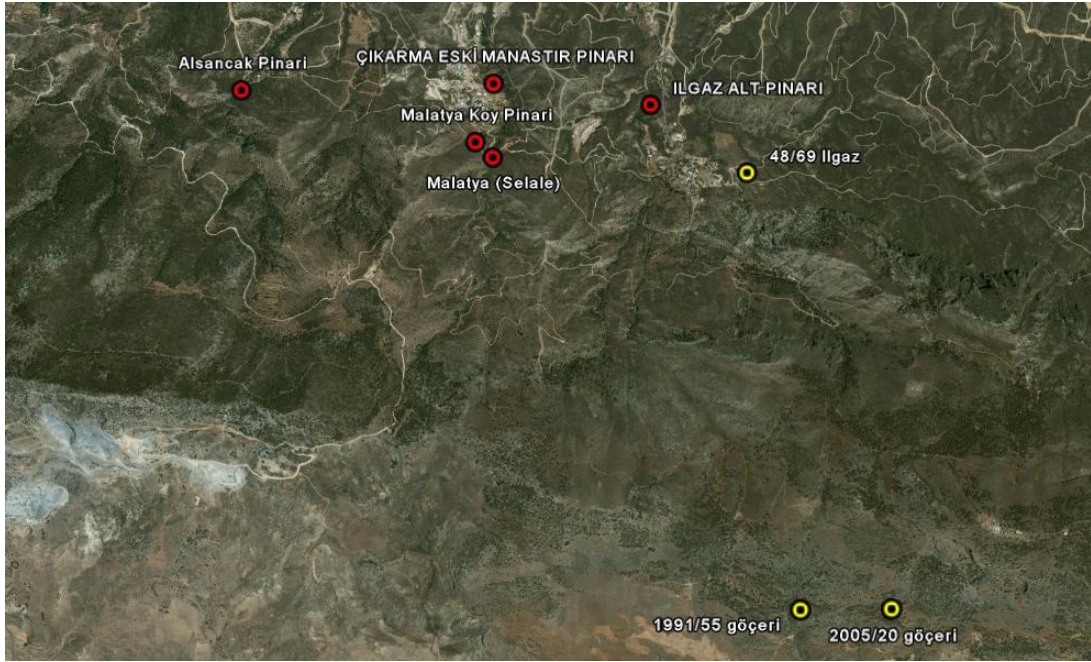


Figure 3.19 Areal picture showing the locations of boreholes (from top view) at Alsancak village Region (scale 1:45,000).

The average flow rates of these springs are 14 m³/day and 72 m³/day respectively. The third spring, (Malatya Upper Spring (Malatya Ust Pınar)) is flowing but its flow rate could not be measured during the site visit since the gate and the valve of the spring were locked. Comparing the elevation of Malatya Upper spring with the elevation of Malatya Köy Pınarı which is 240.79 m and Malatya Ust Pınar which is 233.47 m, it is expected that the flow rate should be almost the same with an around 14 m³/day.

The other two springs are Çıkarma Eski Manastır Spring and Alsancak Spring with elevation 175 m and 215 m, respectively. They are located at northern foothills of Kyrenia Range, away from Malatya Spring 500 m and 1500 m, respectively. The latest measurement recorded on Çıkarma Eski Manastır spring was 0.9 m³/day monitored at 20 February 2006 by Water Works Department. The site visit on this spring was held in June 2009 and the spring was not discharging any more. The yearly discharges of the springs and their pictures in 2009 are given in the Figures (3.21a, 3.21b, 3.22a, 3.22b, 3.23a and 3.23b).

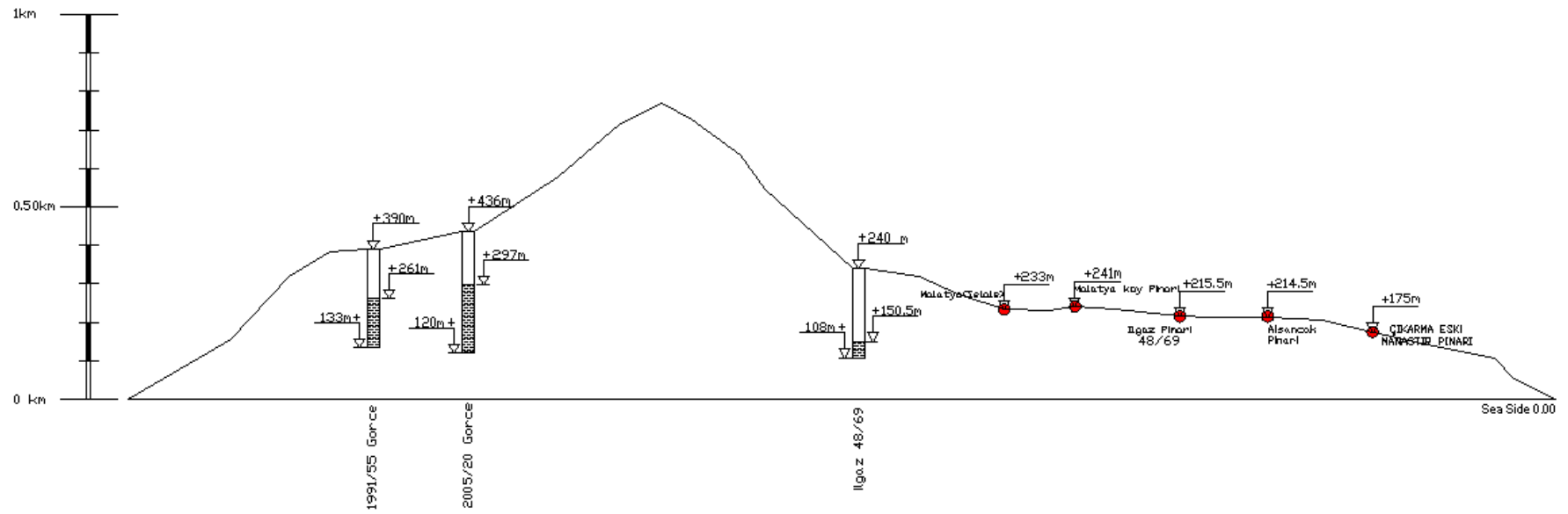


Figure 3.20 Wells depth details and springs elevations at Alsancak Region.

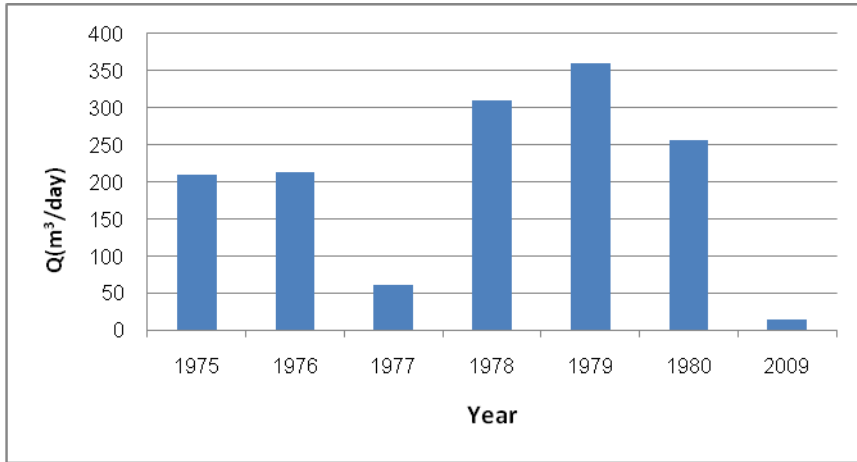


Figure 3.21a Average daily discharges at different years for Malatya Köy Spring based on month June 2009.



Figure 3.21b Malatya Köy Spring.

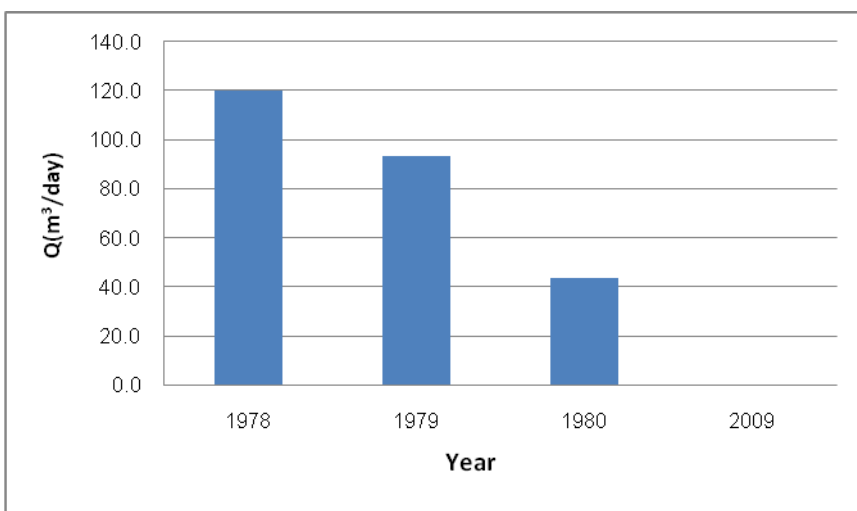


Figure 3.22a Average daily discharges at different years for Çıkarma Eski Manastır Spring based on month June 2009.



Figure 3.22b The picture of Çıkarma Eski Manastır spring Karaolanoğlu.

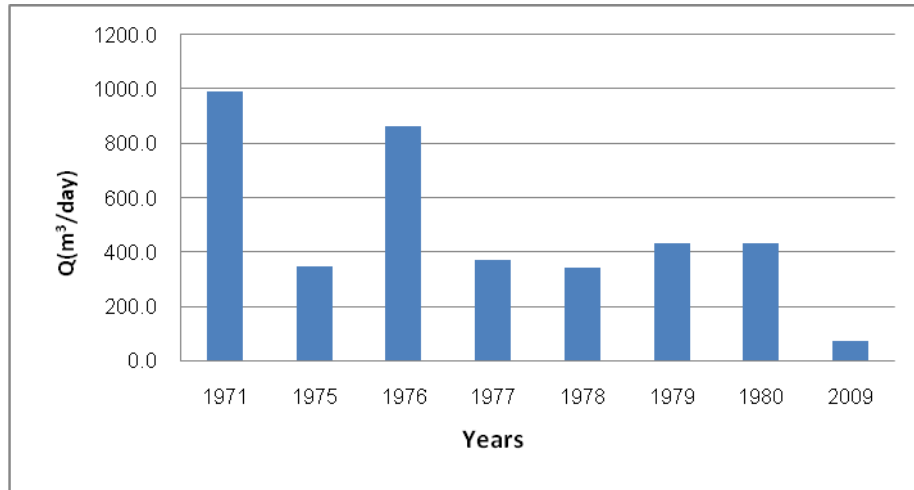


Figure 3.23a Average daily discharges at different years for Ilgaz Lower Spring based on month June 2009.



Figure 3.23b Ilgaz lower Spring (Fetrikha) Ilgaz.

There exists one monitoring well at the Alsancak Region. The well has been drilled at 1969, and has been used since 1972 (Dixey, 1975). The well is called Ilgaz (Fetrikha) 48/69 well. The well is supplying potable water to Ilgaz village, it is observed that the dynamic water level fluctuations at Ilgaz 48/69 are random and the replenishment of the well is independent of the surrounding springs. The discharge of the well is 3-4 m³/hr. Therefore, according to Dixey 1972, at Ilgaz 48/69 well, the flow characteristics are varied which allow unsteady flow conditions within the aquifer. The unsteady flow is due to the isolated block of limestone in which Ilgaz 48/69 is located, separated from the main outcrop by a band of Lapithos formation of about 500 m wide.

Figure 3.24. details the drawdown of dynamic water level of well 48/69.

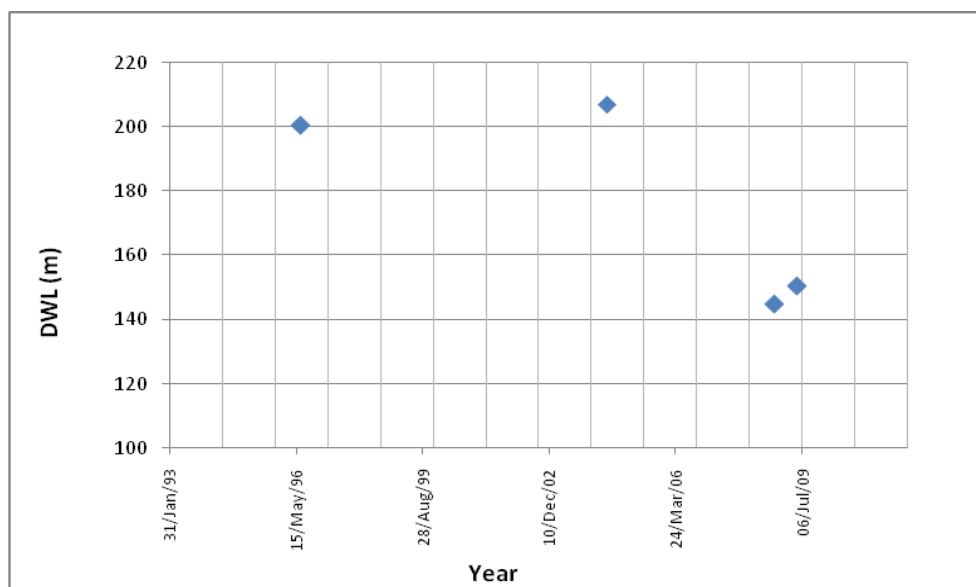


Figure 3.24 Drawdown of dynamic water level of well 48/69 in different years.

At the southern foothills of Kyrenia Range there are two wells. The well named 1991/55 drilled in 1991 to supply water demand for Göçeri village. The dynamic water level was 261 m above sea level. The pumping rate of 1991/55 was recorded as 60 m³/hr at 2002. Figure 3.25. details the drawdown of dynamic water level of well 1991/55. The 2005/20 well drilled in 2005 by Water Works Department (WWD) supplying water to Lefkoşa with dynamic water level of 297 m.

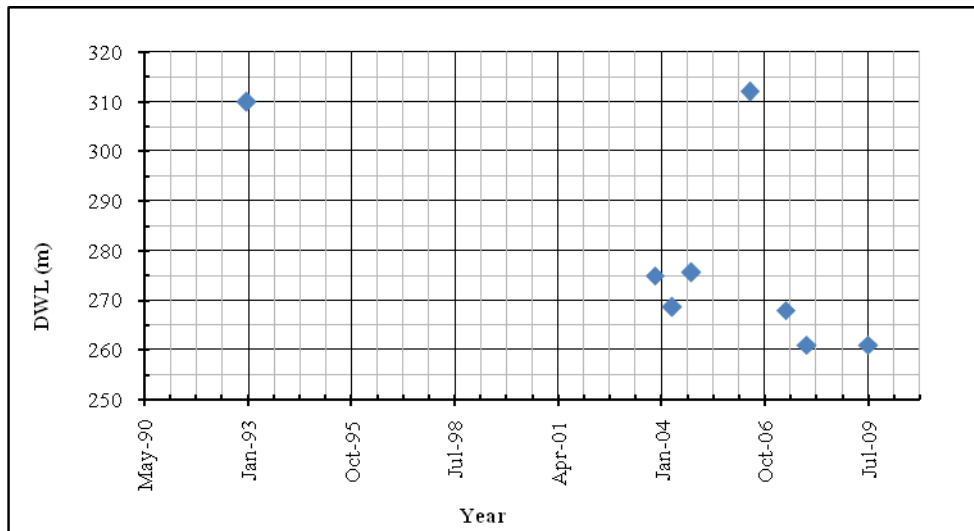


Figure 3.25 Drawdown of dynamic water level of well 1991/55 in different years.

3.4 Karaman (Karmi) Region

In Karaman region there are two groups of wells, in one of the group there are six wells that are located at the northern side of the foothills whereas in the other group there are two wells that are located at the southern foothills of mountains. The wells that are located at the northern foothills of mountains are Karaman Ilgaz (43/34), Karaman 26-A and 26-B, 2004/08, MTA-11 and 2006/17. All these wells were used for domestic water supply purposes for Kyrenia region. On the other hand, the two southern wells are 63/54 and MTA-1 is in use for the domestic water needs of Boğazköy and Gönyeli urban areas. The locations and cross-sectional positions of these wells are given in Figures 3.26 and 3.27.

The yield of Karaman Ilgaz 43/34 well is around 3 m³/day, in which the dynamic water level was observed to be 218 m from mean sea level. This well is supplying domestic water for Karaman village. The other two wells which are also located at Karaman village are 26-A and 26-B. The well 26-A was drilled before 1974 up to a depth of 25 meters. The karst limestone at the region is extended

from Lapithos Formation possessing thick limestone bands and topograph forms a good drainage at that site.

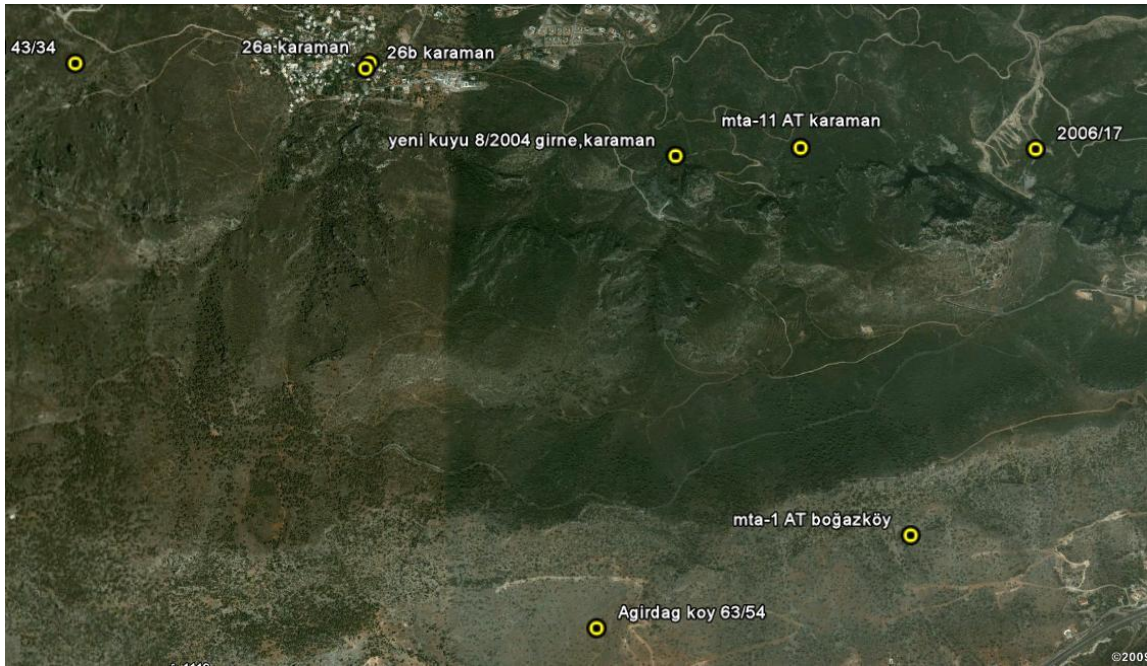


Figure 3.26 Areal picture showing the locations of boreholes (from top view) in Karaman and Boğaz village Regions (scale 1:26,000).

These properties allow deeper drilling opportunities, which can be as deep as 188 meters. At such depths, the yield of borehole is 18 m³/hr. The well 26-B drilled after 26-A, a few meters away. The depth of 26-B was 125 m, with a yield of 20 m³/day. The head difference between the two wells is around 10 meter. This well used for supplying domestic water to Karaman village Figures 3.28 and 3.29 gives the drawdown of dynamic water level of 26-A and 26-B respectively.

The well 2004/08, drilled in 2004 by Girne (Kyrenia) Municipality, and used to supply the domestic water demand of Karaman village and Kyrenia City. The average pumping rate of 2004/08 is 60 m³/hr; this is considerably high, comparing with the other wells at the region. The well was drilled at a depth of 273.5 meters and the dynamic water level at the well was 229 meter.

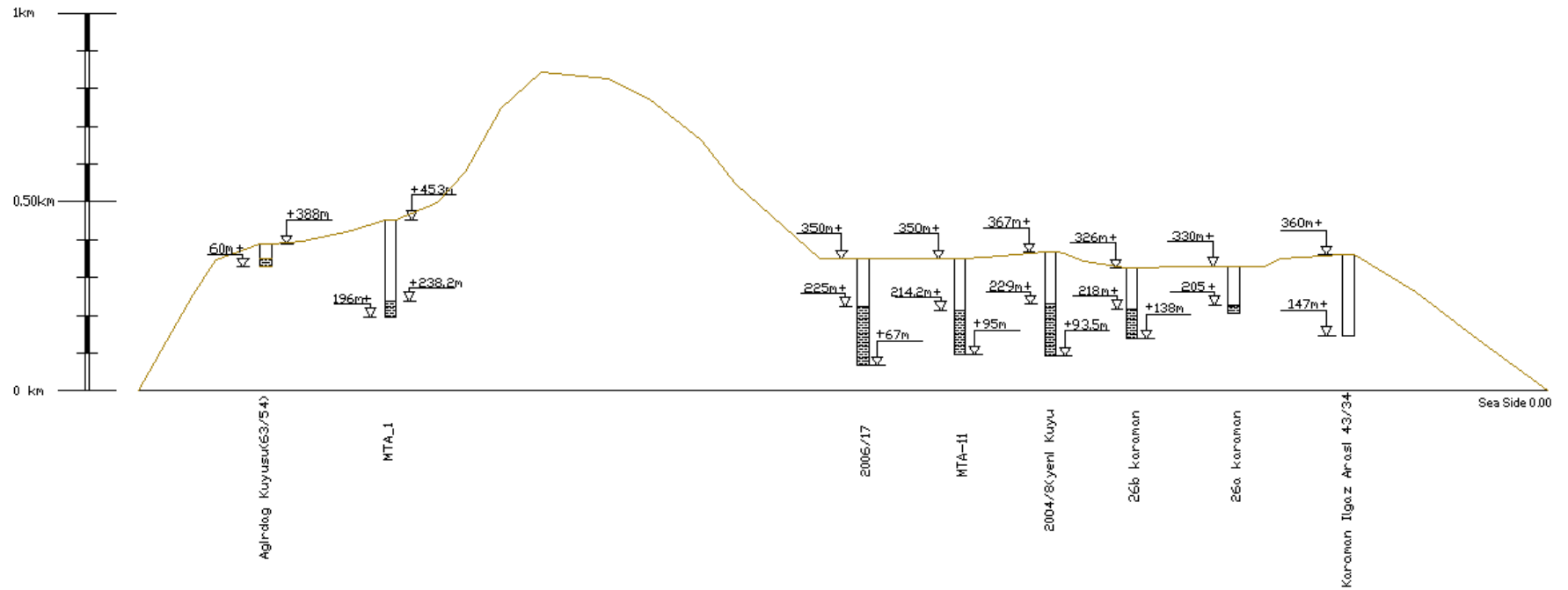


Figure 3.27 Wells depth details and springs elevations at Karaman and Boğaz village regions.

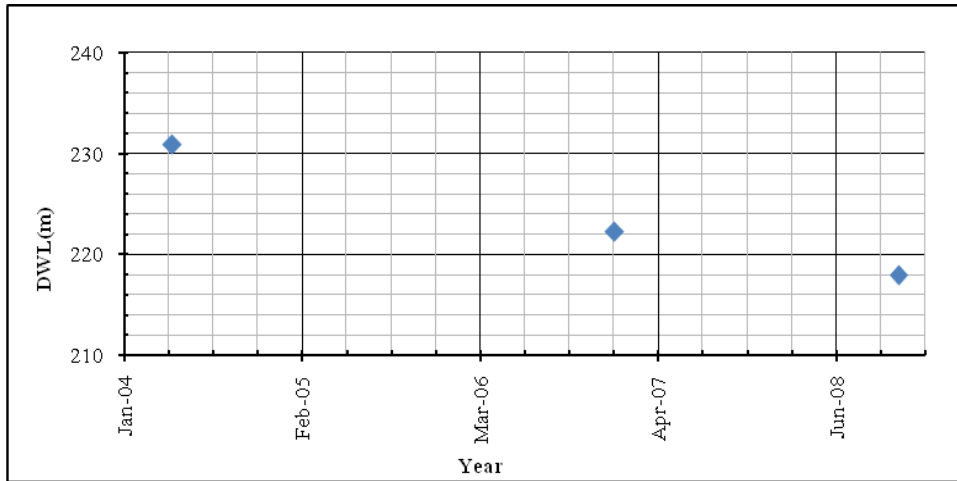


Figure 3.28 Drawdown in dynamic water level of well 26-A in different years.

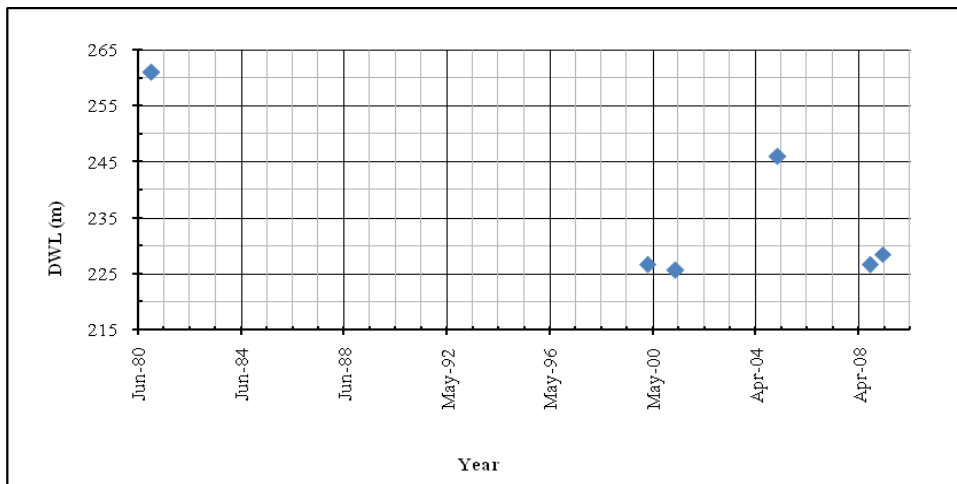


Figure 3.29 Drawdown in dynamic water level of well 26-B in different years.

The well MTA-11, drilled in 1998, dynamic water level at 214.2 meters with a average pumping rate of 36 m³/day. The well supplies domestic water for Girne city. The monitored dynamic water level with respect to years of MTA-11 is given in Figure 3.30.

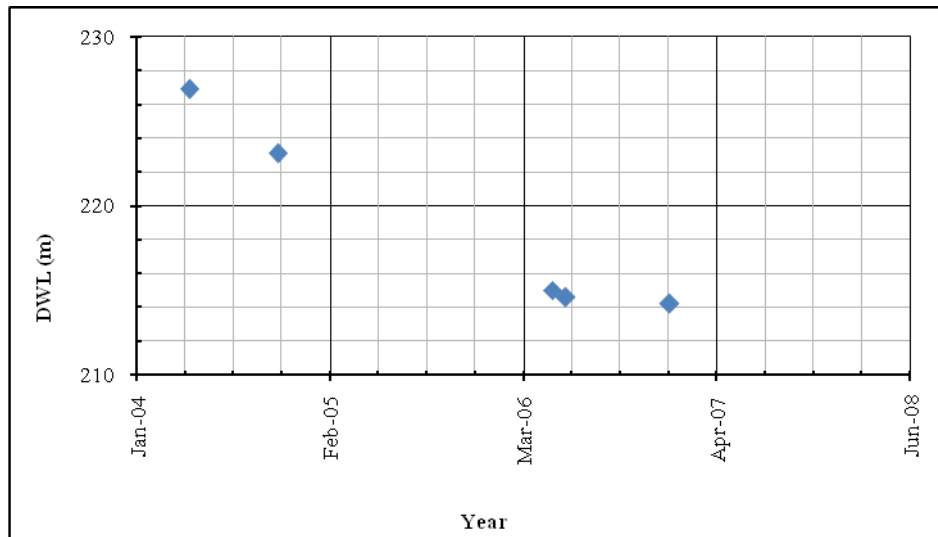


Figure 3.30 Drawdown in dynamic water level of well MTA-11 in different years.

The well 2006/17, known as well St. Hillarion in Kyrenia is located at Zeytinlik village, at the east of Karaman village. The well was drilled in 2006 by Geology and Mining Department (GMD) and Kyrenia Municipality. The pumping rate of the well is about 62 m³/day, supplying water demand of Kyrenia city. The depth of the well is 283 meters. The exact water level of the well did not ever been measured since there is no measurement possibility within the well. However, from the cross section, the water level can be obtained from the general water level from surrounding wells and boreholes; so the water level for well 2006/17 is supposed to be 225 meters.

At the south foothills of Karaman village there are two wells. MTA-1 is located in Boğazköy (Boğaz village); the well was drilled in 1998 by MTA. The yield of MTA-1 is around 27 m³/hr supplying domestic water for Gönyeli. The depth of the well was 257.3 meters with static water level of 238.2 meters above sea level Figure 3.31 details the yearly of well MTA-1. The second well at this region is Ağırdağ village well (63/54). This well was drilled in 1954, and is abandoned for years. There were no springs recorded to flow in this area.

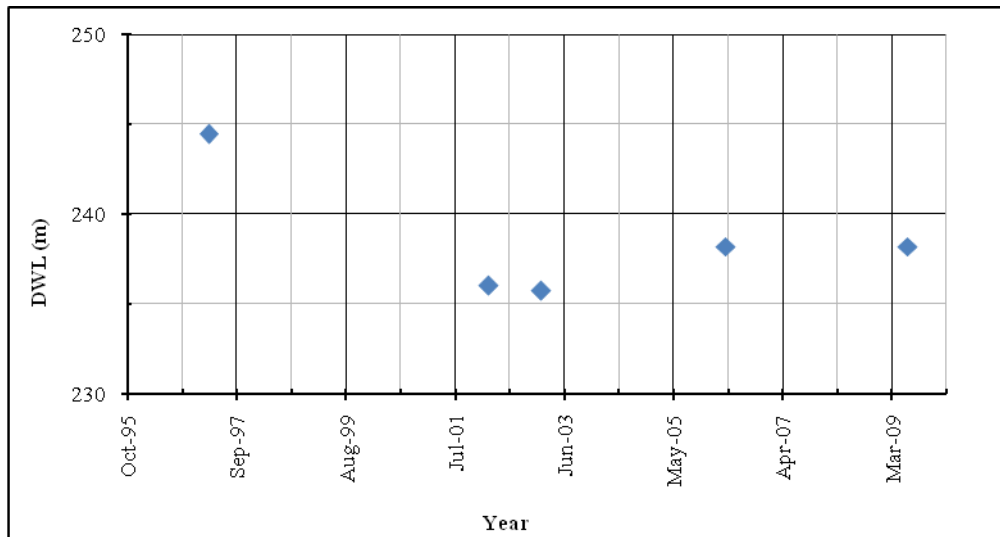


Figure 3.31 Drawdown in dynamic water level of well MTA-1 in different years.

3.5 Dikmen (Dihkomo) Region

Dikmen Region has a group of eight wells, these wells are 173/62, 1/74, 22/74C, 45/79, 36/76, 38/87, 23/46 and 1994/25. The locations and cross-sectional positions of these wells are given in Figures 3.32 and 3.33.

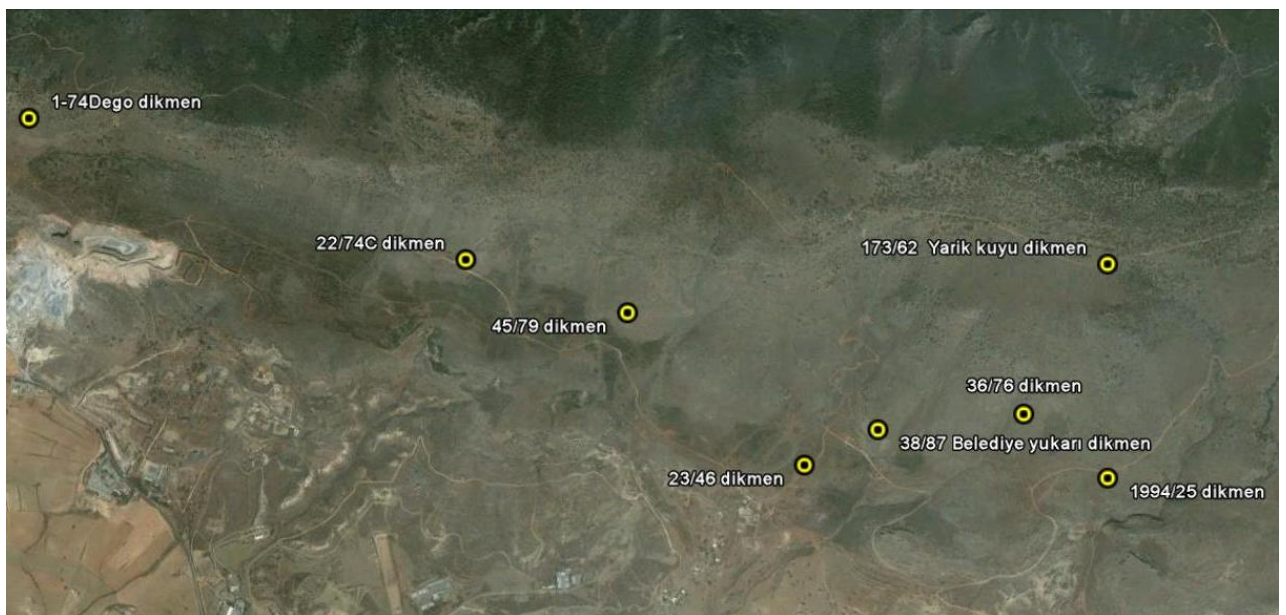


Figure 3.32 The location of borehole from top view in Dikmen Region (scale, 1:30,000).

The well 173/62 is an observation well also known as Dikmen Yarık Well. The well was drilled in 1962 and has been frequently monitored since 2004. As shown in Figure 3.34 the drawdown in the well has reached to around 65 meters within the last 5 years. On the other hand, the literature studies has shown that from 1962 to 1975 which was the first drilling periods of the well, there was no considerable change on the water level elevation within the well. The water level was around 310 m (Dixey, 1975). Also the government archive has shown that in 1981-1982 periods the head in the well was around 320 m. However, after 2004, a rapid drawdown in the head was observed. Such a rapid drawdown can be linked to the operation of DHM1 and DHM2 wells, which are located at the northern face of the Kyrenia range. This is a good indication that the aquifer at northern and southern foothills is connected to each other.

Well 1/74 is also known as Dikmen Dego Well. The well was drilled in 1974. According to long monitoring analysis, it is noticed that the water level in this well has increased from 266 m to 275 m. Therefore, the Dikmen aquifer is believed to occupy large limestone area surrounded by impermeable layer. The pumping rate of the well is 30 m³/hr supporting water demand of Dikmen village.

Well 22/74C is one of the three A, B, and C wells. The well "C" once was supplying water to Lefkoşa (Nicosia) at a pumping rate of 30 m³/hr, A and B wells were stopped pumping so as not to affect the pumping rate of well C since their radius of influences each other.

Well 38/87 is located on the upper site of Dikmen at the south face of mountain foothills. The well is also known as "Belediye Yukari Dikmen well," the water level of Belediye Yukari Dikmen well has dropped 45.5 meters from 1987 to 2009. The well was monitored since 2002 where the yield of the well is 32 m³/hr. Nowadays, the well is out of used due to the lack of continuous uniform discharge from this well. The well 45/79 was drilled in 1979. During the first operation period of the well, the water level was 277 m, by 1994, the water level dropped to 266 m. During the last fifteen years up to 2009, the well is completely dried and it stopped operating after the monitoring in 1994.

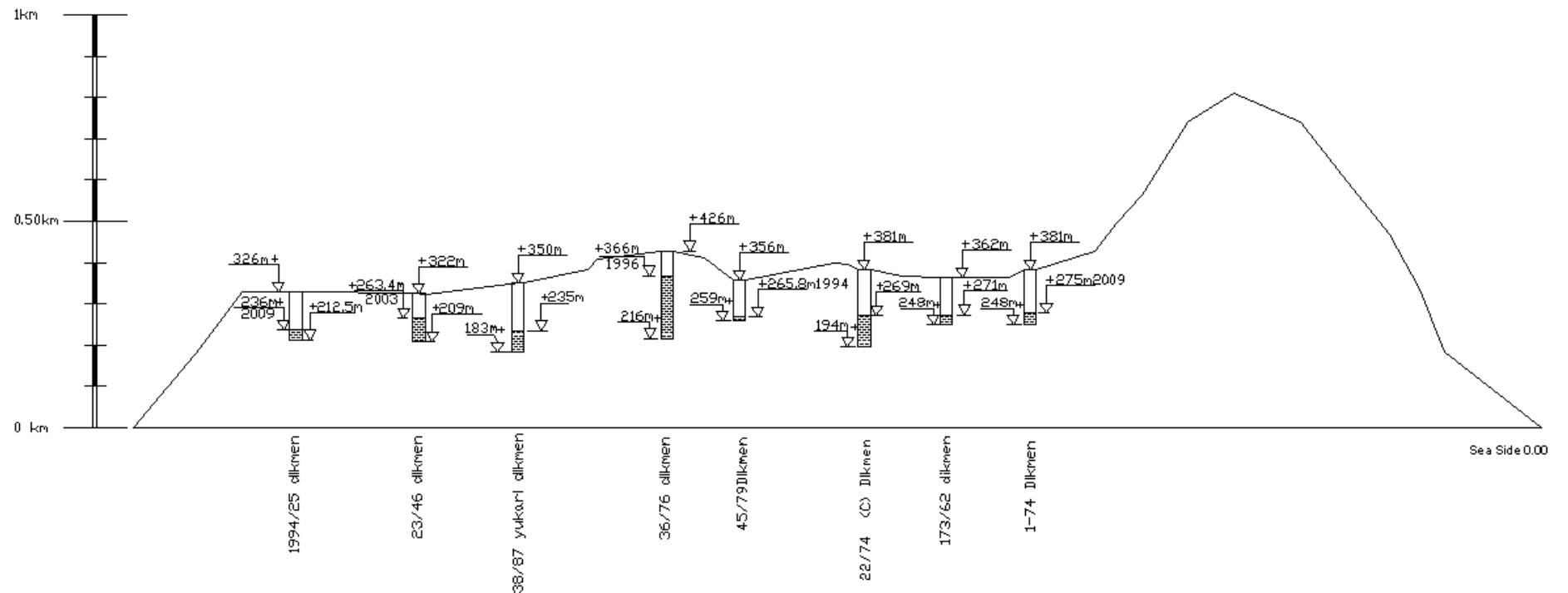


Figure 3.33 Areal picture showing the locations of boreholes (from top view) in 2009 at Dikmen Region.

Well 36/76 and 23/46 drilled in 1976 and 1946 respectively. The wells are not operating since 1996. The main reason is the high pumping rates from the surrounding new wells. Other two wells, 1994/25 and 38/87, are also drilled for domestic water supply purposes but have never worked with high performance due to the same reasons of 36/76 and 23/46. The drawdown graphs of the Dikmen wells are shown in the following Figures 3.34, 3.35, 3.36, 3.37, 3.38 and 3.39.

When the discharges records of the Dikmen borehole 68/62 and of Sihari (Sykhari), late in 1972, recorded, it became evident that the Dikmen aquifer was already being over pumped. Both 68/62 and Sihari were serving Lefkoşa town. The data available for water supply of Dikmen borehole 68/62 during 1963-68 shows that when pumping started at the beginning of 1963, the water level was about 295 m, but following years the water level fell steadily to 271 m. By the year 1966 the water level remained at pump suction or intake level, i.e. 226 m. Meanwhile the yield fell from 15.8 meters to nil position. In 1967 there was a temporary rise in water level 274.8 m with an increased of yield to around 10.4 meters. Thereafter, while slight temporary rises in water level occurred for much or most of the year the water stood at suction level with the yield correspondingly low (Dixey, 1975).

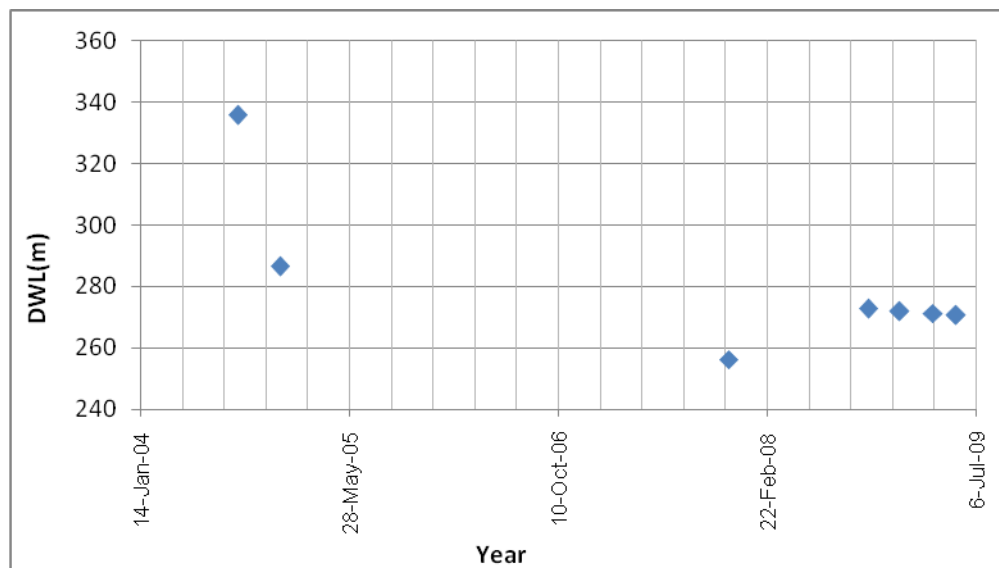


Figure 3.34 Drawdown in dynamic water level in 173/62 in different years.

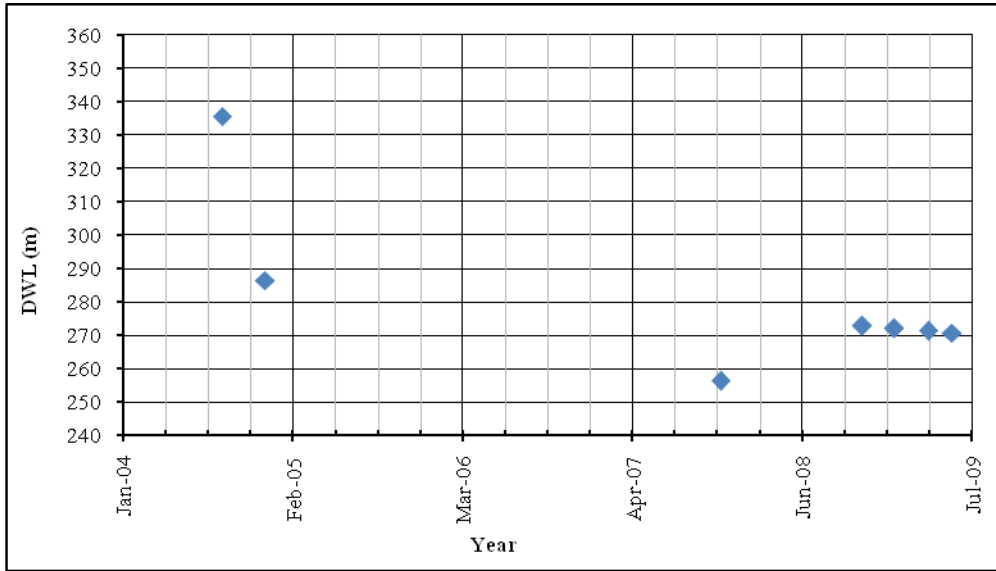


Figure 3.35 Drawdown in dynamic water level of well 1994/25 in different years.

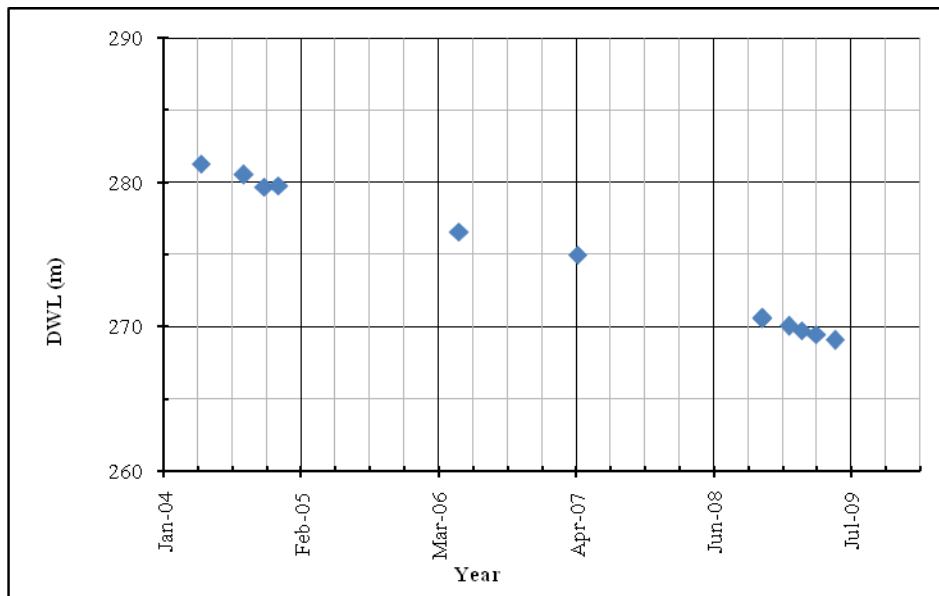


Figure 3.36 Drawdown in dynamic water level of well 22/74 in different years.

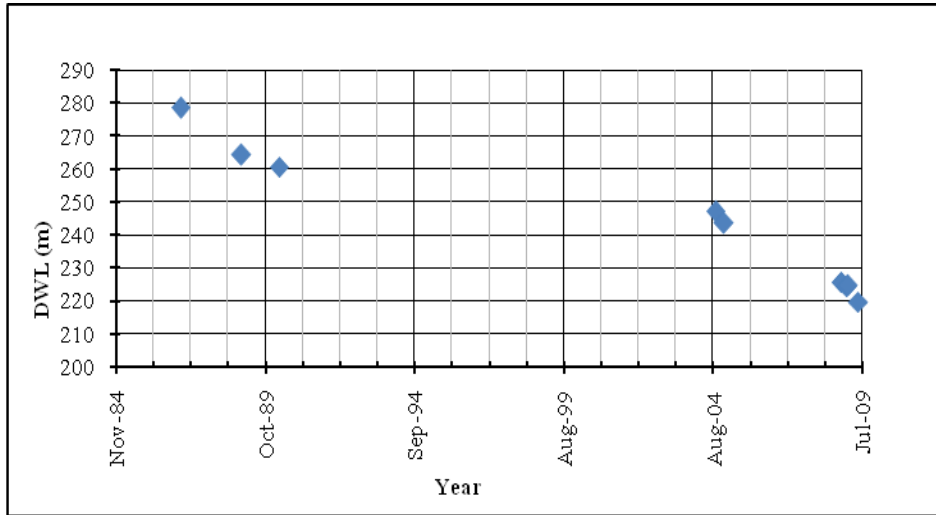


Figure 3.37 Drawdown in dynamic water level of well 38/87 in different years.

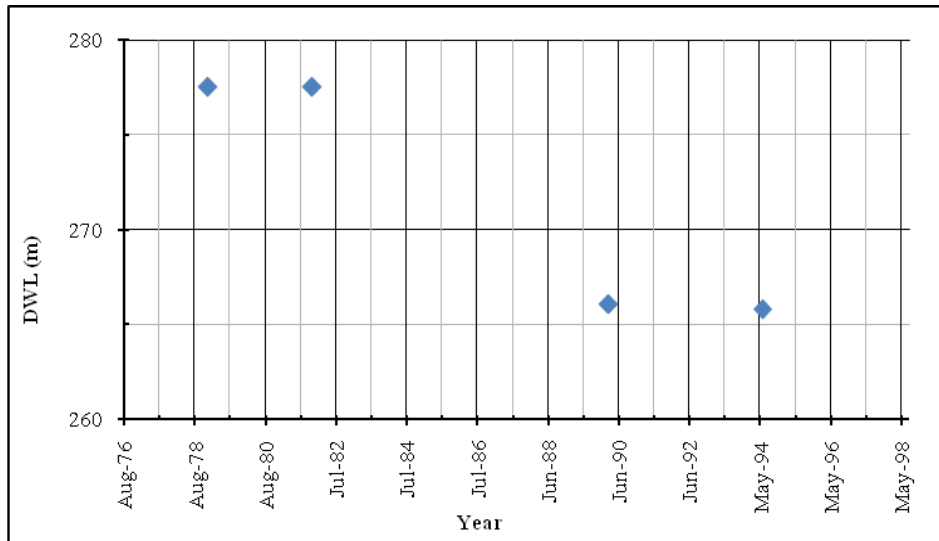


Figure 3.38 Drawdown in dynamic water level of well 45/79 in different years.

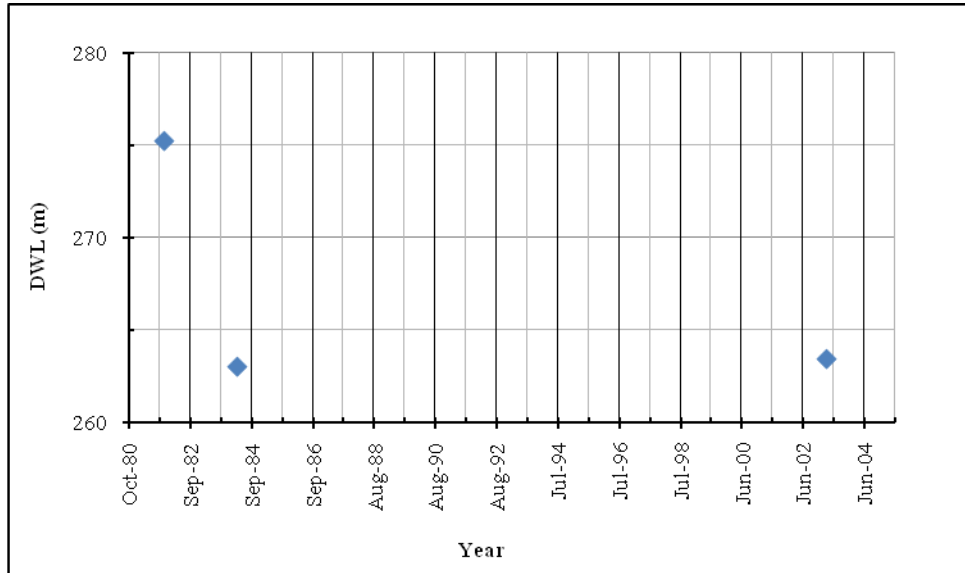


Figure 3.39 Drawdown in dynamic water level of well 23/46 in different years.

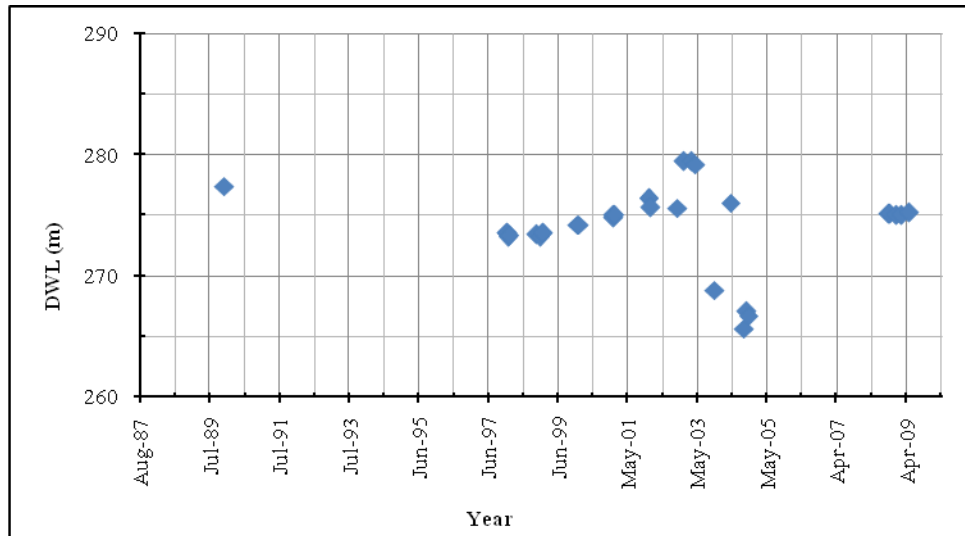


Figure 3.40 Drawdown in dynamic water level of well 1-74 in different years.

3.6 Çatalköy and Beylerbeyi Region

At the center of Kyrenia Range there are two groups of wells located at two different areas; Beylerbeyi (Ballepies) and Çatalköy (Ayios Epiktitos). There is only one spring at the region flowing recently, situated at Ozanköy. This spring is not flowing since December 2001. The locations and cross-sectional positions of wells are given on the Figures 3.41 and 3.42.



Figure 3.41 Areal picture showing the locations of boreholes (from top view) in Çatalköy and Beylerbeyi Region (scale1:40,000).

Among all the wells, only MTA-13 is working at the Beylerbeyi area. The well is pumping at an average rate of 30 m³/hr. The well was drilled in 1998 and the static water level during that time was 183.25 meters above mean sea level. Since 1998, the well is pumping continuously and supplying domestic water for Beylerbeyi Village, the total drawdown on the well since 1998 is around 13.7 meters. The latest drawdown measurement on the well is in November 2008 and has shown that the water level is 169.54 meters above mean sea level.

The well B/20 has been monitored since 1963; it is drilled in Bellapais town, and penetrates Hilarion limestone and Lapithos formation with karstic limestone and lava rocks (Dixey, 1975).

In Beylerbeyi Region the only working well now is MTA-13. It has an elevation of 213m and water table is at 170 m with deeper value comparing with the other two wells B/20 and 14/70. B/20 and 14/70 are not operating now. The depth of these wells is less than the water level at MTA-13. 14/70 was drilled in 1970 and before seven years B/20 existed. Figure 3.47 shows the water level in MTA-13, 55 m less from the depth of the most wells in region and less from all water levels of the other wells. That may explain the reason why operation only one well in this region.

Ozanköy spring is located at 136 m above mean sea level. Although its elevation is far below the elevation of MTA-13, it does not flow since 2001. The distance between the spring and MTA-13 is

2 km, however hydro-geologically they do not have any relationship. There were three wells in Çatalköy, Bademli well (B-30), EB-10, and MTA-4.

Bademli well and the Eđri well, were drilled at 1964. Both of them are supply water demand to Çatalköy, with a pumping rate of 20 m³/hr and 15m³/hr, respectively. The measurements recorded by WWD in 2001, shows that the water level in well EB-10 was 225 meter above mean sea level and in well B-30 263 meters above m.s.l. Both of the wells were drilled in karstified limestone with a productive yielding capacity. For a long period, there were small changes on the dynamic water level of these wells (Dixey, 1972).

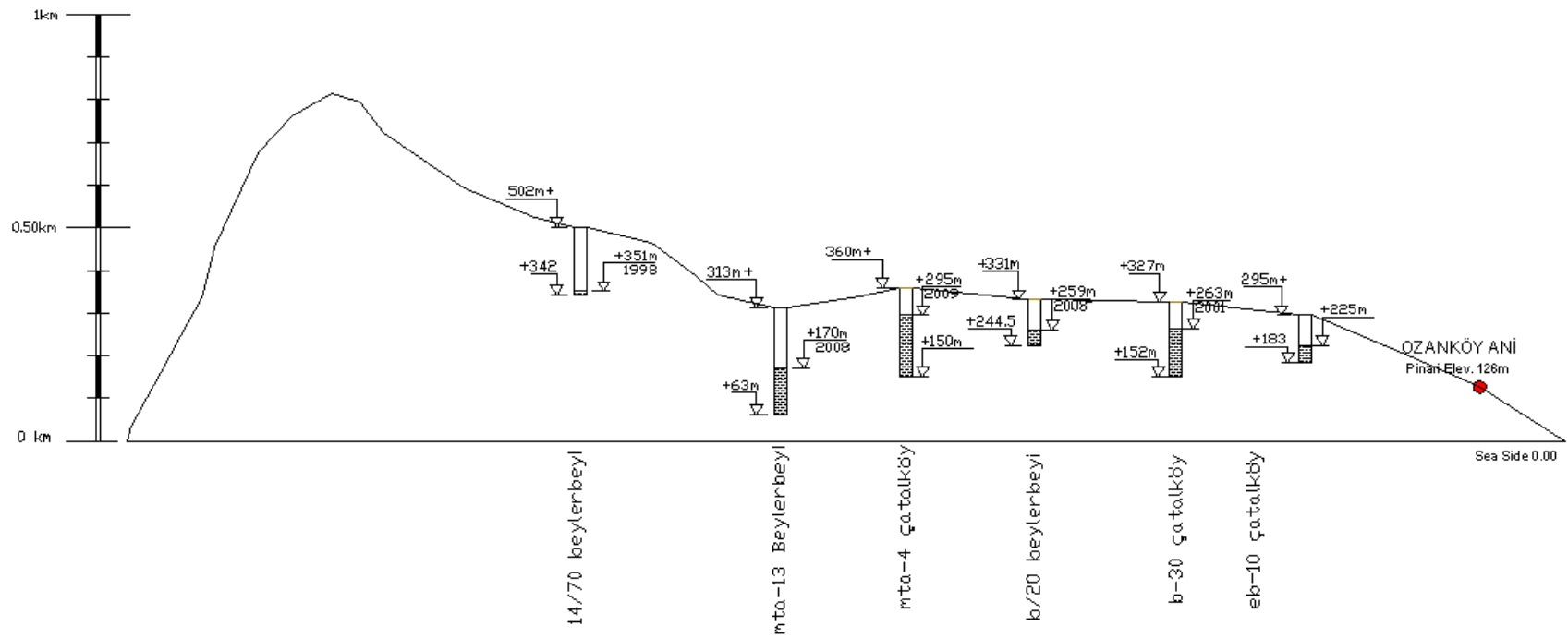


Figure 3.42 Wells depth details and springs elevations at Çatalköy and Beylerbeyi Region

On this principle, MTA drilled MTA-4 at the center of EB-10 and B-30. Their aim was to yield a good pumping rate in this limestone area. MTA-4 was a successful trial and yield 100 m³/hr. The well still supplies water for three villages; namely Çatalköy, Ozanköy and Beylerbeyi. The water level in MTA-4 at 2009 was 295 meter above m.s.l, being higher than EB-10 and B-30, as consider there is no isolation layer in the aquifer and the water level supposed to be the same in all of them. Since MTA-4 was drilled 35 meter deeper than EB-10 and B-30, 100 meters away from each of them, the radius of influence of these wells was affected from the high pumping rates of MTA-4.

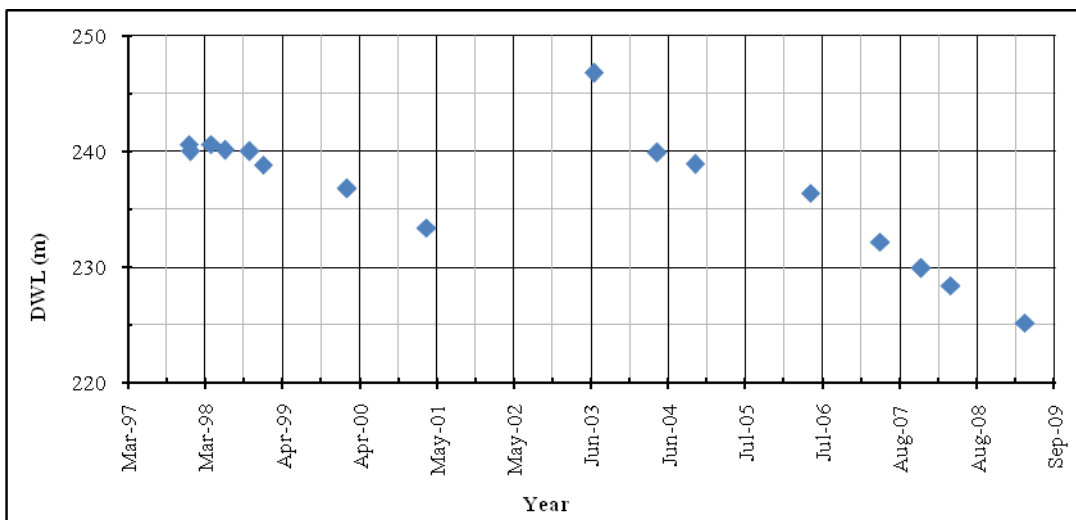


Figure 3.43 Drawdown in dynamic water level of well EB-10 in different years.

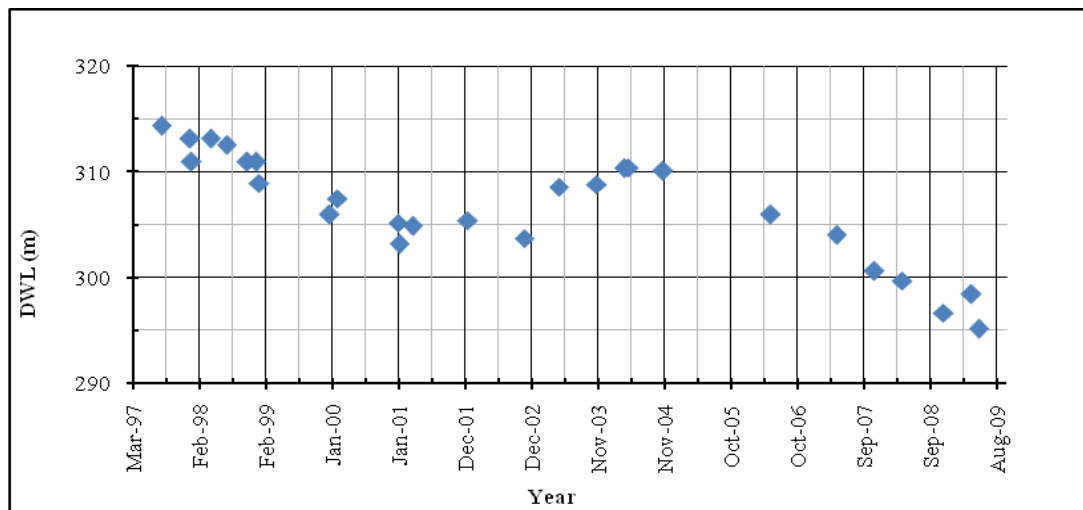


Figure 3.44 Drawdown in dynamic water level of well MTA-4 in different years.

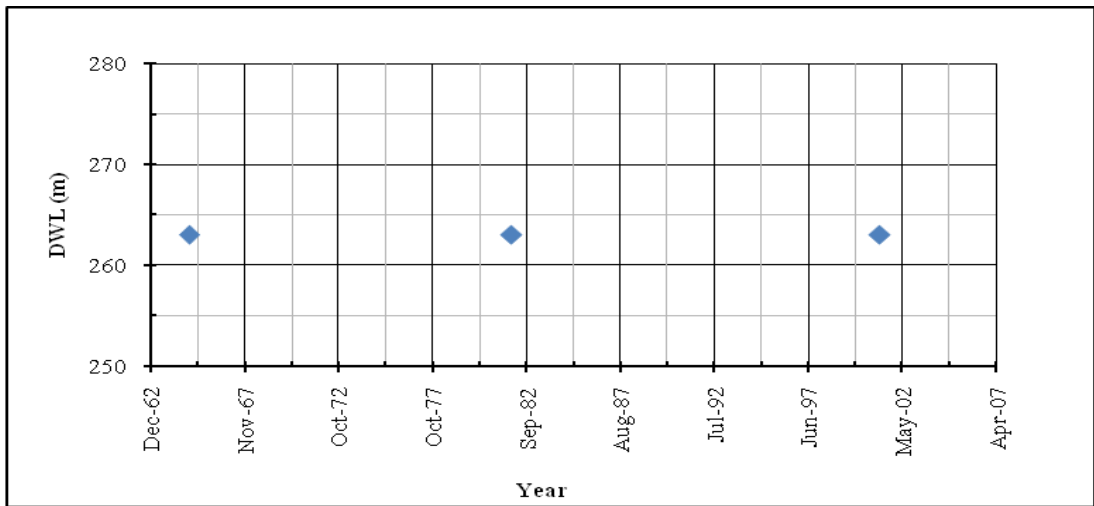


Figure 3.45 Drawdown in dynamic water level of well B-30 in different years.

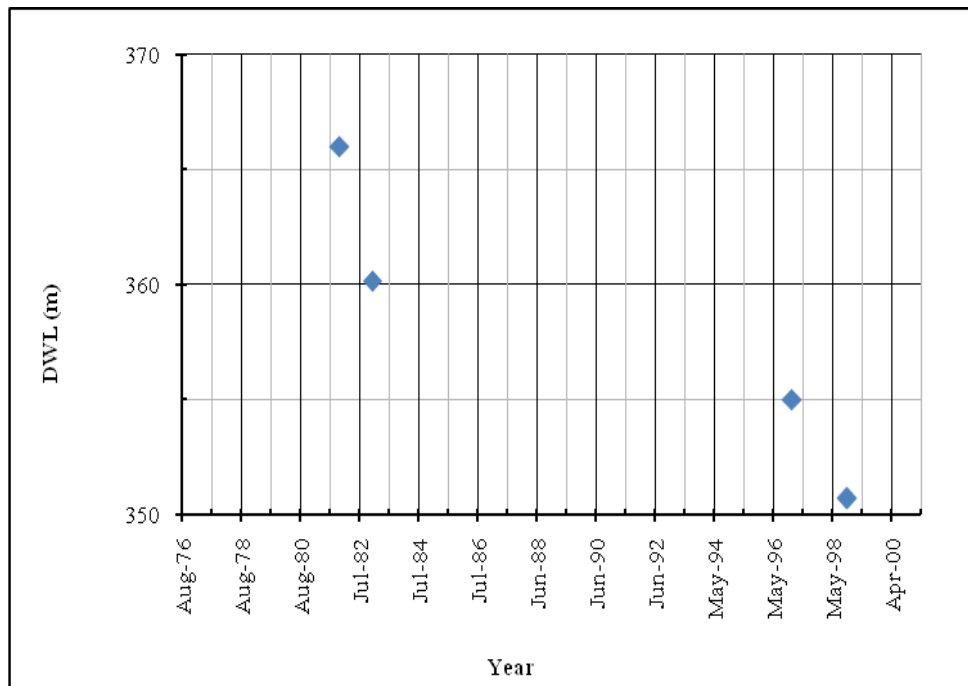


Figure 3.46 Drawdown in dynamic water level of well 14/70 in different years.

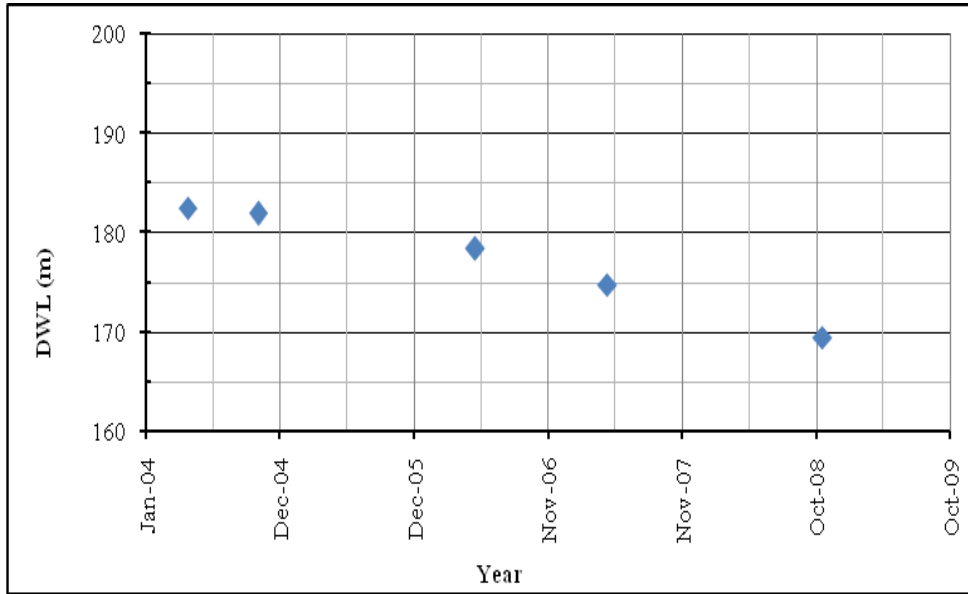


Figure 3.47 Drawdown in dynamic water level of well MTA-13 in different years.

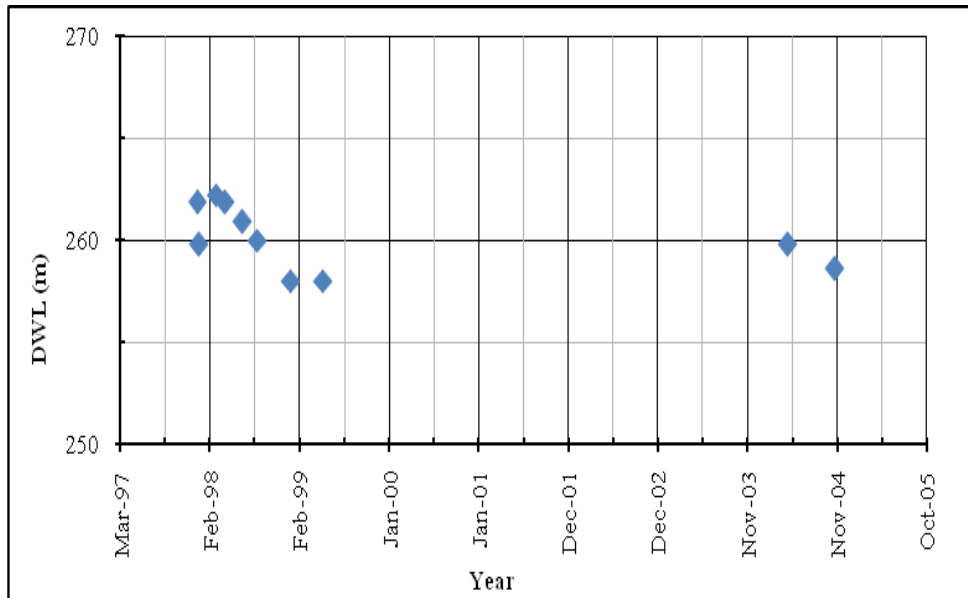


Figure 3.48 Drawdown in dynamic water level of well B-20 in different years.

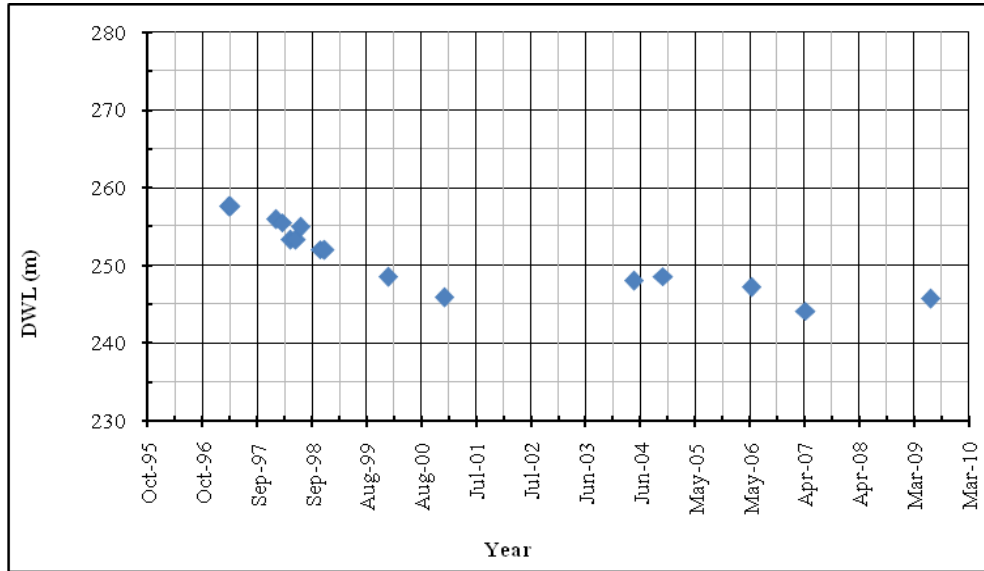


Figure 3.49 Drawdown in dynamic water level of well MTA-2 in different years.

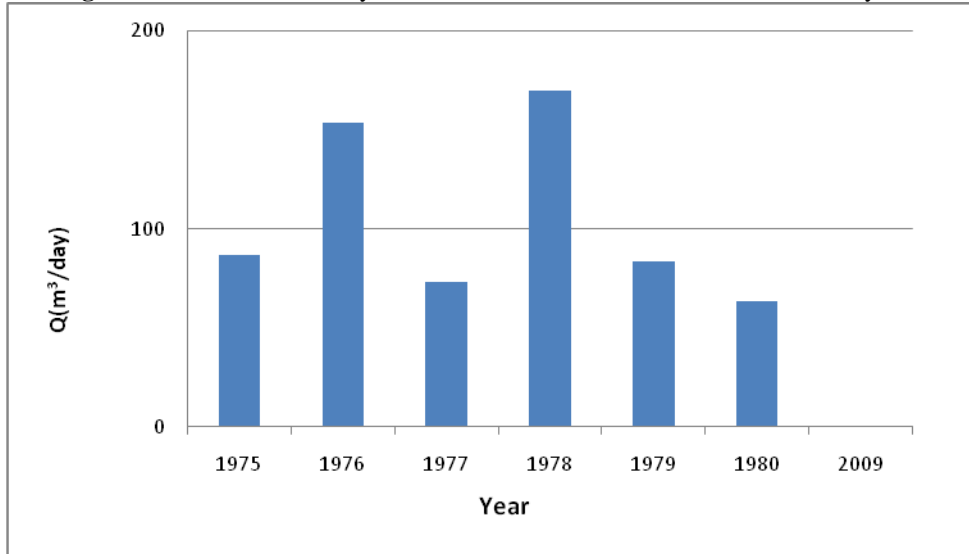


Figure 3.50 Average daily discharges at different years for Ozanköy ANI Spring.

3.7 Değirmenlik Region

In Değirmenlik Region there are five wells. These wells are 19/74, 21/89, 1975/37, 18-b and MTA-2. They are located in one of the most productive aquifer formation. The well 19/74, drilled in 1974 at a depth of 125 m with a pumping rate of 10 m³/hr, and serves water demand of Değirmenlik. By 2009, the water level in the well is monitored as 244 m. The well MTA-2 drilled near 19/74 by MTA as shown in Figure 3.49 the well has an important contribution to domestic water network system. The pumping rate of this well is 75 m³/hr. The MTA-2 well drilled at depth of 114 m from

m.s.l, with water level 246 m which is almost same with 19/74 in evidence that both of 19/74 and MTA-2 are connected without separation. The locations and cross-sectional positions of wells are given on the Figures 3.51 and 3.52.

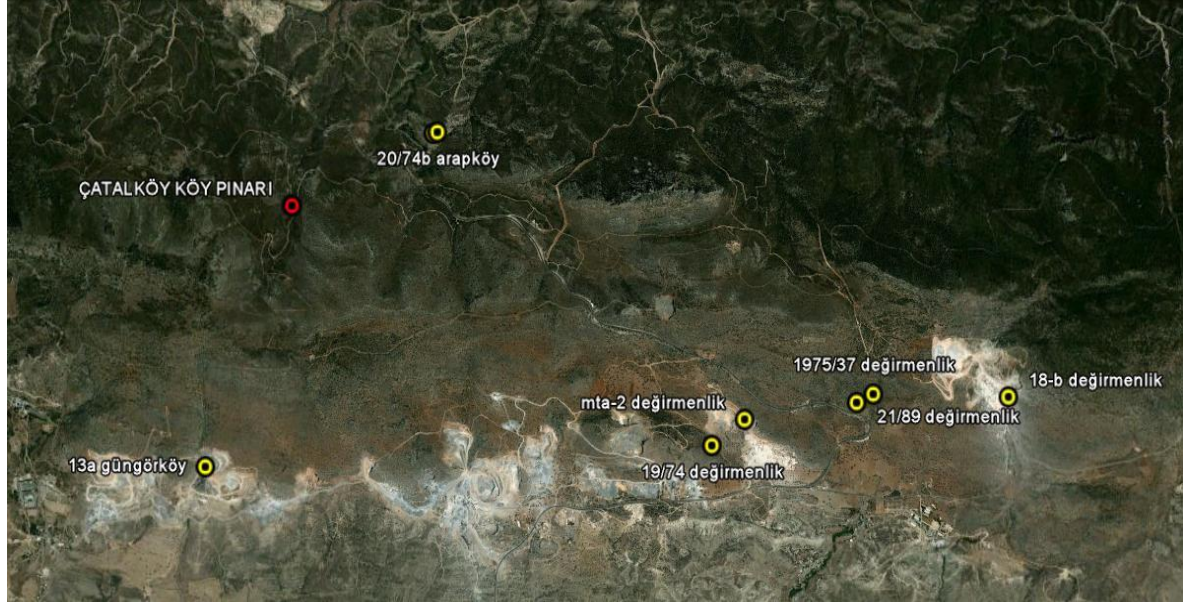


Figure 3.51 Areal picture show the locations of boreholes (from top view) at Değirmenlik Region (scale, 1:53,000).

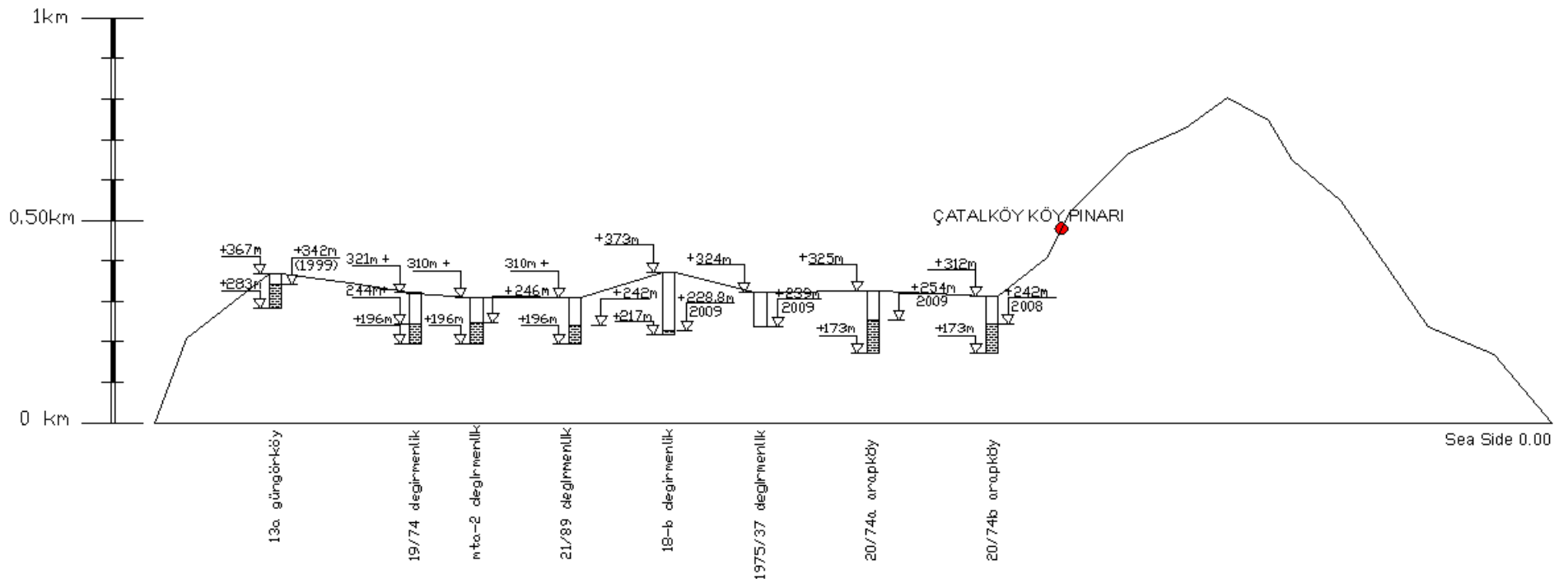


Figure 3.52 Wells depth details and springs elevations at Değirmenlik Region.

The well 18-b is also called Değirmenlik well. The well drilled before 1975, at features which had a narrow gully in limestone, with dark blue shattered and cemented properties; so the well could not go deeper because the geology components can cause mud loss. In the area there is a Kythrea (Değirmenlik) spring at an elevation of 262.7 m. In the last 15 years the spring has dried up due to the over pumping of the surrounding wells.

Two boreholes were drilled at Arapköy (Arab village) named as 20/74-a and 20/74-b. Both of them are in the same location and are drilled in 1974. The pumping rates of the wells are 40 m³/hr. The wells supply water to electric power plants in Arab village. 20/74-a and 20/74-b were drilled at a depth of 152 m and 139 m, respectively. Their water levels are at 250 meter above m.s.l. The only spring available at the region is Çatalköy Spring which is located at an elevation of 481 m. The flow rate of the spring was not a considerable quantity, to be considered as a flow during the site visit at June 2009. Figures 3.59a and 3.59b show the flow rate details and the pictures of the Çatalköy Spring.

The well B13-a (Güngörköy well) is located at Güngör village. The well is used to supply water for military purposes discharging at a rate of 3 m³/hr. Since the amount of water has not been enough for the demand of the existing military people living in that area, later, the well has been closed and another well drilled in the area for the same purpose. The new well name is b13-a, drilled at a depth of 84 meter. The water level was 342 m when it was last monitored at 1999 before abandoned.

The water levels in Değirmenlik and Arab Village are monitored and observed that they have the same elevations and drawdowns. In 2009 the water level is around 250 meters above mean sea level. This result suggests that the aquifer is extending to both sides of the Kyrenia Range. 13-A, which is 4 km away from the other wells is the only water source which is not included into this family of wells. The water level of this well is 113 meter higher than the other wells.

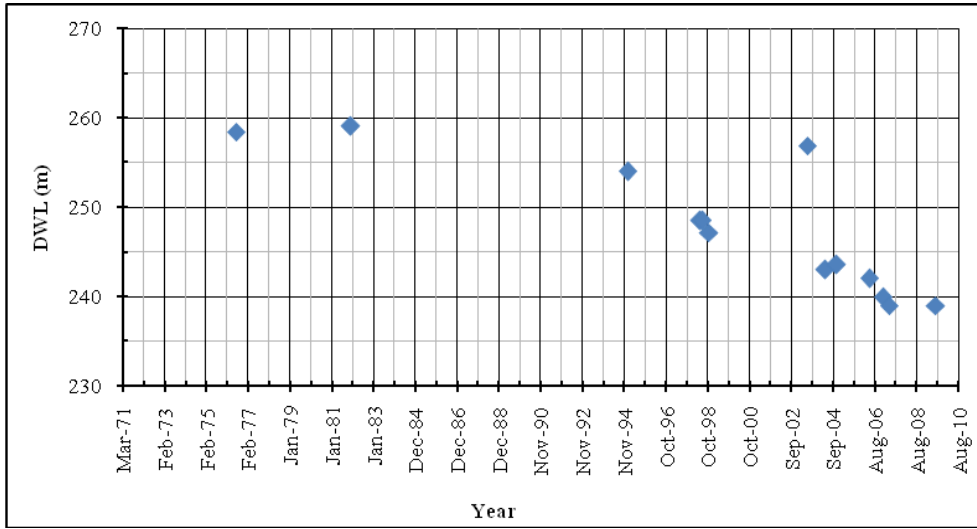


Figure 3.53 Drawdown in dynamic water level of well 1975/37 in different years.

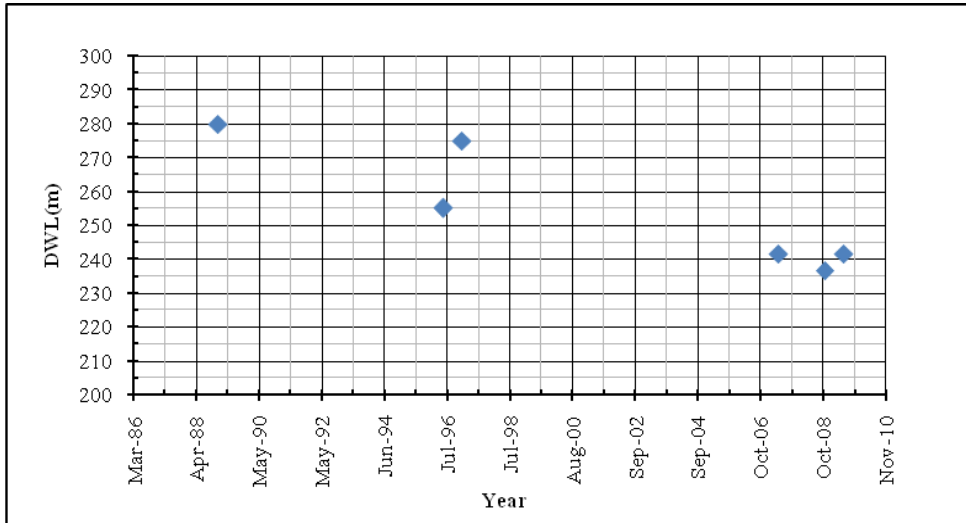


Figure 3.54 Drawdown in dynamic water level of well 21/89 in different years.

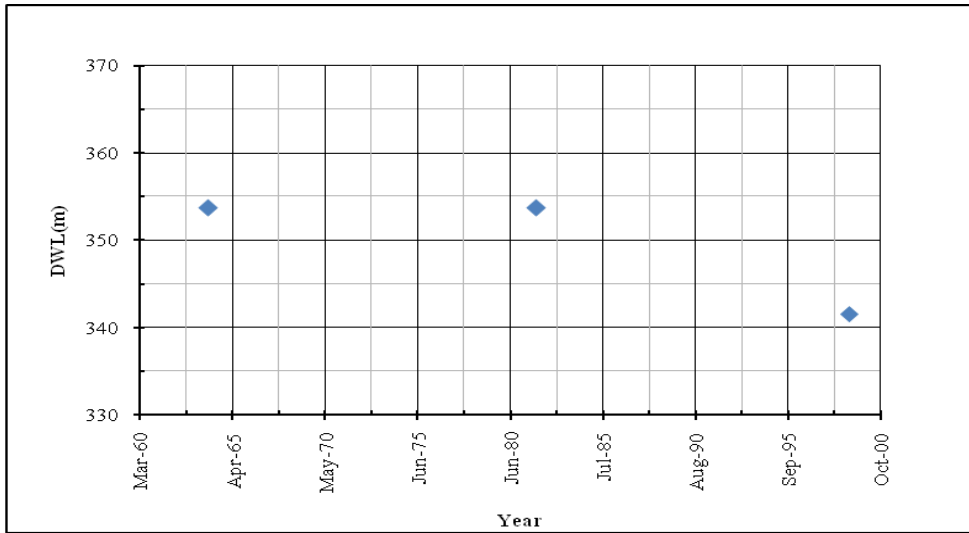


Figure 3.55 Drawdown in dynamic water level of well 13A in different years.

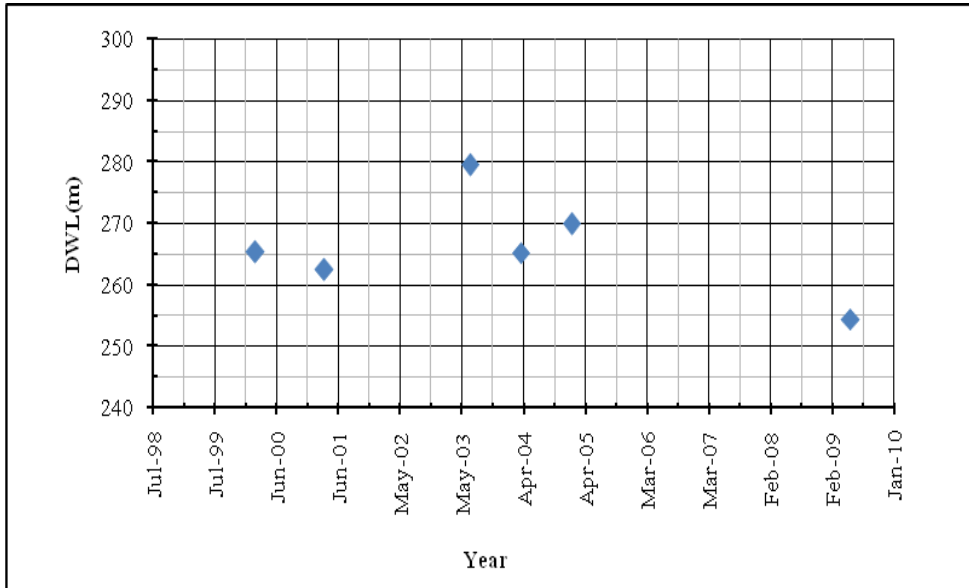


Figure 3.56 Drawdown in dynamic water level of well 20/74a in different years.

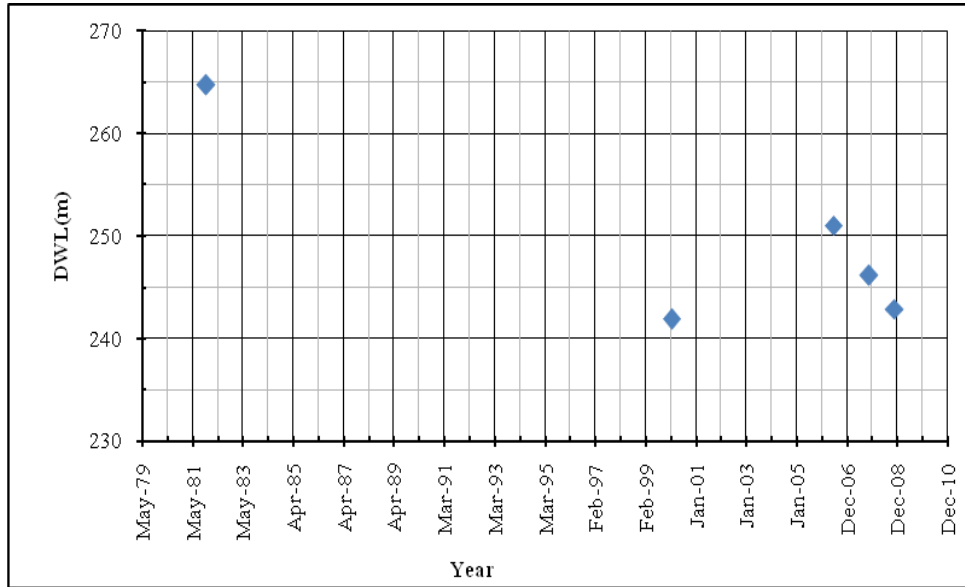


Figure 3.57 Drawdown in dynamic water level of well 20/74 B in different years.

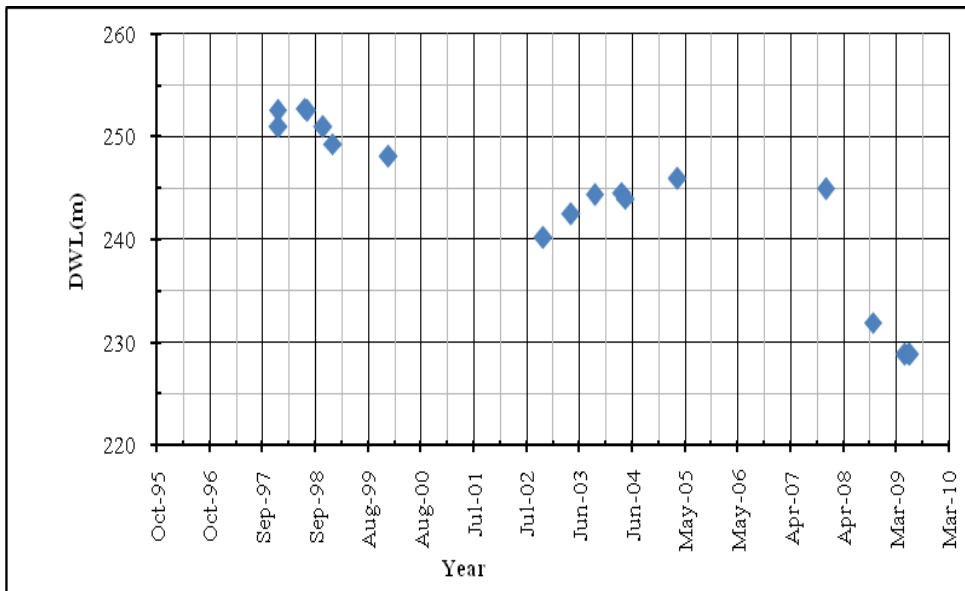


Figure 3.58 Drawdown in dynamic water level of well 18-b in different years.

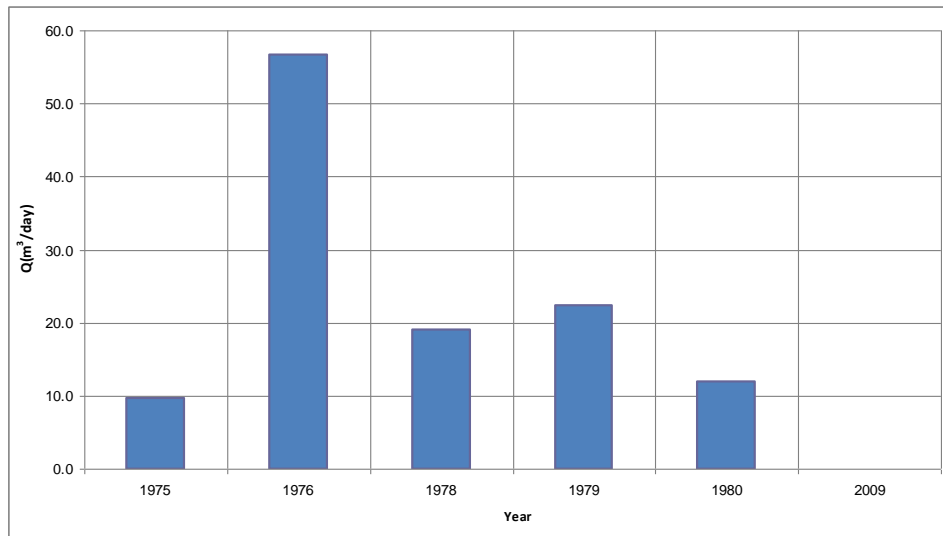


Figure 3.59a Average daily discharges at different years for Çatalköy village spring.



Figure 3.59b Çatalköy village spring.

3.8 Karaağaç-Alevkayası Region

In the region there are two wells, they are MTA-19 located at Karaağaç and 44/67 located at Alevkayası. Two springs known as Çeşmeler (Viysitou) and Karaağaç (Ayyorgi) are located in Karaağaç. The locations and cross-sectional positions of wells are given in Figures 3.60 and 3.61.

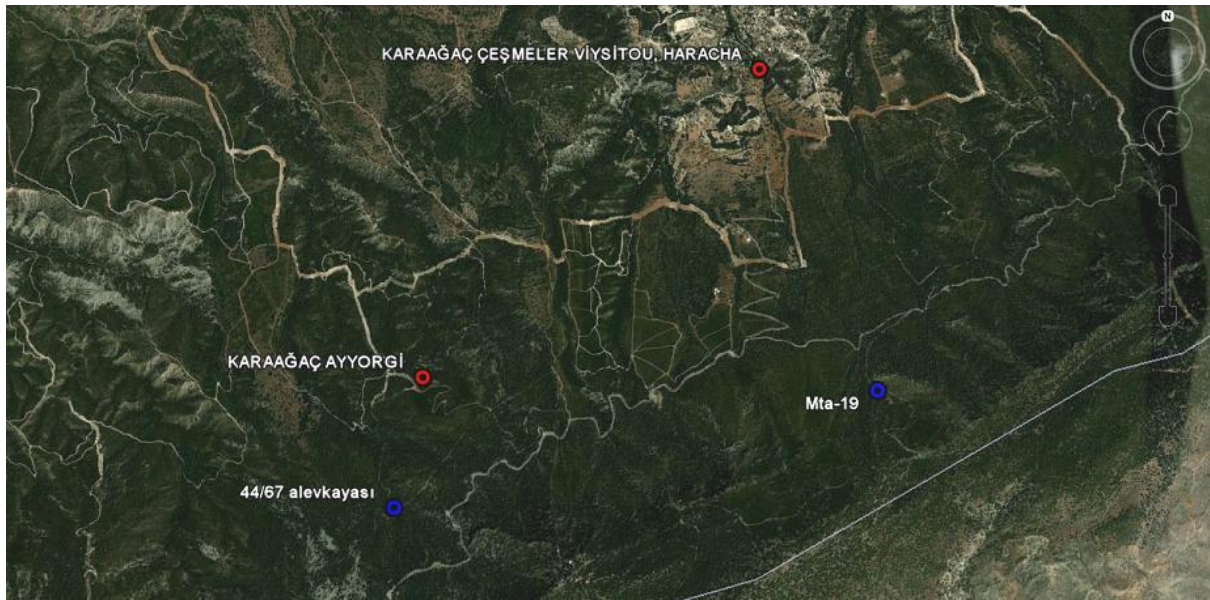


Figure 3.60 Areal picture showing the locations of boreholes (from top view) Karaağaç Alevkayası Region (scale, 1:44,000).

The spring Çeşmeler (Viysitou) is at an elevation of 287 meters under the level of known water table. The spring flow rate is 0.5 m³/hr in the last measurement at June 2009. The Karaağaç (Ayyorgi) Spring, which is discharging at 450 meters, had dried up, since its elevation is higher than the available water table.

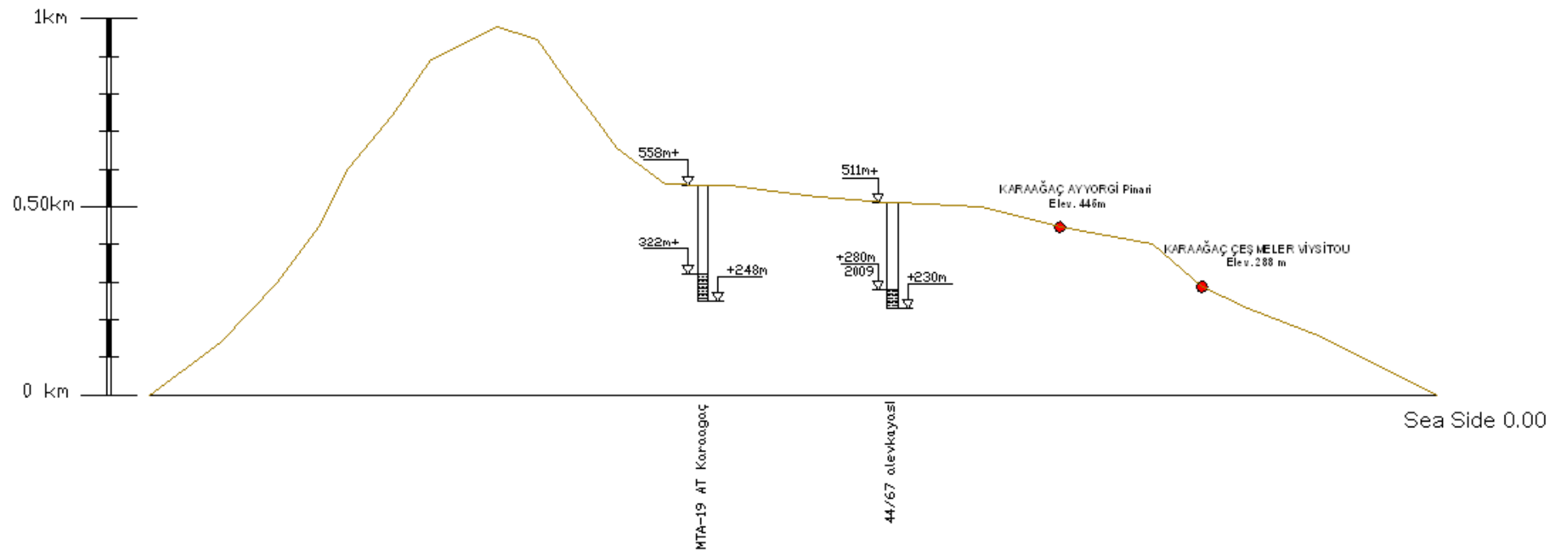


Figure 3.61 Wells depth details and springs elevations at Karaağaç Alevkayası Region.

The MTA-19 has started to operate by MTA at 1998. The well located between the two villages Karaağaç and Esentepe. The well drilled at a depth of 310 meters with water level recorded in 2005 as 322 m. The pumping rate was 20 m³/hr, supplying water demand of Esentepe Village. The head difference between MTA-19 and Çeşmeler spring was 34 meters in 2005 and decreased to 26 meters in 2009. Since still there is a head difference the spring flows at an average 0.52 m³/hr. Since the spring is flowing even in summer season it can be deduced that there is a relation between their locations. It can be concluded that there is a net flow from well towards the north via the cracks on limestone strata. By analyzing the location and from the properties of topography and geology conditions it shows that there is a relation between the well 44/67 and the spring Karaağaç (Ayyorgi). The spring elevation is 445 m and higher than the water table level of 44/67 well which is 280 m above m.s.l, and in the excavation in 2009 summer at month June found out of the spring completely dried, so it is a good understanding that there is a relationship between the well 44/67 and the spring Karaağaç (Ayyorgi). The MTA-19 has water elevation 322 m which is 34 m higher than the elevation of the spring Karaağaç Çeşmeler (Viysitou) 288 m. Since the spring is still flowing with a discharge of 0.52 m³/hr, one can simply make an assumption on the relation between the wells and the springs in that region.

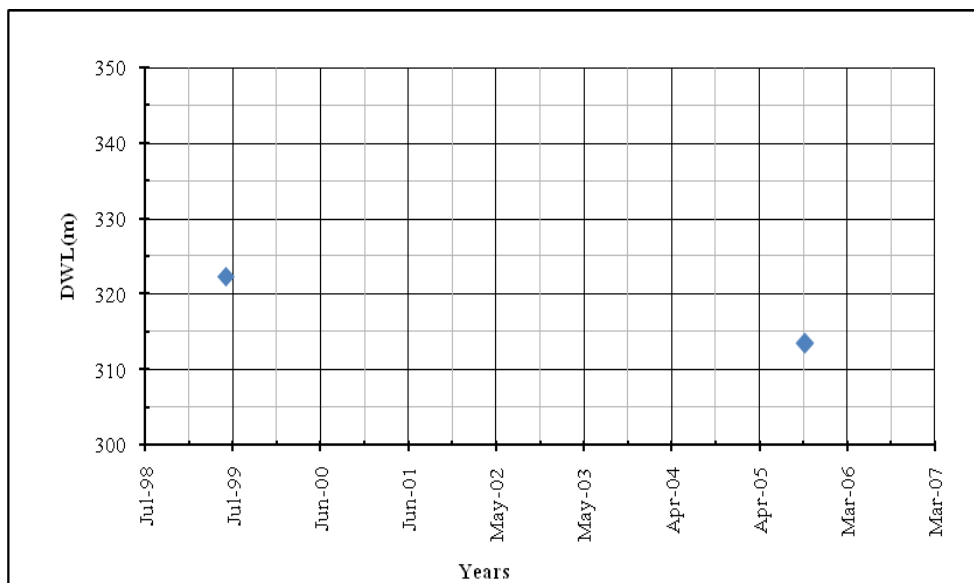


Figure 3.62 Drawdown in dynamic water level of well MTA-19 in different years.

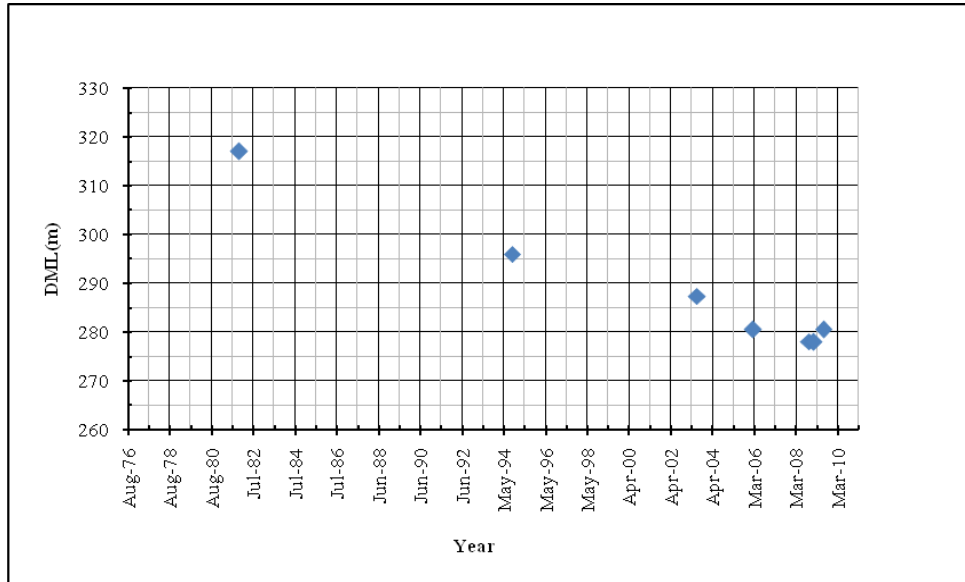


Figure 3.63 Drawdown in dynamic water level of well 44/67 in different years.

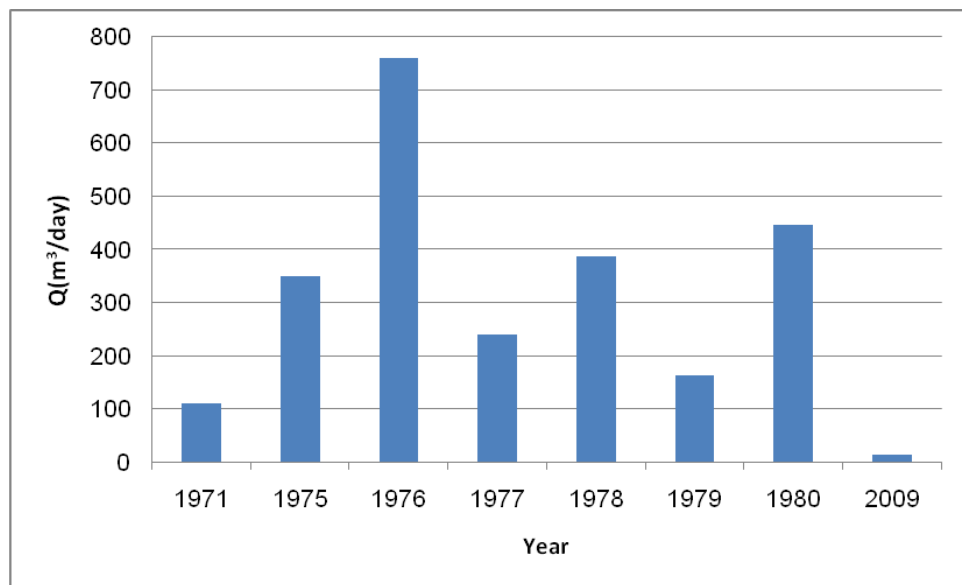


Figure 3.64 Average daily discharges at different years of Karaağaç Çeşmeleri (Viysitou) spring.



Figure 3.65 The Pictures of Karaağaç Çeşmeler (Viysitou) spring.

3.9 Tirmen Region

In Tirmen area there are four wells MTA-3, 17/74, 19/66 and 6/68. Also there are two wells 16/A known as Esentepe well located at Bahçeli, and the well 37/76 located at Ergenekon.

Three of these wells are located at the southern foothills of the Kyrenia Range. These are 37/76, 19/66 and MTA-3. At the northern foothills, the other three wells 16/A, 6/68 and 17/74. There are two springs namely, Aslanbaşı Pınarı and Bahçeli Verysi spring. The locations and cross-sectional positions of these wells are given in Figures 3.66 and 3.67.

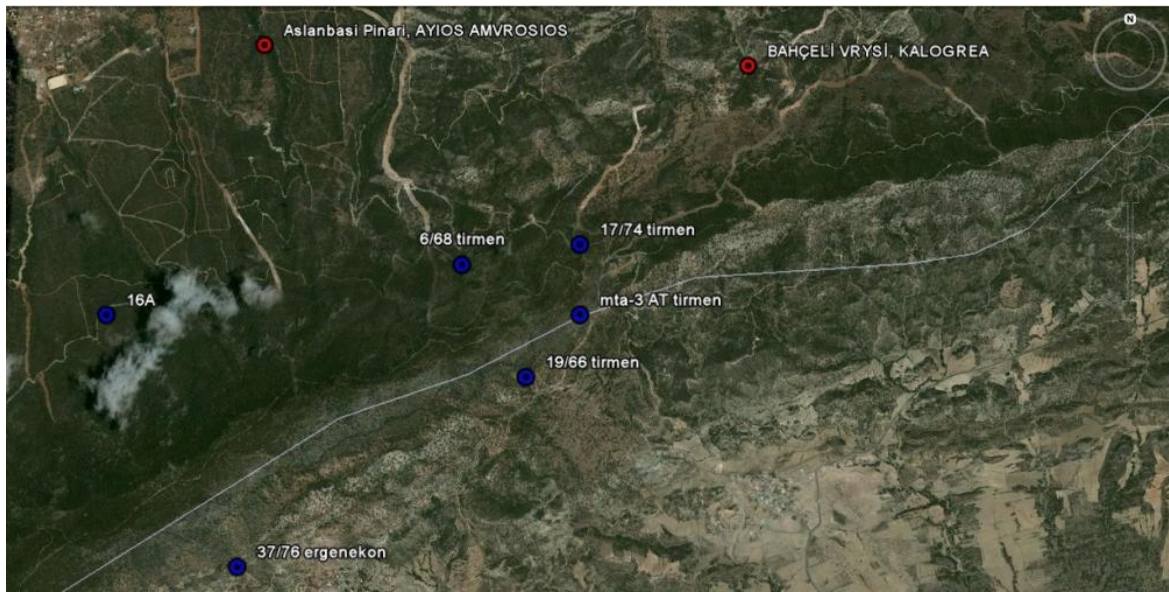


Figure 3.66 Areal picture showing the locations of boreholes (from top view) at Tirmen Region (scale, 1:43,000).

The well MTA-3 started operating at 1998's. The well is used for the water demand of Tirmen Village. The pumping rate is $36 \text{ m}^3/\text{hr}$, recorded by WWD in 2009. The well is located at the southern part of Kyrenia Range at depth of 337.5 m. The water level recorded at 2009 was 285 m above m.s.l. The well 19/66 was drilled in 1966 at a depth of 134 m. The total head of the well has dropped 50 meters during the period 1966 up to 1996. At 1996's the drawdown become steady. The last monitoring shows that the water level was 323 meter, then at 2004 the well was efficiently not working and it has been abandoned.

The 37/76 well is located at Ergenekon village, at the southern foothills of the Kyrenia Range. From the drilling years, 1976, up to 2003 the drawdown was recorded to be decreased 30 meters. The well supplies the water demand of Ergenekon Village. The depth of the well was 150 m. The water level in the well is 233 meters above m.s.l. The wells 37/76 and 19/66 were drilled on the same Lapithos formation which was described by Dixey (1975). Both of the wells are now abandoned.

At the northern foothills the Tirmen region well 6/68 was drilled in 1968, supplying $5 \text{ m}^3/\text{hr}$ for the water demands of Bağçeli (Kalogrea) Village. The well drilled in rubbly crush-breccia of limestone. The well diameter was enlarged 25.4 centimeters in 1971 (Dixey, 1975).

The well 16/A also known as the “Old well” drilled in Bahçeli (Kalogrea) village. The well is supplying domestic water requirements of Esentepe village with a pumping rate $10 \text{ m}^3/\text{hr}$.

The dynamic water level measured in 2004 by WWD was 115.90 meter above m.s.l. The well at Tirmen village 17/74 was drilled in 1975, supplying domestic water to Tirmen Village, with a pumping rate of $36 \text{ m}^3/\text{hr}$. The water level was measured in 2009 as 204 m above m.s.l. Two springs exist in the region. The first spring is located at Esentepe village and called Aslanbaşı Pınarı. The flowing rate of this spring is $1.8 \text{ m}^3/\text{hr}$ with an elevation 224 meters above m.s.l. The other spring is Bahçeli Verysi spring, located at Bahçeli village with an elevation of 222 meters. The spring is dried up since 1980.

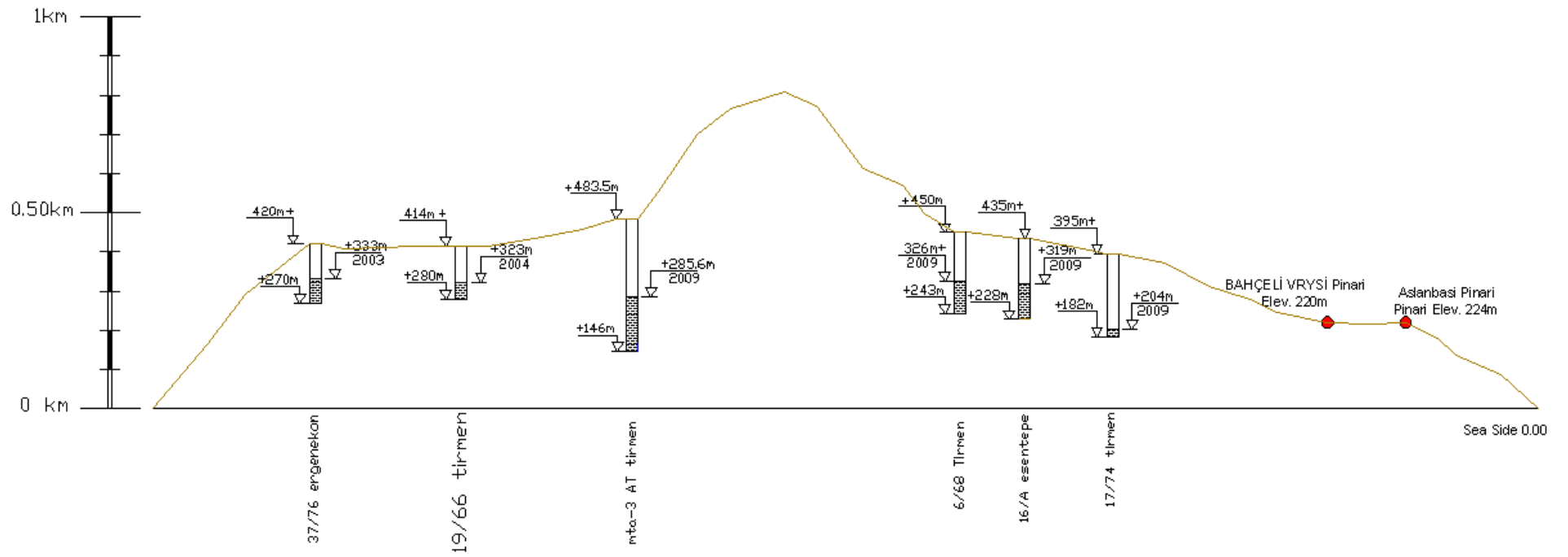


Figure 3.67 Wells depth details and springs elevations at Tirmen Region

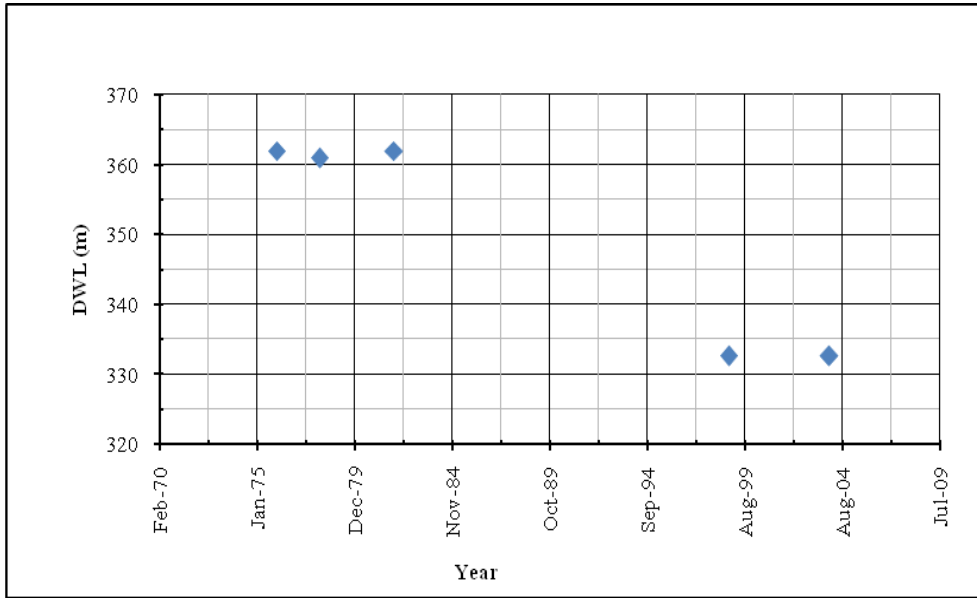


Figure 3.68 Drawdown in dynamic water level of well 37/76 in different years.

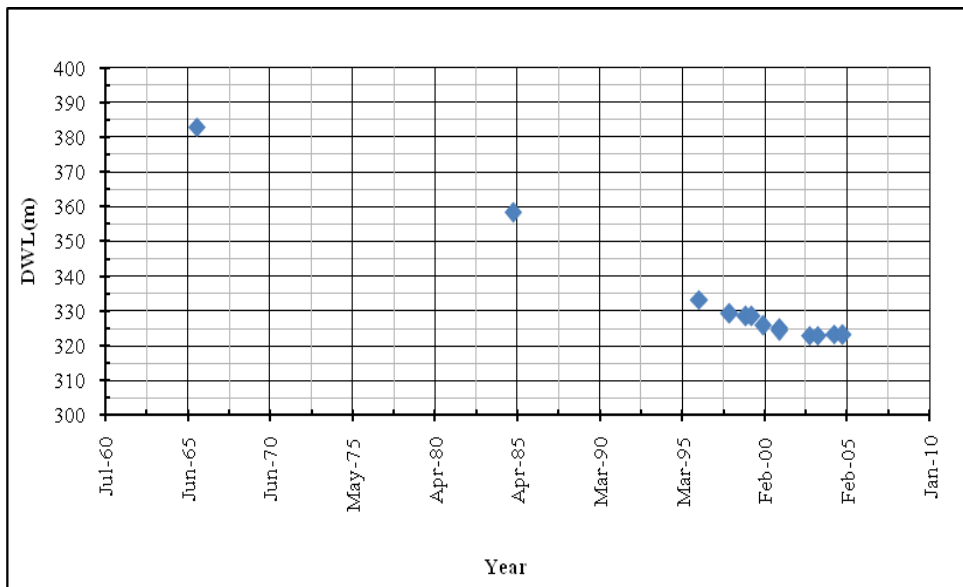


Figure 3.69 Drawdown in dynamic water level of well 19/66 in different years.

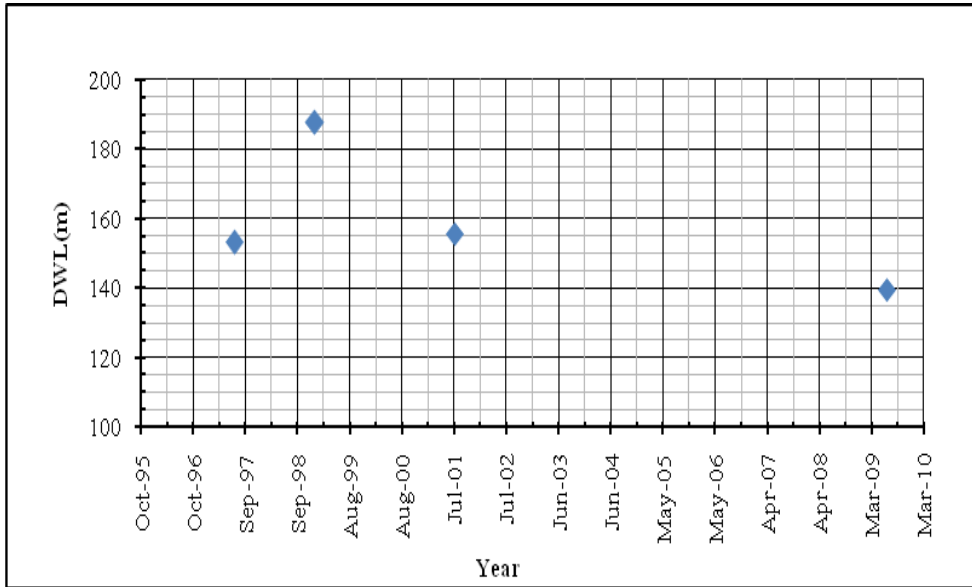


Figure 3.70 Drawdown in dynamic water level of well MTA-3 in different years.

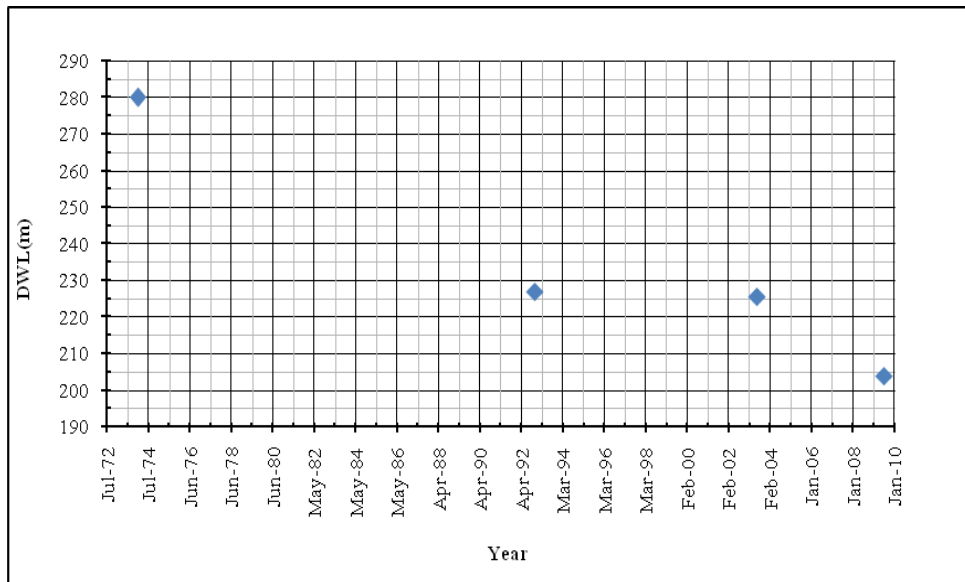


Figure 3.71 Drawdown in dynamic water level of well 17/74 in different years.

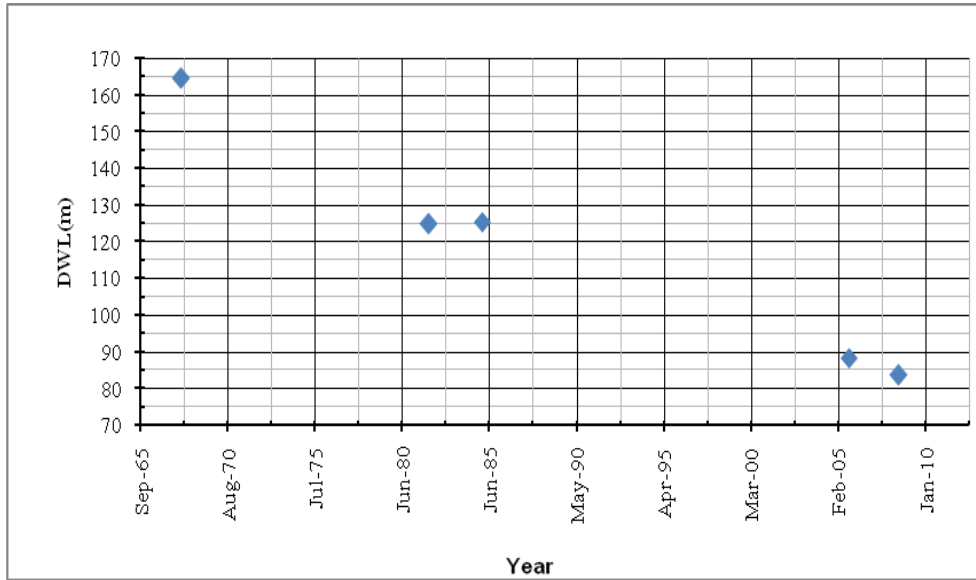


Figure 3.72 Drawdown in dynamic water level of well 6/68 in different years.

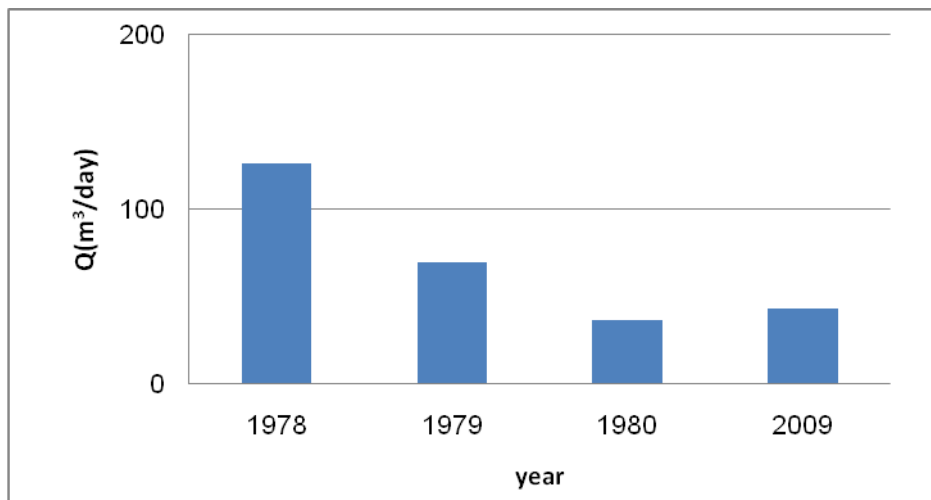


Figure 3.73 Average daily discharges at different years of Aslanbaşı Spring.



Figure 3.74 The Pictures of Aslanbaşı Spring at Tirmen Region.

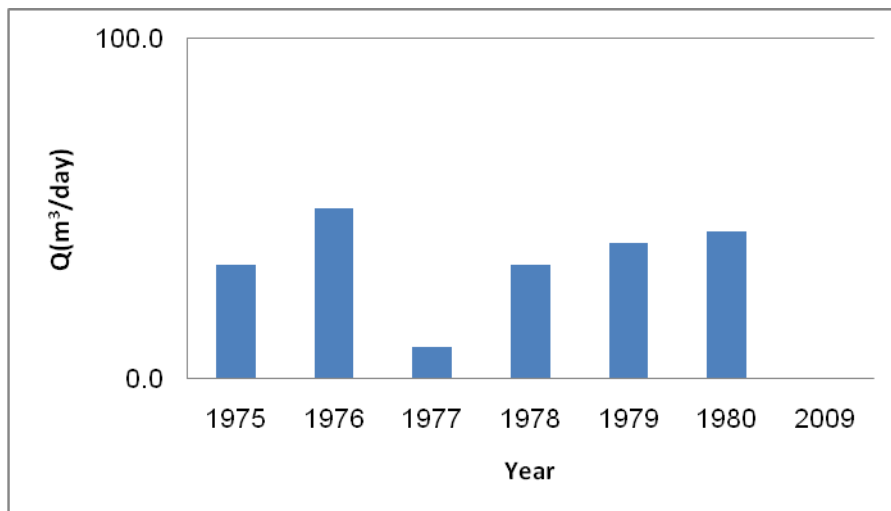


Figure 3.75 Discharges in month June of different years for Bahçeli Verysi spring.



Figure 3.76 The Pictures of Bahçeli Verysi spring.

3.10 Tathisu -Kantara Region

MTA has drilled four wells in Kantara Region. All these wells were drilled in 1998. The wells are MTA-5, MTA-7, MTA-17, and MTA-21. There are four more wells distributed in the region which are 116/65, B-3, 1993/34 and B-1. Dixey in 1975 defines the Kantara limestone block as an isolated mass partly embedded in the surrounding impervious clays, sandstone, breccias, etc. Dixey had notified that, the block is about 2 km in length and good prospect of deep storage. Dixey's observations were a challenging reason for the engineers of MTA to drill several boreholes at the region. The research has started with MTA-5 in which a deep well was drilled. MTA-5 was drilled up to confined layer and brakish (high salt content) water has been burst out from this confined aquifer. The well has been closed by concrete in order to prevent the brakish water potable water interactions within the aquifer. The locations and cross-sectional positions of wells are given in Figures 3.77 and 3.78.



Figure 3.77 Areal picture showing the locations of boreholes (from top view) in Tatlısu Kantara Region (scale, 1:125,000).

MTA-7 drilled in 1998 at Kantara Village. The depth of the well was 209 m, with water level of 395 m above mean sea level. However, the well is considered as a poor water resource with low pumping rate which is 4 m³/hr recorded in 2002. Today, the well is abandoned.

MTA-17 well was drilled at Kantara village at a depth of 156 meters. The purpose of drill was to supply potable water to Kantara and Tatlısu villages. The well was drilled to replace the well 1993/34.

The well 1993/34 has been drilled at 642 meter from mean sea level, whereas MTA-17 was drilled at 673.5 m. The dynamic water levels in both wells were close to each other. The water level was 579 m in 1993/34 well and 583 m at MTA-17 well. Since the geology of region was defined as hard rock, the well drilling was not so easy to drill deep wells. The depth of MTA-17 and 1993/34 were 156 m and 104 m, respectively. Both of the wells have not been in use since they have been drilled.

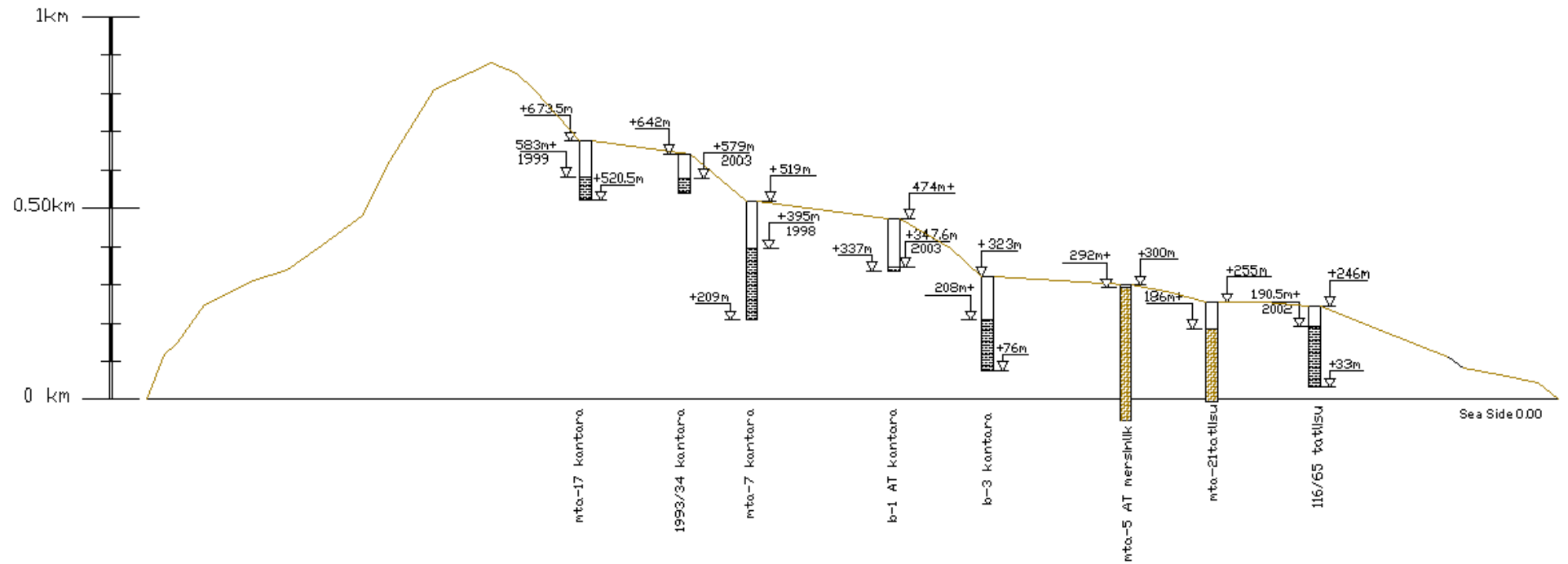


Figure 3.78 Wells depth details and springs elevations at Tatlisu Kantara Region

MTA-21 is located close to Tatlısu, at 1 km west of MTA-17 and 1993/34. The well was drilled at a surface elevation of 255 meters. The well supports the water demand of Tatlısu, Mersinlik and Kaplıca with 72 m³/hr in 2009. The dynamic water level in the well was 186 m above m.s.l. Since the drilling times of the well, the head in the well has been dropped by 17.67 meters.

The well 116/65 was drilled in 1965 at Tatlısu. The well name was later changed to Mersinlik well. The well was used to supply water demand of Mersinlik and Tatlısu villages. The capacity of the well was 25 m³/hr. The water level in the well was 190.5 m above m.s.l. Since 1965 up to 2002, the water level in the well has depleted up to 411 meters.

The B-1 well is situated near Kantara Castle in Kantara village at an elevation of 474 m from m.s.l. The well was drilled by Water Development Department (WDD) in 1965. The reasons motivating WDD to drill near Kantara were the following: Kantara was the only closed settlement on the Kyrenia Range. The concentration of summer houses and temporarily settlements of army at the region for military training camps, required a close water body at the region; the altitude level was 550 m above m.s.l., therefore adequate water supply from the scanty and weak springs in this region was not guaranteed. Six drilling sunk in the years from 1947-1955 had remained without success.

The drilling was located on a steeply dipping major fault separating a 0.5 km² Hilarion limestone block from the southerly neighboring Lapithos calcareous marls. The depth of the B-1 well was 84 m. Later B-1 well was drilled to its final depth which is 137 m. During three pumping test by German mission, the yield of water was 15.5 m³/hr (Mixius et al., 1964). In 2002 the pumping rate of this well was 6 m³/hr, and currently situation is a weak discharging due over pumping stresses.

B-3 well is situated at Tatlısu (Akanthou) in an elevation of 323 meters above m.s.l. It was located on the northern major faults of the long stretched steep dolomitic massif above Tatlısu.

The water table was adapted itself at 114.5 m below surface level 208.5 m.s.l in 1965. The pumping rate was measured by German mission as 20 m³/hr, and in 2002 MTA recorded 15 m³/hr, water supplies from the well used by Tatlısu, Mersinlik and Kaplıca.

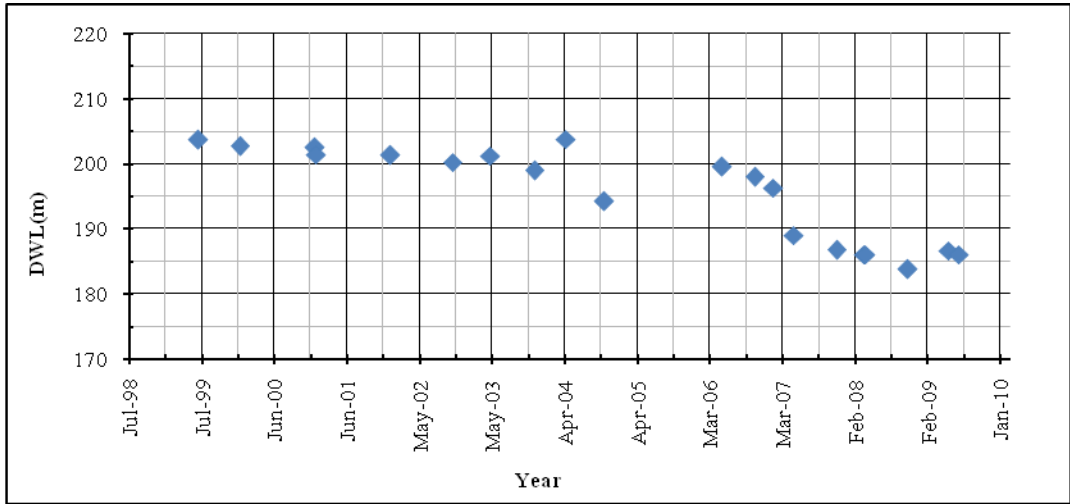


Figure 3.79 Drawdown in dynamic water level of well MTA-21 in different years.

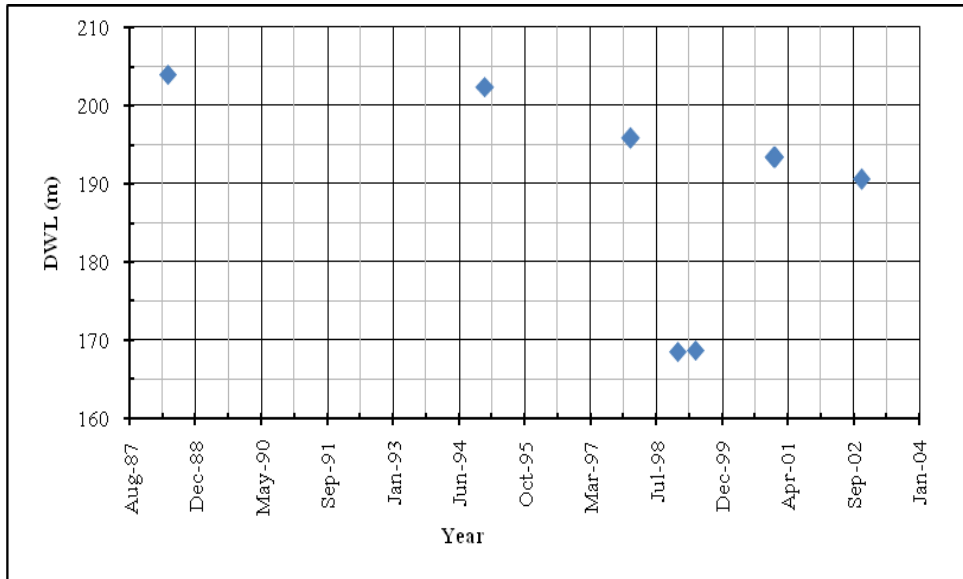


Figure 3.80 Drawdown in dynamic water level of well 116/65 in different years.

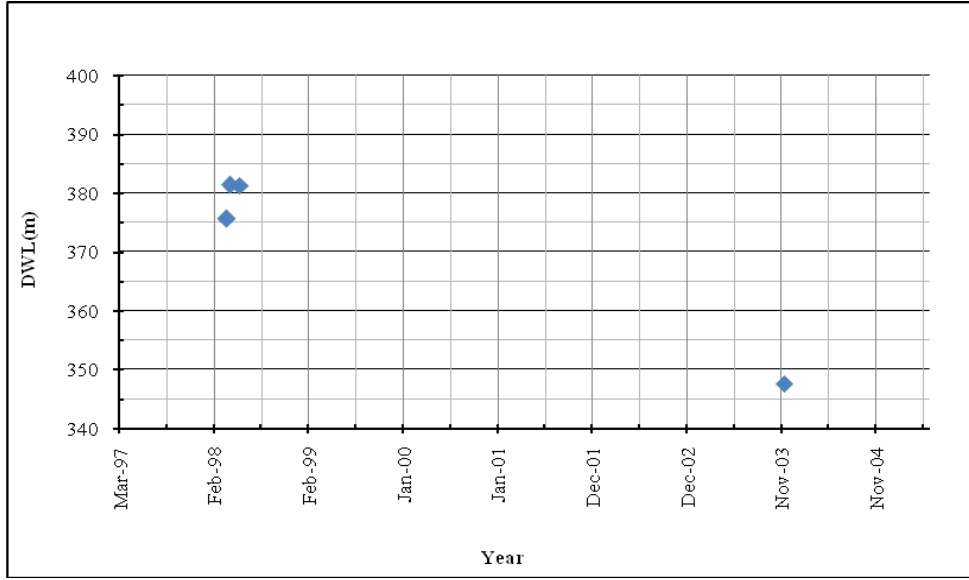


Figure 3.81 Drawdown in dynamic water level of well B-1 in different years.

3.11 Boğaz Region

In Boğaz region there are six wells. The wells are 1/65, 1961/50 (DHM-1), 40/71(DHM-2), MTA-2, 12/74 and 13/74. The locations and cross-sectional drawing of the wells are given at Figures 3.82 and 3.83.



Figure 3.82 The location of borehole from top view in Boğaz Region (scale 1:26,000).

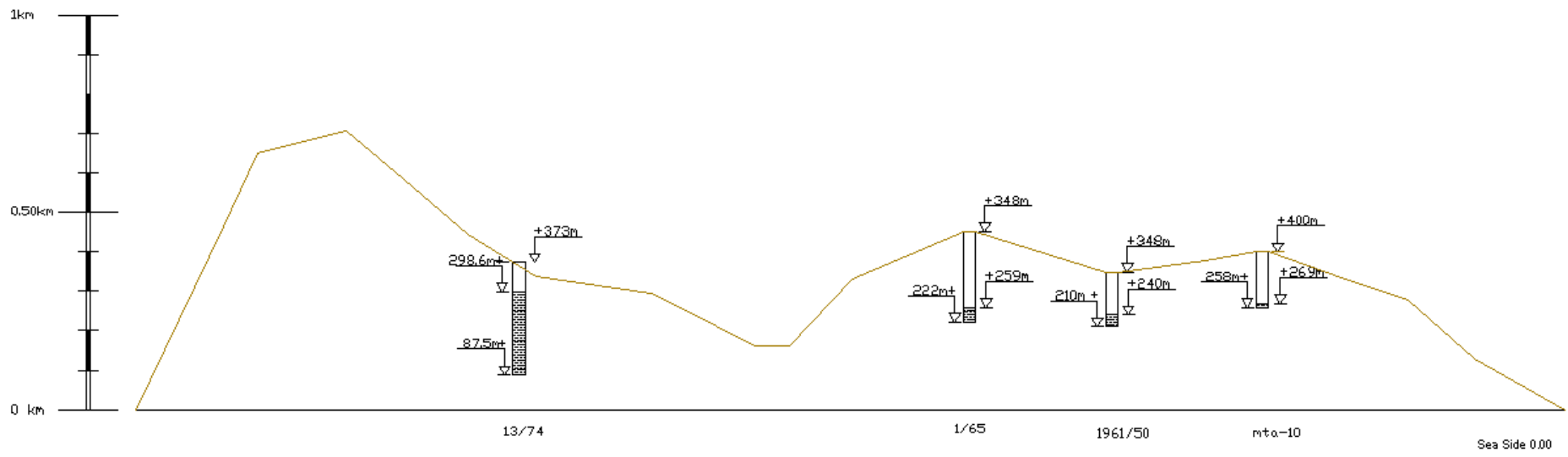


Figure 3.83 Wells depth details and springs elevations at Boğaz Region.

MTA-10 drilled in 1998 at a depth of 258 meter above m.s.l. to supply domestic water of Girne city. The pumping rate 30 m³/hr with water level 269 m above m.s.l. recorded in 2009 by water works department. The well 1971/40 is known as DHM-1 was drilled in 1971. This well also supplies water demand to Girne with pumping rate of 60 m³/hr. The depth of the well is still unknown; because there is no measurement tool inside the well. Beside DHM-1 the well 1961/50 was drilled at 1961. This well is known as DHM-2. DHM-2 is the third well which supplies domestic water to Girne. The yield rate of this well is 70 m³/hr. The well was drilled at a depth of 210 meters above m.s.l. while the water level recorded in 2001 was 240 m above m.s.l. The wells DHM-1 and DHM-2 are considered as an important water source of Girne city. The well 1/65 or Bozdağ well is located at Boğaz village. The well 1/65 was drilled in 1965 at a depth of 222 m and still supplies water demand of different villages with a pumping rate of 45 m³/hr. At Ciklos region, the well 12/74 and the well 13/74 were both drilled in 1974. The 12/74 has no detailed data for it is depth or water level because there is no measurements possibility at the field. The well 13/74 was drilled at a depth of 87.5 m with water level 298.6 m above m.s.l. This well also supplies domestic water to Girne city with 15 m³/hr.

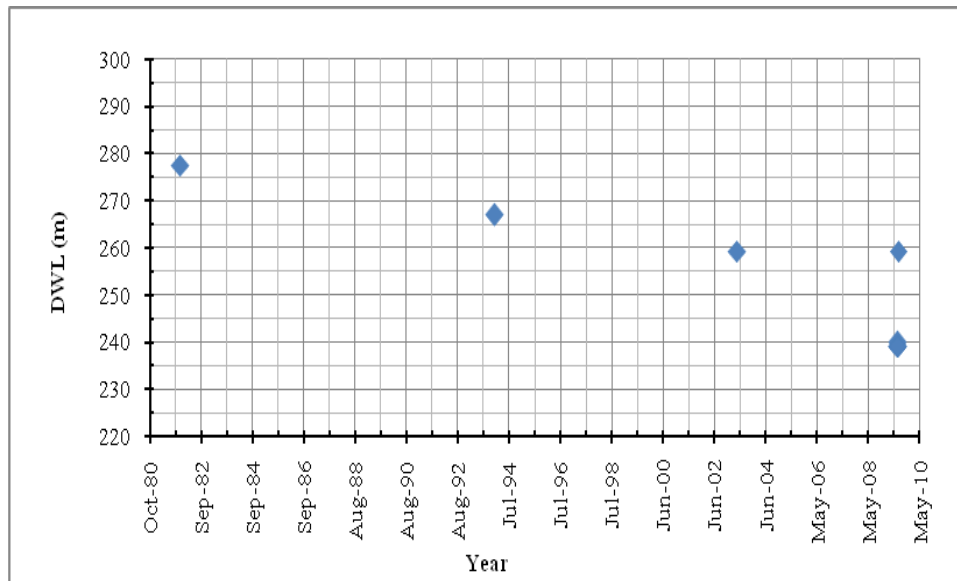


Figure 3.84 Drawdown in dynamic water level of well 1/65 in different years.

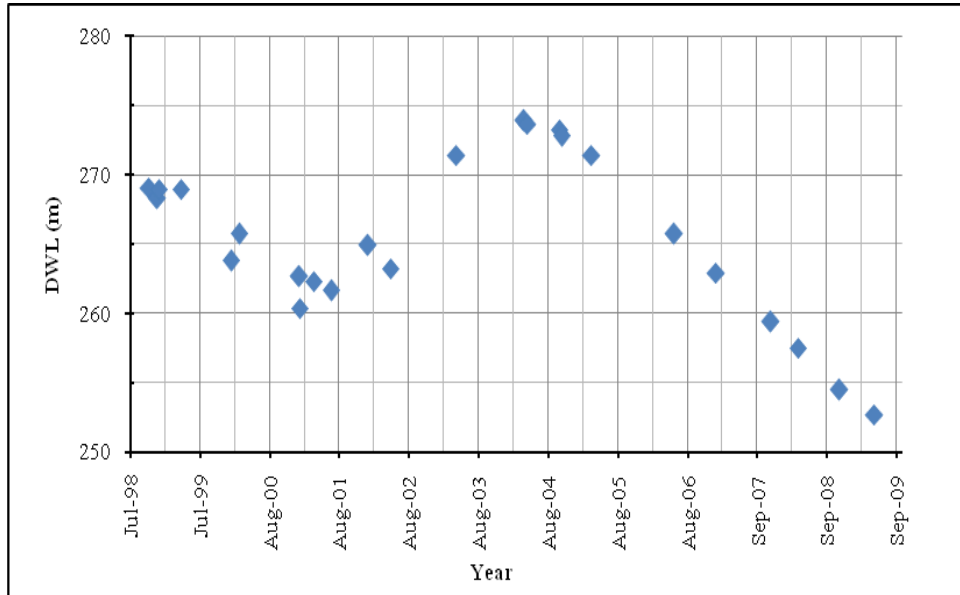


Figure 3.85 Drawdown of dynamic water level of well MTA-10 in different years.

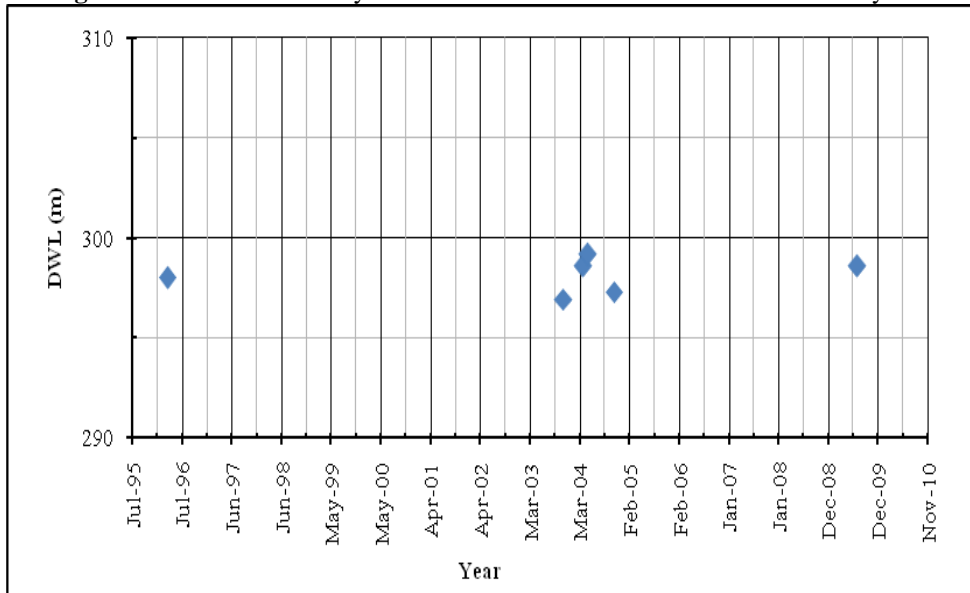


Figure 3.86 Drawdown of dynamic water level of well 13/74 in different years.

3.12 Chapter Conclusion

The information related with each well at Kyrenia Range aquifer is given in Appendix A, in which the detailed data can be easily deducted. Reviewing the data, one can conclude that:

Among these 11 regions, Boğazköy Region wells and Karaman Region wells were the highest discharging wells. The water pumping rates of these regions were 220 and 215 cubic meters per hour, respectively.

The highest yielding capacity well was found to be MTA-4 at Çatalköy region, pumping at rate of 100 m³/hr on the other hand the poorest water yielding wells were located at Kantara Region, including Mersinlik and Tathısu villages. The total pumping rate at the region was 20 m³/hr in total.

The poorest well in the Kyrenia Range is found to be MTA-9 at south foothills of Lapta region, with pumping rate of 2 m³/hr. For sure, the zero yielding wells were outliers for these criteria.

As a result of data compilation, a total abstraction from the wells spatially distributed on Kyrenia Range Aquifer was 1383m³/hr resulting in 12 MCM water consumption per year from the Kyrenia Range Aquifer.

CHAPTER 4

WATER BUDGET ANALYSIS

4.1 Water Budget Development

A ground-water system consists of a mass of water flowing through the pores or cracks below the Earth's surface. This mass of water is in motion. Water is constantly added to the system by recharge from precipitation, and water is constantly leaving the system as discharge to surface water and as evapotranspiration. Each ground-water system is unique in source and the amount of water flowing through the system is dependent upon external factors such as rate of precipitation, location of streams and other surface-water bodies, and rate of evapotranspiration. The one common factor for all ground-water systems, due to one of the basic laws known as the conservation of mass, which impels that, the total amount of water entering, leaving, and being stored in the system must be conserved. An accounting of all the inflows, outflows, and changes in storage is called water budget. Human activities, such as ground-water withdrawals and irrigation, changes in natural flow patterns must be accounted in the calculation of the water budget (Aeyll, et al; 2007).

Some hydrologists believe that a pre-development water budget for a ground-water system (that is, a water budget for the natural conditions before humans used the water) can be used to calculate the amount of water available for consumption (or the safe yield). In this case, the development of a ground-water system is considered to be "safe" if the rate of ground-water withdrawal does not exceed the rate of natural recharge. This concept has been referred to as the "Water-Budget Myth" (Bredehoeft and others, 1982).

It is a myth because it is an oversimplification of the information that is needed to understand the effects of developing a ground-water system. As human activities change the system, the components of the water budget (inflows, outflows, and changes in storage) also will change and must be accounted for in any management decision. Understanding water budgets and how they change in response to human activities is an important aspect of ground-water hydrology; however, a pre-

development water budget by itself is of limited value in determining the amount of ground water that can be withdrawn on a sustained basis (Aeyll, et al; 2007).

4.2 Ground Water Budgets

Under predevelopment conditions, the ground-water system is in long-term equilibrium. That is, averaged over some period of time, the amount of water entering or recharging the system is approximately equal to the amount of water leaving or discharging from that system. Because the system is in equilibrium, the quantity of water stored in the system is constant or varies about some average condition in response to annual or longer-term climatic variations. This predevelopment water budget is shown schematically in Figure 4.1. The equation that describes the water budget of the predevelopment system can be writing as:

$$\text{Recharge (water entering)} = \text{Discharge (water leaving)}$$

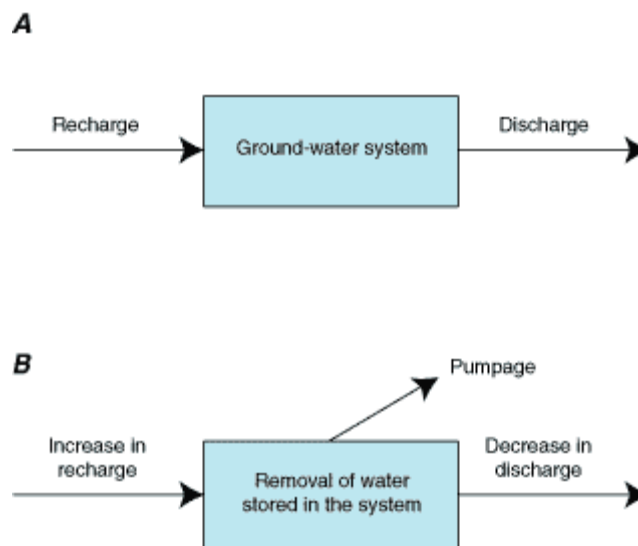


Figure 4.1 Diagrams illustrating water budgets for a ground-water system for predevelopment and development conditions (U.S. Geological Survey, 1999).

(A) Predevelopment water-budget diagram illustrating that inflow equals outflow. (B) Water-budget diagram showing changes in flow for a ground-water system being pumped. The sources of water for the pumpage are changes in recharge, discharge, and the amount of water stored. The initial predevelopment values do not directly enter the budget calculation.

The water leaving often is discharged to streams and rivers are called base flow. The possible inflows (recharge) and outflows (discharge) of a ground-water system under natural (equilibrium) conditions are listed in Table 4.1.

Table 4.1 Possible sources of water entering and leaving a ground-water system under natural conditions

Inflow (Recharge)	Outflow (Discharge)
1. Regional recharges from precipitation that percolates into aquifer system.	1. Discharge to streams, and springs.
2. Recharge from losing streams, lakes and wetlands.	2. Ground-water evapotranspiration

The sources of water for the pumpage are changes in recharge, discharge, and the amount of water stored. The initial predevelopment values do not directly enter the budget calculation.

This statement, illustrated in Figure 4.1B, can be written in terms of rates (or volumes over a specified period of time) as:

$$P = IR + WS + DD \quad (4.1)$$

In which P represents the pumpage from the aquifer (m^3/sec); IR represents the increased recharge rate (m^3/sec); WS is the volumetric rate of water removed from the storage (m^3/sec); and DD is the decreased discharge from the aquifer (m^3/sec).

It is the change in the system that allows water to be withdrawn. That is, the water pumped must come from some change of flows and from removal of water stored in the predevelopment system (Theis, 1940; Lohman, 1972).

Regardless of the amount of water withdrawn, the system will undergo some drawdown in water levels in pumping wells to induce the flow of water to these wells, which means that some water initially is removed from storage. Thus, the ground-water system serves as both a water reservoir and a water-distribution system. For most ground-water systems, the change in storage in response to pumping is a transient phenomenon that occurs as the system readjusts to the pumping stress. The relative contributions of changes in storage, changes in recharge, and changes in discharge evolve with time. The initial response to withdrawal of water is changes in storage. If the system can come to a new equilibrium, the changes in storage will stop and inflows will again balance outflows:

$$P = IR + DD \quad (4.2)$$

Thus, the long-term source of water to discharging wells is typically a change in the amount of water entering or leaving the system. How much ground water is available for use depends upon how these changes in inflow and outflow affect the surrounding environment and what the public defines as undesirable effects on the environment.

Discharge also occurs as seepage to bays or the ocean in coastal areas and as transpiration by plants whose roots extend to near the water table. The three-dimensional body of earth material saturated with moving ground water that extends from areas of recharge to areas of discharge is referred to as a ground-water-flow system as detailed in Figure 2.3 (Aeyll, et al; 2007).

In this local scale ground-water-flow system, inflow of water from areal recharge occurs at the water table. Outflow of water occurs as (1) discharge to the atmosphere as ground-water evapotranspiration (transpiration by vegetation rooted at or near the water table or direct evaporation from the water table when it is at or close to the land surface) and (2) discharge of ground water directly through the streambed. Short, shallow flow paths originate at the water table near the stream. As distance from the stream increases, flow paths to the stream are longer and deeper. For long-term average conditions, inflow to this natural groundwater system must equal outflow. The areal extent of ground-water-flow systems varies from a few square kilometers or less to tens of thousands of square kilometers. The length of ground-water-flow paths ranges from a few meters to tens, and sometimes hundreds, of kilometers. A deep ground-water-flow system with long flow paths between areas of recharge and discharge may be overlain by, and in hydraulic connection with, several shallow, more local, flow systems as given in Figure 4.2. Thus, the definition of a ground-water-flow system is to some extent subjective and depends in part on the scale of a study. (Aeyll, et al; 2007).

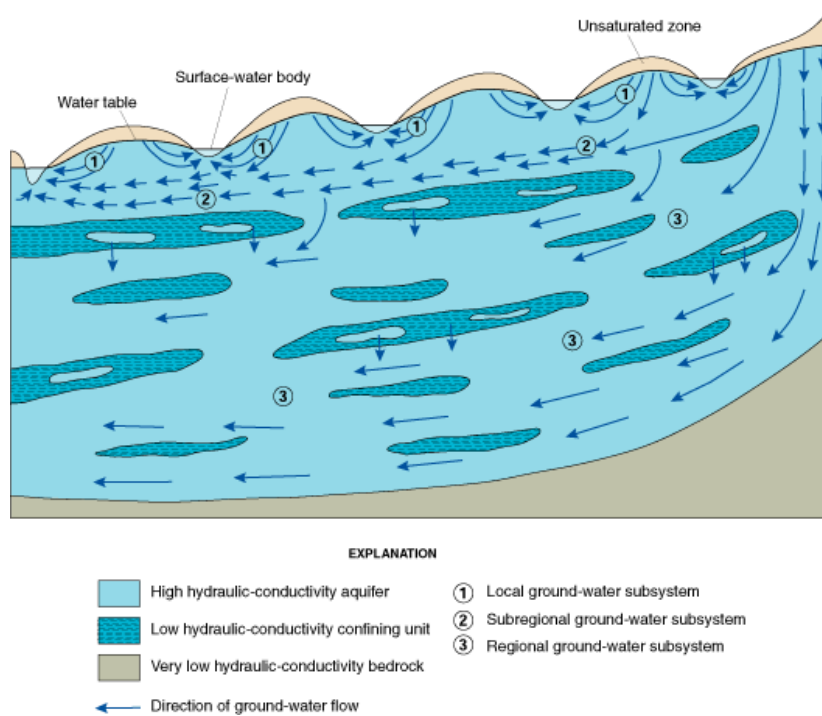


Figure 4.2 Regional ground-water-flow systems that comprises subsystems at different scales and a complex hydrogeologic framework (Sun, 1986).

Significant features of this depiction of part of a regional ground-water-flow system include (1) local ground-water subsystems in the upper water-table aquifer that discharge to the nearest surface-water bodies (lakes or streams) and are separated by ground-water divides beneath topographically high areas; (2) a sub-regional ground-water subsystem in the water-table aquifer in which flow paths originating at the water table do not discharge into the nearest surface-water body but into a more distant one; and (3) a deep, regional ground-water-flow subsystem that lies beneath the water-table subsystems and is hydraulically connected to them. The hydrogeologic framework of the flow system exhibits a complicated spatial arrangement of high hydraulic-conductivity aquifer units and low hydraulic-conductivity confining units. The horizontal scale of the figure could range from tens to hundreds of kilometers (Aeyll, et al; 2007).

4.3 Evapotranspiration (ET_o)

Evapotranspiration is the combination of soil evaporation and crop transpiration. Weather parameters, crop characteristics, management and environmental aspects affect evapotranspiration. The

evapotranspiration rate from a reference surface is called the reference evapotranspiration and is denoted as ETo . A large uniform grass (or alfalfa) field is considered worldwide as the reference surface. The reference grass crop completely covers the soil, is kept short, well watered and is actively growing under optimal agronomic conditions (Figure 4.3).

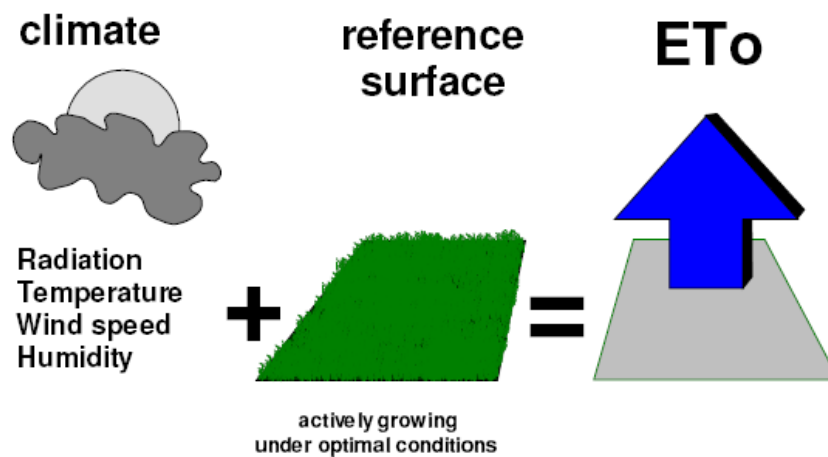


Figure 4.3 Reference evapotranspiration (ETo), source (FAO, 2009).

The concept of the reference evapotranspiration was introduced to study the evaporative demand of the atmosphere independently of crop type, crop development and management practices. As water is abundantly available at the reference evapotranspiring surface, soil factors do not affect ETo . Relating evapotranspiration to a specific surface provides a reference to which evapotranspiration from other surfaces can be related. ETo values measured or calculated at different locations or in different seasons are comparable as they refer to the evapotranspiration from the same reference surface. The only factors affecting ETo are climatic parameters. Consequently, ETo is a climatic parameter and can be computed from weather data. ETo expresses the evaporating power of the atmosphere at a specific location and time of the year and does not consider the crop characteristics and soil factors (Allen et al., 1998).

A revision of the procedures for estimating crop water requirements was undertaken following an expert meeting in Rome in 1990. New procedures were elaborated including a revised method for estimating reference evapotranspiration (ETo), published in 1998 as I&D No. 56 by Allen, Pereira, Raes and Smith (1998). Calculation procedures for crop water management and applications for

planning and management in irrigated and rain fed agriculture were further facilitated by the development of computerized procedures in CROPWAT, published Smith in 1992 (Kassam and Smith, 2001).

Owing to the difficulty of obtaining accurate field measurements, ETo is commonly computed from weather data. A large number of empirical or semi-empirical equations have been developed for assessing reference evapotranspiration from meteorological data. Numerous researchers have analyzed the performance of the various calculation methods for different locations. The FAO Penman-Monteith method is now recommended as the standard method for the definition and computation of the reference evapotranspiration ETo (Raes, 2009).

4.3.1 FAO Penman-Monteith Equation

A consultation of experts and researchers was organized by FAO in May 1990, in collaboration with the International Commission for Irrigation and Drainage and with the World Meteorological Organization, to review the FAO methodologies on crop water requirements and to advice on the revision and update of procedures.

CROPWAT is a decision support system developed by the Land and Water Development Division of FAO for planning and management of irrigation. CROPWAT is meant as a practical tool to carry out standard calculations for reference evapotranspiration, crop water requirements and crop irrigation requirements, and more specifically the design and management of irrigation schemes. It allows the development of recommendations for improved irrigation practices, the planning of irrigation schedules under varying water supply conditions, and the assessment of production under rained conditions or deficit irrigation.

According to the analysis of CROPWAT (Smith, 1992) that is based on the FAO-Penman Monteith method, the mean daily evapotranspiration values in the study area can be found. The FAO Penman-Monteith method calculates the evapotranspiration values (ETo) based on the following equation:

$$ET_o = \frac{0.408\Delta(R_n - G) + \gamma(900/(T + 273))U_2(e_s - e_a)}{\Delta + \gamma(1 + 0.34U_2)} \quad (4.3)$$

where E_{To} is the reference evapotranspiration (mm/day), R_n is the net radiation at the crop surface ($\text{MJ}/\text{m}^2\text{day}$), G is the soil heat flux density ($\text{MJ}/\text{m}^2\text{day}$), T is the mean daily air temperature at 2-m height ($^{\circ}\text{C}$), U_2 is the wind speed at 2-m height (m/sec), e_s is the saturation vapor pressure (kPa), e_a is the actual vapor pressure (kPa), Δ is the slope of the vapor pressure curve ($\text{kPa}/^{\circ}\text{C}$), and γ is the psychrometric constant ($\text{kPa}/^{\circ}\text{C}$).

The parameters that affect the magnitude of evapotranspiration are temperature, humidity, sunshine and wind speed. These parameters affect the results of FAO-Penman Monteith method.

The (average) daily maximum and minimum air temperatures in degrees Celsius ($^{\circ}\text{C}$) are required. Where only (average) mean daily temperatures are available, the calculations can still be executed but some underestimation of E_{To} will probably occur due to the non-linearity of the saturation vapour pressure - temperature relationship. Using mean air temperature instead of maximum and minimum air temperatures yields a lower saturation vapour pressure e_s , and hence a lower vapour pressure difference ($e_s - e_a$), and a lower reference evapotranspiration estimate.

The (average) daily actual vapour pressure, e_a , in kilopascals (kPa) is required. The actual vapour pressure, where not available, can be derived from maximum and minimum relative humidity (%), psychrometric data (dry and wet bulb temperatures in $^{\circ}\text{C}$) or dewpoint temperature ($^{\circ}\text{C}$).

The (average) daily net radiation expressed in mega joules per square meter per day ($\text{MJ m}^{-2} \text{day}^{-1}$) is required. These data are not commonly available but can be derived from the (average) shortwave radiation measured with a pyranometer or from the (average) daily actual duration of bright sunshine (hours per day) measured with a (Campbell-Stokes) sunshine recorder.

The (average) daily wind speed in meters per second (m s^{-1}) measured at 2 m above the ground level is required. It is important to verify the height at which wind speed is measured, as wind speeds measured at different heights above the soil surface differ.

4.4 Infiltration Estimates

Infiltration is the process by which water on the ground surface percolates into the soil. The rate of infiltration decreases as the soil becomes saturated. If the precipitation rate exceeds the infiltration rate the surface runoff will occur. In theory, there are several ways to estimate the volume or the rate of infiltration of water into the soil. The three most famous methods are the Green-Ampt method, SCS method and Horton' method. All these methods require field measurements and soil properties to work accurately. However in this study there are no available data for such calculations. Therefore the Hydrologic balance equation will be used in order to extract the magnitude of infiltration at the Kyrenia Range Aquifers.

Based on the relationship between the hydrologic parameters the following formula can be written:

$$PPt = SF + ETo + INF \quad (4.4)$$

In which (PPt) is precipitation represents the data related with precipitation obtained from Metrological Department for the last fifteen years (mm/month); (SF) is Streamflow accepted to be equivalent to zero since it represents the surface flow; (ETo) is represent Evapotranspiration, the evapotranspiration values calculated by using FAO Penma Monteith equation, using the software CROPWAT (mm/month), and (INF) represent infiltration (mm/month).

4.4.1 Calculation of the Water Budget of Aquifer

According to the conservation of the mass the difference between the net water inflow and outflow from the aquifer will results in net change of volume of water per unit time within the system. The balance equation of the system can be given as in Equation 4.5;

$$Q_{\text{net}} = Q_{\text{inflow}} - Q_{\text{outflow}} \quad (4.5)$$

Where;

$$Q = \frac{\Delta V}{\Delta t} = \left(\frac{dh}{dt} \times \text{Area} \right)$$

Figure 4.4 describe the height of dh and the area of infiltration.

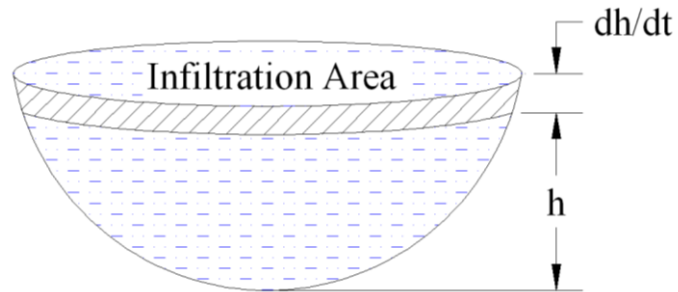


Figure 4.4 Water budget shape.

Then; from equation (4.1):

$$\frac{dh}{dt} \times \text{Area} = Q_{\text{inflow}} - Q_{\text{outflow}} \quad (4.6)$$

By dividing the both sides of the equation into the area of the water budget will result in

$$\frac{dh}{dt} = \frac{Q_{\text{Inflow}}}{\text{Area}} - \frac{Q_{\text{Outflow}}}{\text{Area}} \quad (4.7)$$

$$Q_{\text{inflow}} = \text{Infiltration (m/year)} * \text{Area}$$

Then;

$$\frac{dh}{dt} = \text{Infiltration} - \frac{Q_{\text{outflow}}}{\text{Area}} \quad (4.8)$$

Then;

$$\text{Area} = \frac{Q_{\text{outflow}}}{\frac{dh}{dt} + \text{Infiltration}} \quad (4.9)$$

4.4.2 Volume of Water Stored in the Aquifer

Since there is no information related with the water storage capacity and the shape of the aquifer, it is assumed that the water is stored in a spherical shaped aquifer. The assumption motivates the storage calculations to be done by using the frustum of a sphere (Figure 4.5). The Equation (4.10) is given as

$$V = \frac{1}{3} \pi h^2 (3r - h) \quad (4.10)$$

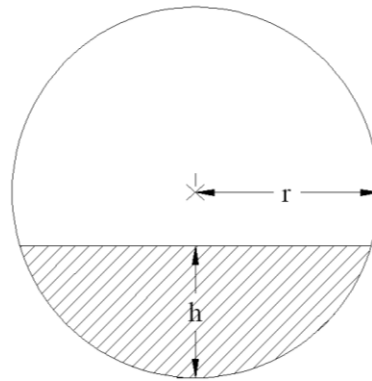


Figure 4.5 Frustum of sphere

The surface area occupied by the water stored in the aquifer can be deducted by the help of Equation (4.9). Since the radius used in the frustum of sphere formula (Equation 4.10) is the same as the radius of the spherical surface area of stored water, then one can easily deduct the radius of stored water by the Equation (4.11). Surface area of infiltration that recharges the aquifer and the change in water level in the aquifer defines the volume of water

$$A = \pi r^2 \quad (4.11)$$

$$r = \sqrt{\frac{A}{\pi}} \quad (4.12)$$

Figure 4.6 simply shows the cross sectional drawing of the aquifer system. The radius of the circular surface area of the frustum shape is then inserted into Equation (4.10) and the volume of water stored in each aquifer system is determined.

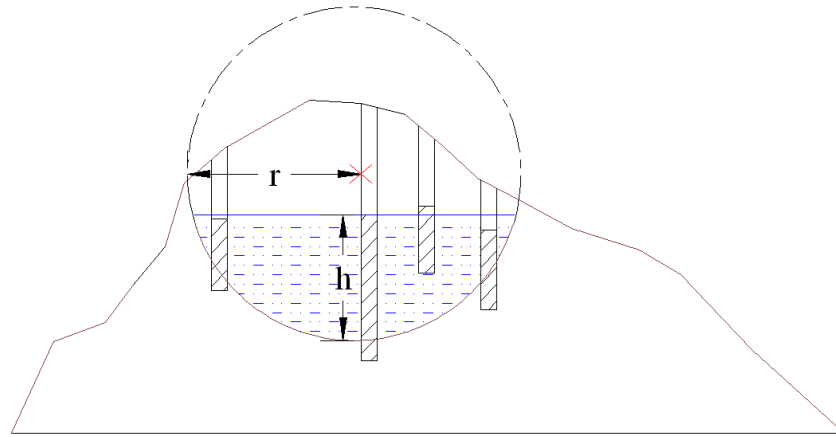


Figure 4.6 Cross section for water storage in an aquifer.

The calculations derived as above are based on the fact that the Kyrenia Range Aquifers are following a homogenous and isotropic property. Also, the assumption of overlap between the aquifer surface area and the infiltration area is another fact that is not reflecting the real conditions. However, due to lack of data and information related with the infiltration rates at the region, these assumptions were inevitable during the water budget calculations of the aquifers. Since there have been no geological and geophysical studies at the aquifers, there is no information related with the porosity of the aquifers. Hence, the information given by Dixey, 1975 will be used to define the porosity of the aquifer systems. Dixey has mentioned that the porosity of the aquifer is around 25% at Kyrenia Range.

CHAPTER 5

WATER BUDGET CALCULATIONS FOR 11 REGIONS

5.1 Calculation Procedures for Evapotranspiration

In the first section of this chapter, the Penman Monteith Formula is applied to Lapta region as an example for calculating the evapotranspiration. The second section shows the result for determining the water budget for all the regions of Kyrenia Range Aquifer. The process of calculation and results are shown as follow;

5.1.1 The Penman Monteith Formula

$$ET_o = \frac{0.408\Delta(R_n - G) + \gamma \frac{900u_2(e_s - e_a)}{T + 273}}{\Delta + \gamma(1 + 0.34u_2)} \quad (5.1)$$

5.1.2 The Psychrometric Constant (γ)

$$\gamma = \frac{c_p P}{\epsilon \lambda} = 0.665 \times 10^{-3} P \quad (5.2)$$

$$P = 101.3 \left(\frac{293 - 0.0065z}{293} \right)^{5.26} \quad (5.3)$$

From equation (5.3), where; P= 98.96 kPa, at z = 200 m for (Lapta Region);

Solved by equation (5.2)

$$\gamma = \frac{1.013 \times 10^{-3} \times 98.96}{0.622 \times 2.45}$$

$$\gamma = 0.066 \text{ kPa } ^\circ\text{C}^{-1}$$

5.1.3 Saturation vapour pressure $e^{\circ}(T)$

$$e^{\circ}(T) = 0.6108 \exp\left(\frac{17.27T}{T + 237.3}\right) \quad (5.4)$$

According to the data gathered from Department of Meteorology (Table 5.1 and 5.2) maximum temperature for Lapta region $T_{\max} = 26.5^{\circ}\text{C}$ and $T_{\min} = 15.8^{\circ}\text{C}$. As shown in Tables 5.1 and 5.2.

From equation (5.4):

$$e^{\circ}(T_{\max}) = 3.462 \text{ kPa, minimum } e^{\circ}(T_{\min}) = 1.795 \text{ kPa,}$$

$$e_s = \frac{e^{\circ}(T_{\max}) + e^{\circ}(T_{\min})}{2} \quad (5.5)$$

$$e_s = \frac{e^{\circ}(3.462) + e^{\circ}(1.795)}{2}$$

$$e_s = 2.629 \text{ kPa}$$

$$e^{\circ}(T_{\max}) = 3.462 \text{ kPa}$$

$$e^{\circ}(T_{\min}) = 1.795 \text{ kPa}$$

Table 5.1 Minimum Monthly Temperature Averages for Lapta, Boğaz, Alevkayası and Esentepe regions. (Meteorology Department, 2010).

Min average T(°C)		Jan	Feb	Mar	Apr	May	Jun	July	Agu	Sep	Oct	Nov	Dec	Yearly
LAPTA	1985-2010	9.2	9.0	10.4	12.9	16.5	20.7	23.5	23.8	21.1	18.1	13.9	10.7	15.8
BOĞAZ	1995-2010	5.2	3.7	5.6	8.4	12.8	18.4	21.2	21.0	18.1	14.0	8.5	6.8	12.0
ALEVKAYASI	1985-2010	4.8	4.6	6.4	9.6	13.7	17.9	20.7	20.9	18.0	14.8	10.0	6.4	12.3
ESENTEPE	1985-2010	8.1	7.9	9.3	12.1	16.6	20.6	23.4	23.5	21.0	17.8	13.2	9.7	15.3

Table 5.2: Maximum Monthly Temperature Averages for Lapta, Boğaz, Alevkayası and Esentepe region. (Meteorology department, 2010).

Max average T(°C)		Jan	Feb	Mar	Apr	May	Jun	July	Agu	Sep	Oct	Nov	Dec	Yearly
LAPTA	1985-2010	18.0	18.8	20.9	23.9	29.8	32.3	35.1	35.1	32.0	29.3	23.5	19.7	26.5
BOĞAZ	1995-2010	15.1	15.5	18.4	22.6	28.0	32.6	35.9	35.6	31.6	27.0	21.5	16.8	25.0
ALEVKAYASI	1985-2010	11.4	11.6	14.5	19.3	24.5	28.7	31.0	31.6	28.4	23.5	17.7	13.1	21.4
ESENTEPE	1985-2010	13.9	14.5	16.7	20.8	25.2	29.7	32.7	32.4	29.6	25.4	19.8	15.4	23.0

5.1.4 Actual Vapour Pressure (e_a)

$$e_a = e(T_{\text{dew}} \approx T_{\text{min}}) = 0.611 \exp \left[\frac{17.27 T_{\text{min}}}{T_{\text{min}} + 237.3} \right] \quad (5.6)$$

$$e_a = e(T_{\text{dew}} \approx T_{\text{min}}) = 0.611 \exp \left[\frac{17.27(15.8)}{(15.8) + 237.3} \right]$$

Where T_{min} is in °C. then,

$$e_a = 1.796 \text{ kPa.}$$

5.1.5 Slope of the Vapour Pressure Curve (Δ)

$$\Delta = \frac{4098 \left[0.6108 \exp \left(\frac{17.27 T}{T + 237.3} \right) \right]}{(T + 237.3)^2} \quad (5.7)$$

$$\Delta = \frac{4098 \left[0.6108 \exp \left(\frac{17.27(21.15)}{21.15 + 237.3} \right) \right]}{(21.15 + 237.3)^2}$$

T: the mean air temperature, $T = \frac{15.8 + 26.5}{2} = 21.15$ °C then,

$$\Delta = 0.153 \text{ kPa } ^\circ\text{C}^{-1}$$

5.1.6 The soil heat flux (G)

$$G = c_s \frac{T_j + T_{j-1}}{\Delta t} \Delta z \quad (5.8)$$

$$G_{\text{month},j} = 0.14 \left(T_{\text{month},j} - T_{\text{month},j-1} \right) \quad (5.9)$$

$$G = 0.14(13.9 - 13.6)$$

$$G = 0.042 \text{ MJ m}^{-2} \text{ day}^{-1}$$

5.1.7 Wind Speed (u_2)

$$u_2 = u_z \frac{4.87}{\ln(67.8z - 5.42)} \quad (5.10)$$

$$u_2 = 2 \frac{4.87}{\ln(67.8z - 5.42)}$$

$$u_2 = 2.0 \text{ m s}^{-1}$$

5.1.8 Calculation Procedure of the Net Radiation (R_n)

5.1.8.1 Extraterrestrial Radiation for Daily Periods (R_a)

$$R_a = \frac{24 \times 60}{\pi} G_{sc} d_r \left(\omega_s \sin \varphi \sin \delta + \cos \varphi \cos \delta \sin \omega_s \right) \quad (5.11)$$

$$d_r = 1 + 0.033 \cos \left(\frac{2\pi}{365} J \right) = 1 + 0.033 \cos(0.0172J) \quad (5.12)$$

$$d_r = 1.033$$

$$\delta = 0.409 \sin \left(\frac{2\pi}{365} J - 1.39 \right) = 0.409 \sin(0.0172J - 1.39) \quad (5.13)$$

$$\delta = -0.0403$$

Then, solved by following equation,

$$R_a = \frac{24 \times 60}{\pi} 0.0820 \times 1.033 (1.751 \times 0.027 \times (-0.007) + 0.819 \times 1 \times 0.027)$$

$$R_a = 1.966 \text{ MJ m}^{-2} \text{ day}^{-1}$$

5.1.8.2 Solar Radiation (R_s)

5.1.8.2.1 Clear-Sky Solar Radiation (R_{so})

$$R_{so} = 0.75 R_a \quad (5.14)$$

$$R_{so} = 1.475 \text{ MJ m}^{-2} \text{ day}^{-1}$$

$$R_s = \left(a_s + b_s \frac{n}{N} \right) R_a \quad (5.15)$$

$$R_s = k_{Rs} (T_{\max} + T_{\min})^{1/2} R_a$$

$$R_s = 2.43 \text{ MJ m}^{-2} \text{ day}^{-1}$$

5.1.8.2.2 Net Solar or Net Shortwave Radiation (R_{ns})

$$R_{ns} = (1 - \alpha) R_s \quad (5.16)$$

$$R_{ns} = (1 - 0.23) \cdot 2.43$$

$$R_{ns} = 1.871 \text{ MJ m}^{-2} \text{ day}^{-1}$$

5.1.8.2.3 Net Longwave Radiation (R_{nl})

$$R_{nl} = f \cdot \varepsilon \cdot \sigma \cdot \frac{(T_{\max}^4 + T_{\min}^4)}{2} \quad (5.17)$$

$$f = \left(a_c \frac{R_s}{R_{so}} + b_c \right) \quad (5.18)$$

To find f from Equation (5.18),

$$f = \left(1.35 \frac{2.34}{1.475} + (-0.35) \right)$$

$$f = 1.874$$

$$\varepsilon = (a_1 + b_1 \sqrt{e_a}) \quad (5.19)$$

To find ε from Equation (5.19),

$$\varepsilon = (0.34 + (-0.14) \sqrt{1.796})$$

$$\varepsilon = 0.152$$

Then by substitute in equation (5.17),

$$R_{nl} = 1.874 \times 0.152 \times 4.903 \times 10^{-9} \frac{(26.5^4 + 15.8^4)}{2}$$

$$R_{nl} = 0.00039 \text{ MJ m}^{-2} \text{ day}^{-1}$$

5.1.8.3 Net Radiation (R_n)

$$R_n = R_{ns} - R_{nl} \quad (5.20)$$

$$R_n = 1.871 - 0.00039$$

$$R_n = 1.871 \text{ MJ m}^{-2} \text{ day}^{-1}$$

Finally from all the result of calculation by substitute at Equation (5.1):

$$ET_{oLapta} = 51.047 \text{ mm/month}$$

5.2 Calculating the Infiltration of the Kyrenia Range

5.2.1 Process of Calculating the Water Budget at Karşıyaka Region

The calculation process to find the volume of water budget; the infiltration quantity and the evapotranspiration (ET_o) of Karşıyaka region have been determined as shown below in Table 5.3.

Table 5.3 Result of Infiltration and Evapotranspiration

Month	Min Temp °C	Max Temp °C	Humidity %	Wind m/s	ETo mm/month	Ppt (mm)/month	Infiltration (mm)/month	Total Infiltration m/year
January	9.2	18	66	3.8	73.78	98.5	24.7	0.025
February	9	18.8	66	4.2	79.8	117.5	37.7	0.038
March	10.4	20.9	65	4.1	110.36	52.8	-57.6	0
April	12.9	23.9	63	4.1	136.5	17.6	-118.9	0
May	16.5	29.8	65	4.1	184.45	11.1	-173.4	0
June	20.7	32.3	61	4.4	204.9	6.3	-198.6	0
July	23.5	35.1	60	4.2	226.61	1.9	-224.7	0
August	23.8	35.1	63	3.7	203.98	1.7	-202.3	0
September	23.1	32	64	4.2	165.3	4.7	-160.6	0
October	18.1	29.3	66	3.6	132.99	28.4	-104.6	0
November	13.9	23.5	66	2.3	76.2	62.2	-14	0
December	10.7	19.7	68	3.6	72.54	131.4	58.8	0.059
							Total Infiltration	0.121

where in Table 5.3; minimum temperature, maximum temperature and precipitation (ppt) information's are gathered from the database of State Meteorology Department, Northern Cyprus.

ET_o: the evapotranspiration is calculated by using the Penman-Monteith method using FAO-CROPWAT 8 program.

The infiltration results found as:

$$\text{Infiltration} = \text{PPt} - \text{ET}_o$$

Depending on the data analysis for water well pumping, at Karşıyaka region there are two separate water budgets at areas of MTA-14 and MTA-1, as shown in Figure 5.1, to calculate the water budget, assumed the shape of aquifer as a frustum of sphere shape, so the volume is obtained from Equation (4.10), the Table 5.3 shows the result of calculation for water budget of the aquifer at Karşıyaka region.

$$\text{Area} = \frac{Q_{\text{outflow}}}{\frac{dh}{dt} + \text{Infiltration}} \quad (5.21)$$

Where the infiltration unit is (m/year) and;

$\frac{dh}{dt}$: The yearly change in water level by time in meters (m/year).

Q : is the total pumping rate (m³/year).

A : surface area of the aquifer.

$$A = \frac{455520}{10.28 + 0.121}$$

$$A = \frac{455520}{10.401}$$

$$A = 43796 \text{ m}^2$$

$$r = \sqrt{\frac{A}{\pi}} \quad r = \sqrt{\frac{43796}{\pi}} = 118.1 \text{ m}$$

Example for calculating the volume of water budget at Karşıyaka region:

$$V = \frac{1}{3} \pi h^2 (3r - h)$$

$$V = \frac{1}{3} \pi 54^2 (3 \times 118 - 54)$$

$$V = 916,246.0 \text{ m}^3$$

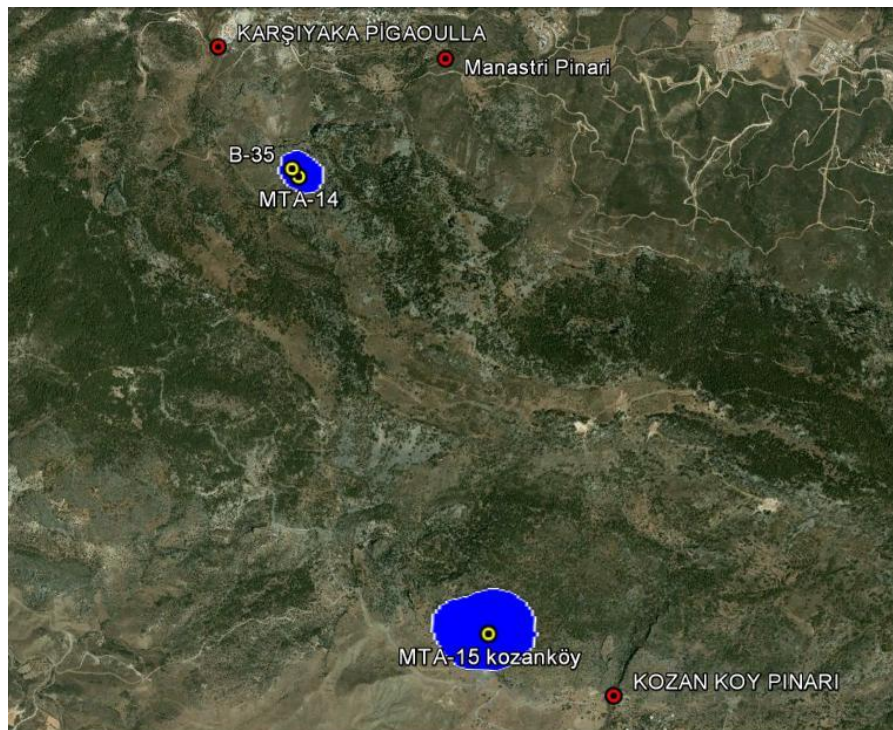


Figure 5.1 Top view of the aquifer at Karşıyaka Region (scale, 1:37,000).

At Karşıyaka region both MTA-14 and MTA-15 as shown in Figure 5.1 exist and the area of the water budget had been drawn after determining the surface area for each pumping well. Where the final calculations are shown at Table 5.4, summarizes the data which used for finding the area of infiltration and the volume of water budgets.

Table 5.4 Results of Calculation for aquifer of Karşıyaka Region

Karşıyaka region	(dh/dt) (m/year)	Infiltration (m/year)	Q (m ³ /year)	Area (m ²)	Water level(m)	Well depth(m)	h (m)	r (m)	V (m ³)
MTA-14	10.28	0.121	455,520	43,772	152	98	54	118.1	916,246.3
MTA-15	2.8	0.121	157,680	53,982	280	105	175	131.1	6,999,021.6

Where in table 5.4:

Q: The total pumping rate (m³/year).

A: The surface area of the aquifer (m²), it is assumed that the catchments area of the aquifer is overlapping with the connect saturation surface area of the aquifer.

V: volume of aquifer which assumed as a frustum of a sphere (m³).

h: difference in height between well depth and water level (m).

r: radius of assumed frustum (m).

Apart from the site location, the FAO Penman-Monteith equation requires latitude and elevation, the minimum and maximum daily air temperature, maximum relative humidity, solar radiation and wind speed data for even just monthly calculations.

Table 5.5 Results of Infiltration and Evapotranspiration of Karşıyaka Region.

Month	Min Temp °C	Max Temp °C	Humidity %	Wind m/s	ETo mm/month	PPt (mm)/month	Infiltration (mm)/month	Total Infiltration m/year
January	9.2	18	66	3.78	73.78	98.5	24.7	0.025
February	9	18.8	66	4.24	79.8	117.5	37.7	0.038
March	10.4	20.9	65	4.13	110.36	52.8	-57.6	0
April	12.9	23.9	63	4.10	136.5	17.6	-118.9	0
May	16.5	29.8	65	4.13	184.45	11.1	-173.4	0
June	20.7	32.3	61	4.40	204.6	6.3	-198.3	0
July	23.5	35.1	60	4.19	226.92	1.9	-225.1	0
August	23.8	35.1	63	3.72	203.98	1.7	-202.3	0
September	23.1	32	64	4.25	165.6	4.7	-160.9	0
October	18.1	29.3	66	3.63	132.99	28.4	-104.6	0
November	13.9	23.5	66	2.30	76.2	62.2	-14	0
December	10.7	19.7	68	3.61	72.54	131.4	58.8	0.059
								0.121 m/year

5.3 The Result of Water Budget Calculation of Kyrenia Region

5.3.1 Water Budget of Lapta Region

The final calculations to find the area of infiltration and the volume of the aquifers are shown at Table 5.6 and 5.7; for Lapta Region.

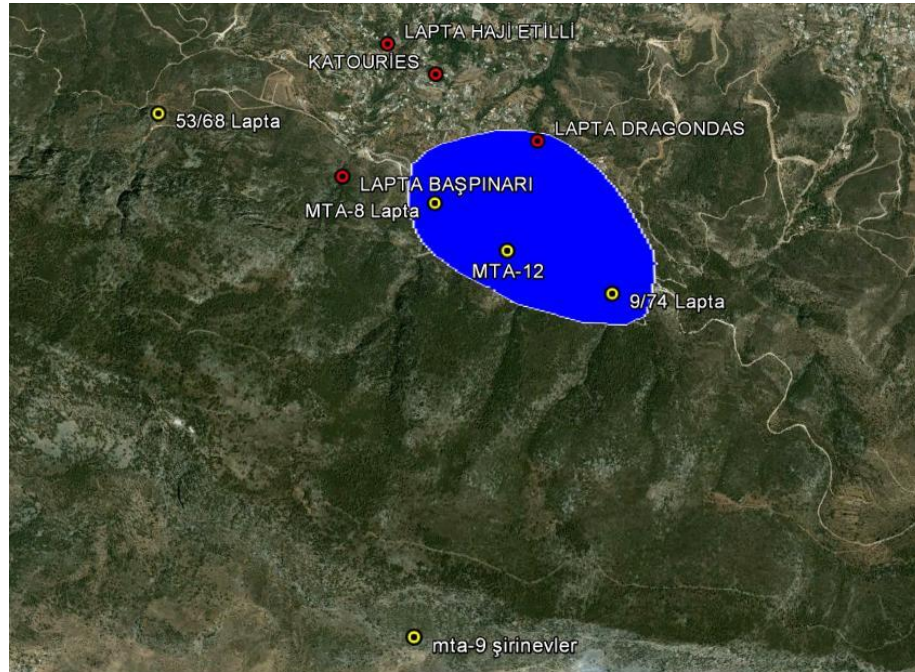


Figure 5.2 Top view of the aquifer at Lapta Region (scale, 1:37,000).

Table 5.6 Result of Infiltration and Evapotranspiration of Lapta Region.

Month	Min Temp °C	Max Temp °C	Humidity %	Wind m/s	ETo mm/month	Ppt (mm)/month	Infiltration (mm)/month	Total Infiltration m/year
January	9.2	18	66	3.78	73.78	98.5	24.7	0.025
February	9	18.8	66	4.24	79.8	117.5	37.7	0.038
March	10.4	20.9	65	4.13	110.36	52.8	-57.6	0
April	12.9	23.9	63	4.10	136.5	17.6	-118.9	0
May	16.5	29.8	65	4.13	184.45	11.1	-173.4	0
June	20.7	32.3	61	4.40	204.6	6.3	-198.3	0
July	23.5	35.1	60	4.19	226.92	1.9	-225.1	0
August	23.8	35.1	63	3.72	203.98	1.7	-202.3	0
September	23.1	32	64	4.25	165.6	4.7	-160.9	0
October	18.1	29.3	66	3.63	132.99	28.4	-104.6	0
November	13.9	23.5	66	2.30	76.2	62.2	-14	0
December	10.7	19.7	68	3.61	72.54	131.4	58.8	0.059
								0.121 m/year

Table 5.7 Calculation Result of the Aquifer of Lapta Region.

Lapta Region	dh/dt (m/year)	Infiltration m/year	Q (m ³ /year)	Area (m ²)	Water level(m)	well depth (m)	h (m)	r (m)	V (m ³)
MTA-8	0.75	0.121	35,040	40,230	268	108	160	113.2	4,811,520.1
MTA-12	3.14	0.121	280,320	85,886	266	192	74	165.4	2,419,604.6
9/74	5.60	0.121	306,600	53,592	241	38	203	130.6	8,148,868.2

5.3.2 Water Budget of Alsancak Region

The final calculations to find the area of infiltration and the volume of the aquifers are shown at Table 5.8 and 5.9; for Alsancak Region.



Figure 5.3 Top view of the aquifer at Alsancak region (scale, 1:46,000).

Table 5.8 The Result of Infiltration and Evapotranspiration of Alsancak Region.

Month	Min Temp °C	Max Temp °C	Humidity %	Wind m/s	ETo mm/day	ETo mm/month	PPt (mm)/month	Infiltration (mm)/month	Total Infiltration m/year
January	9.2	18	66	3.8	2.38	73.78	98.5	24.7	0.025
February	9	18.8	66	4.2	2.85	79.8	117.5	37.7	0.038
March	10.4	20.9	65	4.1	3.56	110.36	52.8	-57.6	0
April	12.9	23.9	63	4.1	4.55	136.5	17.6	-118.9	0
May	16.5	29.8	65	4.1	5.95	184.45	11.1	-173.4	0
June	20.7	32.3	61	4.4	6.83	204.9	6.3	-198.6	0
July	23.5	35.1	60	4.2	7.32	226.92	1.9	-225.1	0
August	23.8	35.1	63	3.7	6.59	204.29	1.7	-202.6	0
September	23.1	32	64	4.2	5.52	165.6	4.7	-160.9	0
October	18.1	29.3	66	3.6	4.3	133.3	28.4	-105	0
November	13.9	23.5	66	2.3	2.54	76.2	62.2	-14	0
December	10.7	19.7	68	3.6	2.34	72.54	131.4	58.8	0.059
									0.121

Table 5.9 The Calculation Result of the Aquifer of Alsancak Region

Alsancak region	dh/dt (m/year)	Infiltration m/year	Q (m ³ /year)	Area (m ²)	Water level(m)	well depth (m)	h (m)	r (m)	V (m ³)
1991/55	3.06	0.121	394,200	123,826	261	133	128	199	8,046,766
2005/20	3	0.121	262,800	84,204	297	120	177	164	10,334,410

5.3.3 Water Budget of Karaman Region

The final calculations to find the area of infiltration and the volume of the aquifers are shown at Table 5.10 and 5.11; for Karaman Region.

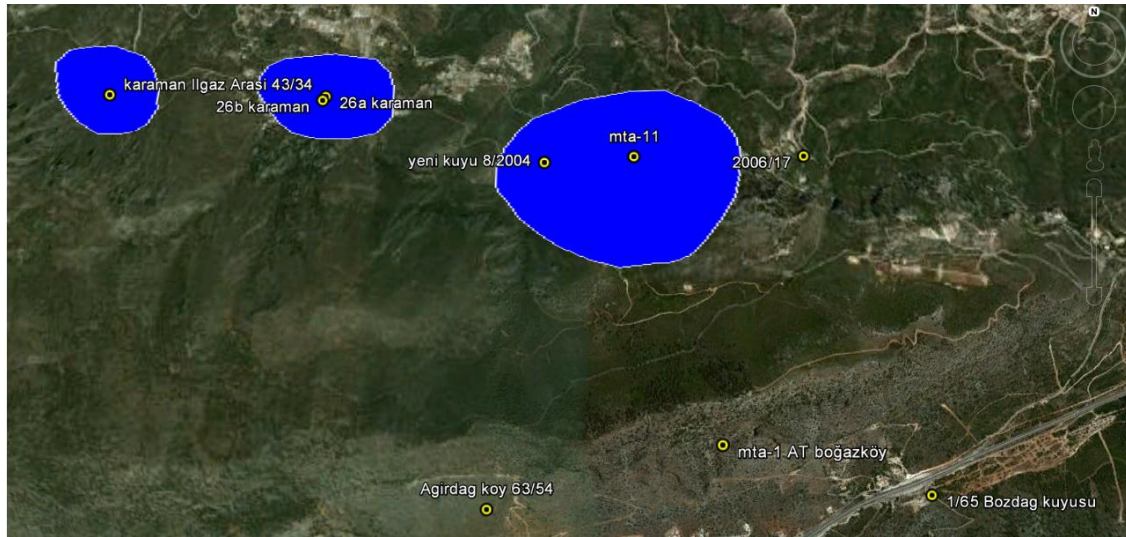


Figure 5.4 Top view of the aquifer at Karaman Region (scale, 1:35,000).

Table 5.10. The Result of Infiltration and Evapotranspiration of Karaman Region.

Month	Min Temp. °C	Max Temp. °C	Humidity %	Wind m/s	ETo mm/day	ETo mm/month	Ppt (mm)/month	Infiltration (mm)/month	Total Infiltration m/year
January	5.2	15.1	74	3.8	1.82	56.42	71.9	15.48	0.015
February	3.7	15.5	73	4.2	2.21	61.88	76.3	14.42	0.014
March	5.6	18.4	70	4.1	3	93	44	-49	0
April	8.4	22.6	65	4.1	4.21	126.3	15.9	-110.4	0
May	12.8	28	61	4.1	5.81	180.11	11.2	-168.91	0
June	18.4	32.6	59	4.4	6.93	207.9	8.1	-199.8	0
July	21.2	35.9	60	4.2	7.4	229.4	3.7	-225.7	0
August	21.2	35.6	63	3.7	6.63	205.53	0.2	-205.33	0
September	18.1	31.6	64	4.2	5.39	161.7	3.4	-158.3	0
October	14	27	66	3.6	3.99	123.69	24.2	-99.49	0
November	8.5	21.5	70	2.3	2.25	67.5	42.5	-25	0
December	6.8	16.8	74	3.6	1.85	57.35	79.2	21.85	0.022
								Total Infiltration	0.052

Table 5.11 The calculation result of the aquifer of Karaman region

Karaman	dh/dt (m/year)	Infiltration m/year	Q (m ³ /year)	Area (m ²)	Water level(m)	well depth (m)	h (m)	r (m)	V (m ³)
26A	2.6	0.052	175,200	49,324	205	190	15	125.3	85,015.3
26B	3.25	0.052	43,800	8,670	218	138	80	52.5	520,073.3
2004/8	5.5	0.052	525,600	94,669	229	94	136	173.6	7,451,452.2
MTA-11	4.33	0.052	350,400	79,903	214	95	119	159.5	5,329,355.9

5.3.4 Water Budget of Dikmen Region

The final calculations to find the area of infiltration and the volume of the aquifers are shown at Table 5.12 and 5.13; for Dikmen Region.



Figure 5.5 Top view of the aquifer at Dikmen Region (scale, 1:31,000).

Table 5.12. The Result of Infiltration and Evapotranspiration of Dikmen Region.

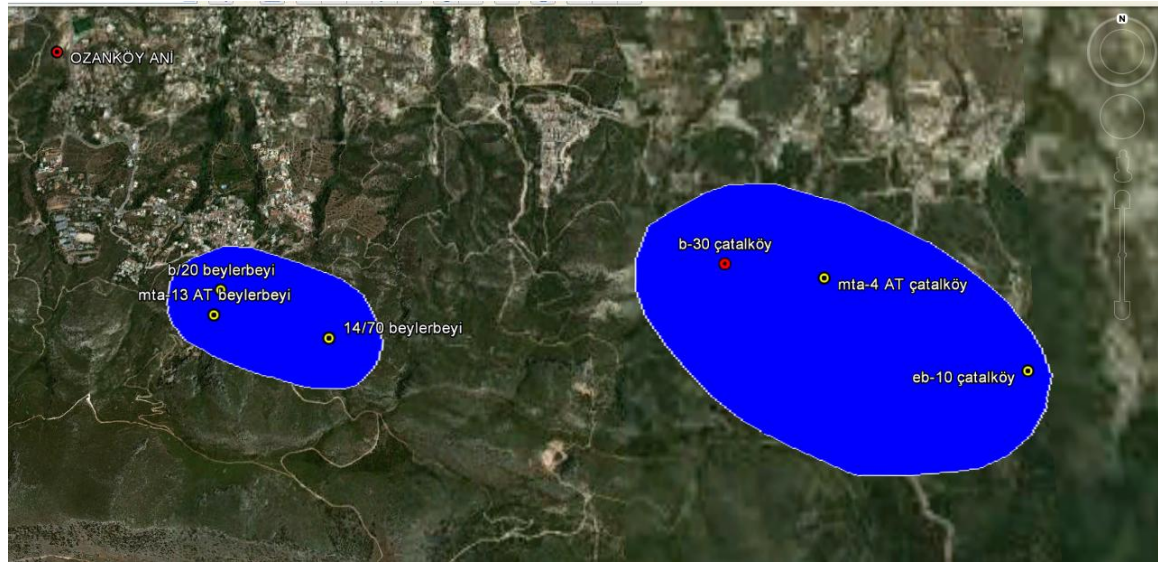
Month	Min Temp °C	Max Temp °C	Humidity %	Wind m/s	ETo mm/month	PPt (mm)/month	Infiltration (mm)/month	Total Infiltration m/year
January	5.2	15.1	74	1.5	41.23	71.9	30.67	0.031
February	3.7	15.5	73	1.6	48.16	76.3	28.14	0.028
March	5.6	18.4	70	1.3	73.78	44	-29.78	0
April	8.4	22.6	65	1.3	101.4	15.9	-85.5	0
May	12.8	28	61	1.4	146.32	11.2	-135.12	0
June	18.4	32.6	59	1.5	162.6	8.1	-154.5	0
July	21.2	35.9	60	1.4	177.94	3.7	-174.24	0
August	21.2	35.6	63	1.4	165.23	0.2	-165.03	0
September	18.1	31.6	64	1.4	120	3.4	-116.6	0
October	14	27	66	1.3	92.69	24.2	-68.49	0
November	8.5	21.5	70	1.2	54.6	42.5	-12.1	0
December	6.8	16.8	74	1.1	37.82	79.2	41.38	0.041
							Total Infiltration	0.1 (m/year)

Table 5.13. The Calculation Result of the Aquifer of Dikmen Region

Dikmen Region	dh/dt (m/year)	Infiltration m/year	Q (m ³ /year)	Area (m ²)	Water level(m)	well depth (m)	h (m)	r (m)	V (m ³)
1/74	0.69	0.1	262,800	1,280,308	275	248	27	326.0	725,640.6
22/74C	2.20	0.1	87,600	45,310	269	194	75	110.1	1,503,687.8
38/87	2.34	0.1	280,320	134,946	366	216	150	191.3	9,981,361.7

5.3.5 Water Budget of Çatalköy and Beylerbeyi Region

The final calculations to find the area of infiltration and the volume of the aquifers are shown at Table 5.14 and 5.15; for Çatalköy and Beylerbeyi Region.

**Figure 5.6** Top view of the aquifer at Çatalköy and Beylerbeyi region (scale, 1:36,000).**Table 5.14** The result of Infiltration and Evapotranspiration for Çatalköy and Beylerbeyi Region.

Month	Min Temp °C	Max Temp °C	Humidity %	Wind m/s	ETo mm/month	PPt (mm)/month	infiltration (mm)/month	Total Infiltration m/year
January	4.8	11.4	73	2.2	41.23	76.3	35.07	0.03507
February	4.6	11.6	72	2.9	48.72	80	31.28	0.03128
March	6.4	14.5	69	2.5	74.4	45.2	-29.2	0
April	9.6	19.3	63	2.3	105	26.7	-78.3	0
May	13.7	24.5	60	2.3	146.32	24.7	-121.62	0
June	17.9	28.7	57	2.4	176.4	11.4	-165	0
July	20.7	31	56	2.3	194.68	3.8	-190.88	0
August	20.9	31.6	59	2.2	182.28	1.6	-180.68	0
September	18	28.4	59	2.3	143.4	6	-137.4	0
October	14.8	23.5	62	2	99.51	26.8	-72.71	0
November	10	17.7	67	2.1	61.8	59.6	-2.2	0
December	6.4	13.1	73	2.2	42.78	95.1	52.32	0.05232
							Total Infiltration	0.11867 m/year

Table 5.15 The Calculation Result of the aquifer of Çatalköy and Beylerbeyi Region.

Çatalköy Region	dh/dt (m/year)	Infiltration m/year	Q (m ³ /year)	Area (m ²)	Water level(m)	well depth (m)	h (m)	r (m)	V (m ³)
MTA-13	3.25	0.119	262,800	168,605.3	78,005	63	107	157.6	4,384,023.0
B/20	1.00	0.119	140,160	280,320	125,255	244.5	14.5	199.7	128,664.5
14/70	0.88	0.119	26,280	29,863.64	26,244	342	9	91.4	22,489.4
B-30	0.00	0.119	175,200	0	1,472,269	152	111	684.7	25,059,912.2
MTA-2	0.83	0.119	175,200	185,150	183,969	196	50	242.1	1,769,270.7
MTA-4	1.64	0.119	876,000	534,146.3	499,042	150	163	398.7	28,726,101.7
EB-10	1.45	0.119	131,400	90,620.69	83,506	183	58	163.1	1,518,360.6

5.3.6 Water Budget of Değirmenlik Region

The final calculations to find the area of infiltration and the volume of the aquifers are shown at Table 5.16 and 5.17; for Değirmenlik Region.

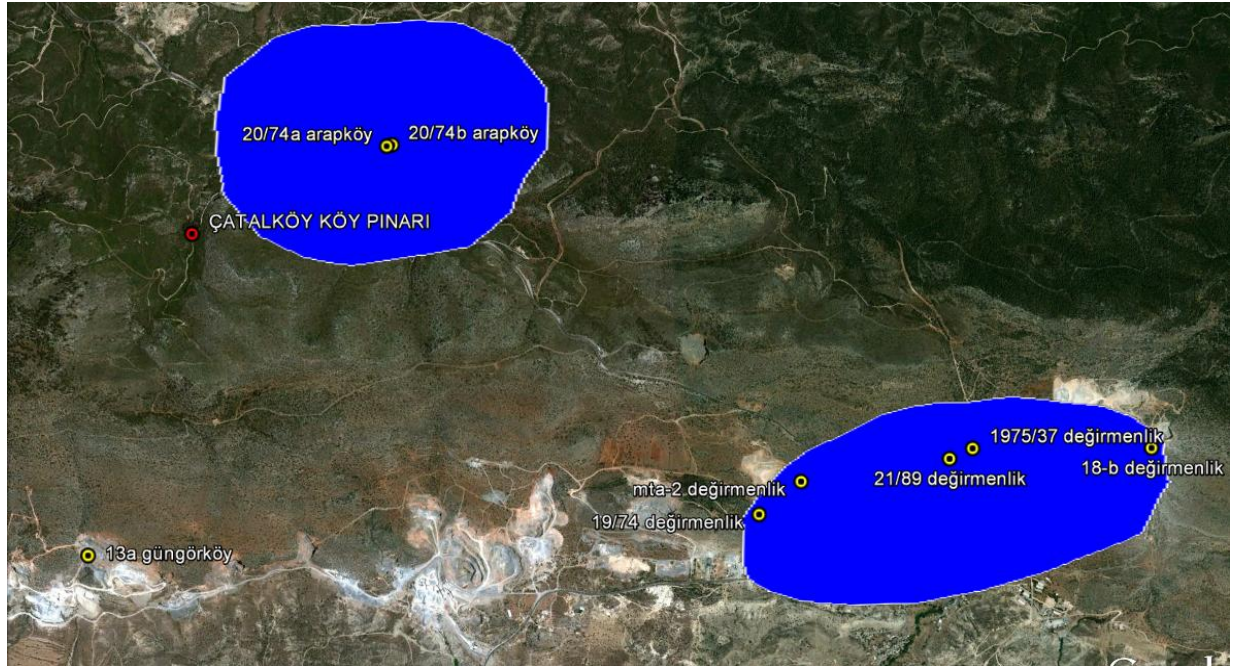


Figure 5.7 Top view of the aquifer at Değirmenlik Region (scale, 1:45,000).

Table 5.16 Result of Infiltration and Evapotranspiration of Değirmenlik Region.

Month	Min Temp °C	Max Temp °C	Humidity %	ET _o mm/day	ET _o mm/month	PPT (mm)/month	infiltration (mm)/month	Total Infiltration m/year
January	4.8	11.4	73	1.33	41.23	56.1	14.87	0.015
February	4.6	11.6	72	1.74	48.72	54.2	5.48	0.005
March	6.4	14.5	69	2.4	74.4	34.8	-39.6	0
April	9.6	19.3	63	3.51	105.3	16.9	-88.4	0
May	13.7	24.5	60	4.72	146.32	18.5	-127.82	0
June	17.9	28.7	57	5.89	176.7	10.2	-166.5	0
July	20.7	31	56	6.28	194.68	4.4	-190.28	0
August	20.9	31.6	59	5.89	182.59	2.3	-180.29	0
September	18	28.4	59	4.79	143.7	5.6	-138.1	0
October	14.8	23.5	62	3.21	99.51	23	-76.51	0
November	10	17.7	67	2.06	61.8	47.7	-14.1	0
December	6.4	13.1	73	1.38	42.78	59.6	16.82	0.017
							Total Infiltration	0.037

Table 5.17 The Calculation Result of the aquifer at Değirmenlik Region.

Değirmenlik	dh/dt (m/year)	Infiltration m/year	Q (m ³ /year)	Area (m ²)	Water level(m)	well depth (m)	h (m)	r (m)	V (m ³)
20/74A	1.10	0.037	350,400	308,179	254	173	81	313.3	5,897,873.1
20/74 B	0.84	0.037	350,400	399,207	242	173	69	356.6	4,986,586.7
75/37	0.59	0.037	930,750	1,046,330	239	85	154	577.3	39,164,636.3
21/89	1.90	0.037	260,640	135,674	242	196	46	207.9	1,279,231.9
18-B	2.09	0.037	438,000	205,836	229	217	12	256.0	113,959.2

5.3.7 Water Budget of Karaağaç Alevkayası Region

The final calculations to find the area of infiltration and the volume of the aquifers are shown at Table 5.18 and 5.19; for Karaağaç Alevkayası Region.

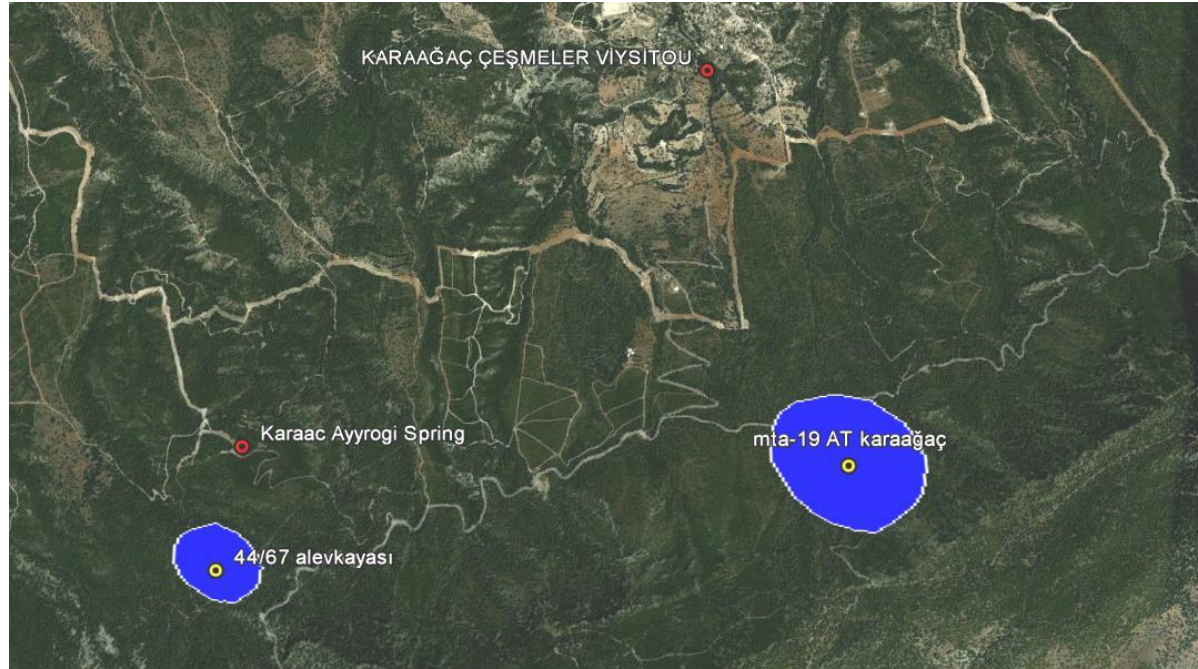


Figure 5.8 Top view of the aquifer at Karaağaç Alevkayası Region (scale, 1:33,000).

Table 5.18 The result of Infiltration and Evapotranspiration of Karaağaç Alevkayası Region

Month	Min Temp °C	Max Temp °C	Humidity %	ETo mm/day	ETo mm/month	Ppt (mm)/month	Infiltration (mm)/month	Total Infiltration m/year
January	4.8	11.4	73	1.19	36.89	76.3	39.41	0.039
February	4.6	11.6	72	1.53	42.84	80	37.16	0.037
March	6.4	14.5	69	2.18	67.58	45.2	-22.38	0
April	9.6	19.3	63	3.23	96.9	26.7	-70.2	0
May	13.7	24.5	60	4.39	136.09	24.7	-111.39	0
June	17.9	28.7	57	5.46	163.8	11.4	-152.4	0
July	20.7	31	56	5.78	179.18	3.8	-175.38	0
August	20.9	31.6	59	5.45	168.95	1.6	-167.35	0
September	18	28.4	59	4.31	129.3	6	-123.3	0
October	14.8	23.5	62	2.89	89.59	26.8	-62.79	0
November	10	17.7	67	1.75	52.5	59.6	7.1	0.007
December	6.4	13.1	73	1.22	37.82	95.1	57.28	0.057
							Total Infiltration	0.141

Table 5.19 The Calculation Result of the aquifer at Karaağaç Alevkayası Region.

Karaağaç Alevkayasi Region	dh/dt (m/year)	Infiltration m/year	Q (m ³ /year)	Area (m ²)	Water level(m)	well depth (m)	h (m)	r (m)	V (m ³)
44/67	1.32	0.141	105,120	71,883	280	230	50	151	1,055,051
MTA-19	1.12	0.141	175,200	182,665	322	248	74	241	3,721,660

5.3.8 Water Budget of Tirmen Region

The final calculations to find the area of infiltration and the volume of the aquifers are shown at Table 5.20 and 5.21; for Tirmen Region.

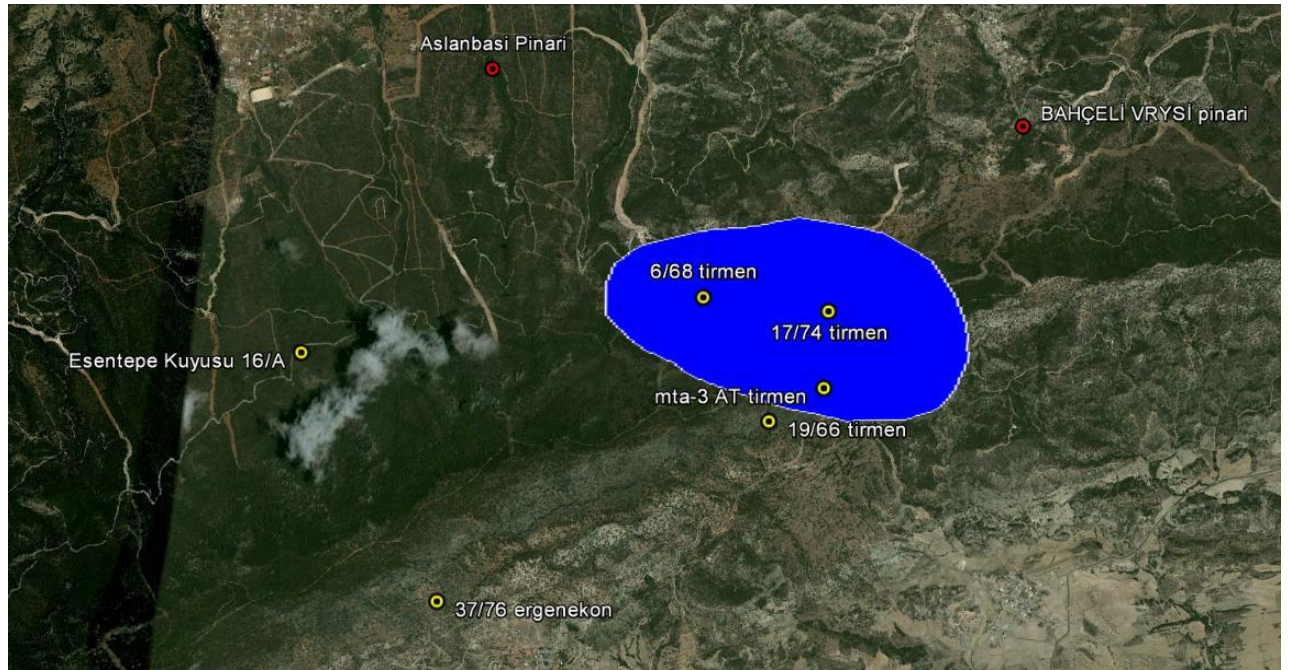


Figure 5.9 Top view of the aquifer at Tirmen Region (scale, 1:45,000).

Table 5.20 The Result of Infiltration and Evapotranspiration of Tirmen Region.

Month	Min Temp °C	Max Temp °C	Humidity %	ETo mm/month	PPt (mm)/month	Infiltration (mm)/month	Total Infiltration m/year
January	8.1	13.9	69	48.67	78.4	29.73	0.03
February	7.9	14.5	68	58.52	74.6	16.08	0.016
March	9.3	16.7	68	82.77	45.5	-37.27	0
April	12.1	20.8	65	109.8	22.4	-87.4	0
May	16.6	25.2	63	150.04	19.4	-130.64	0
June	20.6	29.7	60	181.2	10	-171.2	0
July	23.4	32.7	60	203.67	1.6	-202.07	0
August	23.5	32.4	62	188.17	1.6	-186.57	0
September	21	29.6	62	148.5	10.4	-138.1	0
October	17.8	25.4	64	104.47	31.6	-72.87	0
November	13.2	19.8	69	65.4	64.1	-1.3	0
December	9.7	15.4	65	53.63	92.6	38.97	0.039
						Total Infiltration	0.085

Table 5.21 The Calculation Result of the aquifer of Tirmen Region.

Tirmen Region	dh/dt (m/year)	Infiltration m/year	Q (m ³ /year)	Area (m ²)	Water level(m)	well depth (m)	h (m)	r (m)	V (m ³)
68/6	2.02	0.085	727,080	20,795	326	243	83	81.4	1,161,896.1
17/74	2.17	0.085	1,787,040	139,761	204	182	22	211.0	309,484.0
MTA-3	4.27	0.085	1,226,400	72,368	285	146	139	151.8	6,399,223.4

5.3.9 Water Budget of Kantara Region

The final calculations to find the area of infiltration and the volume of the aquifers are shown at

Table 5.22 and 5.23; for Kantara Region.



Figure 5.10 Top view of the aquifer at Kantara Region (scale, 1:135,000).

Table 5.22 The Result of Infiltration and Evapotranspiration of Kantara Region.

Month	Min Temp °C	Max Temp °C	Humidity %	ETo mm/month	Ppt (mm)/month	infiltration (mm)/month	Total Infiltration mm/year
January	8.1	13.9	69	48.67	105.4	56.73	0.057
February	7.9	14.5	68	58.52	85.5	26.98	0.027
March	9.3	16.7	68	82.77	58.8	-23.97	0
April	12.1	20.8	65	109.8	27.5	-82.3	0
May	16.6	25.2	63	150.04	28.3	-121.74	0
June	20.6	29.7	60	181.5	13.2	-168.3	0
July	23.4	32.7	60	203.67	3.4	-200.27	0
August	23.5	32.4	62	188.17	2.9	-185.27	0
September	21	29.6	62	148.5	5.5	-143	0
October	17.8	25.4	64	104.47	42	-62.47	0
November	13.2	19.8	69	65.1	66.3	1.2	0.001
December	9.7	15.4	65	53.63	118.9	65.27	0.065
						Total Infiltration	0.15

Table 5.23 The Calculation Result of the aquifer of Kantara Region

Kantara Region	dh/dt (m/year)	Infiltration m/year	Q (m ³ /year)	Area (m ²)	Water level(m)	well depth (m)	h (m)	r (m)	V (m ³)
116/65	2.12	0.139	219,000	196,538	191	33	158	250.2	15,482,757.1
B-3	2.75	0.139	131,400	45,310	208	76	132	120.1	4,164,909.2
B-1	5.6	0.15	52,560	9,141	347	337	10	54	15,917

5.3.10 Water Budget of Boğaz Region

The final calculations to find the area of infiltration and the volume of the aquifers are shown at Table 5.24 and 5.25; for Boğaz Region.

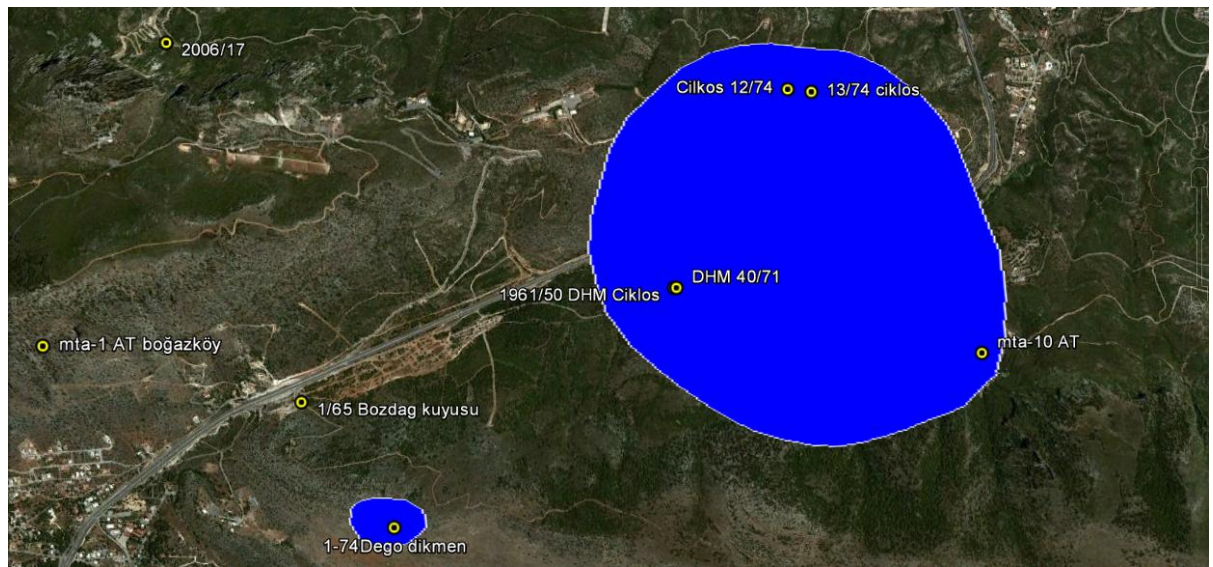


Figure 5.11 Top view of the aquifer at Boğaz Region (scale, 1:3,000).

Table 5.24 The Result of Infiltration and Evapotranspiration of Boğaz Region.

Month	Min Temp °C	Max Temp °C	Humidity %	ETo mm/month	PPt (mm)/month	Infiltration (mm)/month	Total Infiltration mm/year
January	5.2	15.1	74	46.81	71.9	25.09	0.025
February	3.7	15.5	73	56	76.3	20.3	0.02
March	5.6	18.4	70	83.39	44	-39.39	0
April	8.4	22.6	65	111.9	15.9	-96	0
May	12.8	28	61	159.34	11.2	-148.14	0
June	18.4	32.6	59	178.5	8.1	-170.4	0
July	21.2	35.9	60	196.54	3.7	-192.84	0
August	21.2	35.6	63	182.28	0.2	-182.08	0
September	18.1	31.6	64	135.3	3.4	-131.9	0
October	14	27	66	103.23	24.2	-79.03	0
November	8.5	21.5	70	65.4	42.5	-22.9	0
December	6.8	16.8	74	45.88	79.2	33.32	0.033
						Total Infiltration	0.079

Table 5.25 The Calculation Result of the aquifer of Boğaz Region

Boğaz Region	dh/dt (m/year)	Infiltration m/year	Q (m ³ /year)	Area (m ²)	Water level(m)	well depth (m)	h (m)	r (m)	V (m ³)
MTA-10	3.67	0.079	262,800	70,161	269	258	11	227	55,400.3
DHM-1	1.43	0.079	525,600	348,310	240	210	30	333	912,958.4
BOZDAG WELL 1/65	1.34	0.079	394,200	277,941	259	222	37	412	1,225,907.1

5.4 Overall capacity of the Kyrenia Range Aquifers

The water budget calculations based on hydrologic assumptions and field analysis presented the total volume of water stored in Kyrenia Range Aquifers. The summary of the results are shown in Table 5.26 in which the total water stored in the Aquifer is sum up to 322.5 MCM. The table summarizes the individual water capacities of each region.

Table 5.26 Water Stored Areas and Volume of Aquifer of 11 regions

Region Name	Infiltration (m/year)	Surface Areas of Aquifers (m ²)	Volume (m ³)
1 Karşıyaka (Vasillia) Region	0.121	97,753	7,915,267.9
2 Lapta (Lapithos) Region	0.121	179,708	15,379,992.9
3 Alsancak (Karavas) Region	0.121	215,741	18,326,517.9
4 Karaman (Karmi) Region	0.052	693,135	13,385,896.7
5 Dikmen (Dihkomo) Region	0.100	486,686	12,210,690.1
6 Çatalköy and Beylerbeyi (Ayios Epiktitos) Region	0.119	2,468,290	61,608,822.1
7 Değirmenlik (Kythrea) Region:	0.037	2,095,226	51,442,287.2
8 Karaağaç-Alevkayası (Alevga) Region	0.141	210,269	4,242,502.7
9 Tirmen (Trypimeni) Region	0.085	232,924	7,870,603.5
10 Kantara (Kantara) Region	0.150	250,990	19,663,561.4
11 Boğaz (Boghaz) Region	0.079	696,412	2,194,265.80
Total	1.126	7,627,134	214,240,408.20

The above calculation does not take into consideration the effect of porosity. Therefore, the resultant total volume represents as if there is no rocks or sediments in the karst system and the frustum shape is like a cave or hole. Since this is not the case and it is well known that the karst system is consisting of cracks on limestone formation, the porosity of the aquifer will be used to find the resultant volume of the water available in the aquifers. As a result 25 percent of the total volume will reflect the actual volume of water available in the aquifer system which is 53 million cubic meters.

CHAPTER 6

CONCLUSIONS

In this study, the spatial distributions of water supply wells at Kyrenia Range Aquifers are investigated. The study was initiated with a field visit, in which the dramatic situation of water resources of North Cyprus was once more approved.

Nevertheless, the information based on the monitoring program done by Water Works Department and the compilation of information from previous studies carried out at the region was the positive and useful inputs of this research. Except the wells drilled in 1996-1998 period and well monitoring studies of W.W.D at the region, the literature survey has shown that there were no serious studies carried out in the region after 1974.

Depending on the well monitoring program and the spatial distribution of wells, the Kyrenia Range Aquifer is divided into 11 regions, each region defined by well locations, springs, water levels and other properties.

Among these 11 regions, Boğazköy Region wells and Karaman Region wells were the highest discharging wells. The water pumping rates of these regions were 220 and 215 cubic meters per hour, respectively.

The highest yielding capacity well was found to be MTA-4 at Çatalköy region, pumping at rate of 100 m³/hr. On the other hand, the poorest water yielding wells were located at Kantara Region, including Mersinlik and Tatlısu villages. The total pumping rate at the region was 20 m³/hr in total.

The poorest well in the Kyrenia Range is found to be MTA-9 at south foothills of Lapta region, with pumping rate of 2 m³/hr. The well yielding data were summarized while zero yielding wells accepted as outliers.

As a result of data compilation, total pumping rate from the wells spatially distributed on Kyrenia Range Aquifers was 1383 m³/hr which yields annually 12 MCM consumption from Kyrenia Range Aquifer.

The spring water flow outflows are not considered in this study since the spring outflows were not worth to consider as water consumption from the existing aquifer system. On the other hand, it was observed that the highest spring flow rate was in Lapta Dragondas with 7.2 m³/hr discharging rate. The lowest spring flow rate was from Lapta Şht. Ahmet Kamil sokak Alt haji etilli spring with pumping rate of 0.0967 m³/hr. it should be mentioned that the flow of the springs increase in the winter season while approaching to nill flow during summer.

Evapotranspiration (ET_o), infiltration and precipitation were important factors of this study in order to determine the water budget of the aquifer. The Penman Monteith Formula was used to find the ET_o, and the groundwater budgets were determined by using the evapotranspiration ET_o, infiltration and precipitation simulations which were created by the help of CROPWAT, V 0.8 software.

Even though one of the scopes of the study was to find traces of common sharing between the wells and their properties drilled at southern and northern foothills of the Kyrenia Range aquifers, it was not possible to extract any result. Further analysis like isotope analysis is compulsory in order to extract such relationship.

The results of the water balance calculations depicted that still there exist 214 MCM water storage in the Kyrenia Range Aquifers. Neglecting the infiltration rate of precipitated water and assuming that the discharge will continue steadily (12 MCM/year) results in 5 years lifetime estimation for the Kyrenia Range Aquifers.

REFERENCES

- Allen, R.G., Pereira, L.S., Raes, D., Smith, M., 1998. Crop evapotranspiration: guidelines for computing crop water requirements. FAO Irrigation and drainage paper n. 56. Rome, Italy.
- Aeyll, W.M., 2007. T.E. Reilly, and O.L. Franke, Sustainability of Ground-Water Resources, U.S. Geological Survey Circular 1186.
- Batu V., 1998 Aquifers Hydraulics John Wiley & Sons, 27 Feb. 1998-727 Pages
- Bonacci, O., 2001. Analysis of maximum discharge of karst springs. Hydrogeology Journal; 328–338
- Bredehoeft JD, Papadopulos SS, Cooper HH Jr (1982) the Water Budget Myth. In: Scientific basis of water resource management, studies in geophysics. National Academy Press, Washington, DC.
- Bruker, R. W., J. W. Hess, & W. B. White. 1972. Role of vertical shafts in the movement of groundwater in carbonate aquifers. Ground Water 10, no 6:5-13.
- Currens, 2002. Kentucky is a karst country, Kentucky Geological Survey, 228 Mining and Mineral Resources Building university of Kentucky. Series XII, 2002.
- Dixey F., 1975. The Geology and Hydrogeology of the Kyrenia Range, Cyprus. Ministry of Overseas Development, London.
- Dixey F., 1971. Proc. Soc. London. No. 166, p 308-311.
- DSİ, 1982. Aydın, S. and Çultu, L.Kıbrıs Türk Federe Devleti Su ve Toprak Kaynakları, Master Plan Mühendeslik Hidrolojisi. Ön Çalışma Raporu, Enerji ve Tabii Kaynaklar Bakanlığı, Ankara.
- Ducloz, C., 1968. The quaternary terraces of Klepini. Archives des sciences, Geneva. Vol. 20, p 123-198.

El-Hakim M. and Bakalowicz M., 2006. Significance and origin of very large regulating power of some karst aquifers in the Middle East. Implication on karst aquifer classification.

Ewers, R. O., et al. 1978. The Origin of Distributary and Tributary flow within karst aquifers. Geological Society of America, Abstracts with Programs 10, no. 7:398-99.

FAO (1995) Cyprus: country report to the international conference and program on plant genetic resource. F. a. A. O. o. t. U. Nations, United Nations, p 38.

Fetter, C. W. 1942, Applied Hydrology. University of Wisconsin-Oshkosh, Third Edition, Prentice Hall, Upper Saddle River, New Jersey 07458, 691 p.

Freeze R. Allan, and Cherry A. John, 1979: Ground water. Prentice-Hall, V 1, 1979, Pages no 604.

Ford, D. C., & R. O. Ewers. 1978. The development of limestone cave system in the dimensions of length and depth. Canadian Journal of Earth Science 15:1783-98.

Gokcekus H. and Endreny TA., (2009) Ancient eco-technology of qanats for engineering sustainable water supply in the Mediterranean Island of Cyprus. Environmental Geology, 57 (2): 249-257.

Hadjicharalambous K. (2008) Karstic Phenomena - Problems In Gypsum Rocks of Cyprus Geological Survey Department, Cyprus, p 2.

Kassam A. and Smith M., 2001, FAO Methodologies on Crop Water Use and Crop Water Productivity. Paper No Cwp-M07.

Kansas Geological Survey, 1993, Kansas Ground Water, Comments to webadmin@kgs.ku.edu, Web version Jan. 2005, Original publication date August 1993. URL=http://www.kgs.ku.edu/Publications/Bulletins/ED10/04_occur.html

Lohman S. W. 1972 Ground water Hydraulics. Geological survey professional paper 708. US Government printing office Washington :1972.

Mangin, A., 1975. Contribution the study of hydrodynamic aquifers karstification. Ph.D Thesis, University of Dijon, p. 124.

Mixius and Kreysing, 1964. Hydrological Investigation and ground water development in the kyrenia range of Cyprus.(German Technical Assistance).

MOA (2005) Vegetation and flora of Cyprus. Ministry of Agriculture, Natural Resources and Environment, Forestry Department.

Moore, T.A., 1967 Geology and mineral resources of the Astromeritis and Kormakiti area. Geological Department, Nicosia, publ. no. 6, pp 17-81, pp 51-54.

Monroe, W. H., 1970, A glossary of karst terminology: U.S. Geological Survey, Water- Supply Paper 1899, 26 p.

Necdet M. (2003) Enriched: overview of the karst occurrences in northern Cyprus. *Acta Carsologica* 32(2):269–276.

Palmer, A. N., 1984. Recent trends on karst geomorphology. *Journal of Geological Education* 32: 247-53.

Pinault, J.L., Plagnes, V., Aquilina, L., Bakalowicz, M., 2001. Inverse modeling of the hydrological and the hydrochemical behavior of hydrosystems; characterization of karst system functioning. *Water Resources Research* 37, 2191–2204.

Plummer, L. N., T. M. L. Wigley, & D. L. Parkhurst. 1978. The Kinetics of Calcite Dissolution in CO₂ –Water system at 50 to 60 C and 0.00 to 1.0 atm CO₂. *American Journal of Science* 278: 176-216.

Price C, Michaclides S et al (1999) Long term changes in diurnal temperature range in Cyprus *Atmos Res* 51(2):85–98.

Raes D., 2009. The ETo Calculator, Evapotranspiration from a reference surface, Food and Agriculture Organization of the United Nations. Land and water Division Reference Manual, version 3.1, January, 2009. Rome, Italy.

Robertson AHF, Woodcock NH (1996).The role of the Kyrenia Range Lineament, Cyprus, in the geological evolution of the eastern Mediterranean area. *Philos Trans Roy Soc Lond Ser A* 317(1539):141–177.

Rozos E, Koutsoyiannis D, (2005) A multicell karstic aquifer model with alternative flow equations, Department of Water Resources, School of Civil Engineering, National Technical University of Athens, Heroon Polytechniou 5, GR 15780 Zographou, Greece.

Scanlona R. Robert E. Maceb, Michael E. Barrettc, Brian Smith, 2003.Can we simulate regional groundwater flow in a karst system using equivalent porous media models? Case study, Barton Springs Edwards aquifer, USA Bridget.

Shuster, E. T., & W. B. White. 1971. Seasonal fluctuations in the chemistry of limestone springs: A possible means for characterizing carbonate aquifers. *Journal of Hydrology* 14:93-128.

Smith, M., 1992. CROPWAT - a computer program for irrigation planning and management. FAO Irrigation and Drainage Paper N°46. Rome, Italy.

Sophocleous, M., 2002. Interactions between groundwater and surface water: the state of the science', *Hydrogeology Journal*, vol. 10, pp. 52-67.

Stavrinou Y.Hji., 1963. Groundwater Resources of the Krastic Regions of Cyprus. Geological Survey Department, Bulletin No. 5 pp 1-21.

Sun, R.J., ed., 1986, Regional Aquifer-System Analysis program of the U.S. Geological Survey, Summary of projects, 1978-84: U.S. Geological Survey Circular 1002, 264 p.

Theis, C. V. (1940). The source of water derived from wells: Essential factors controlling the response of an aquifer to development. *Civil Engineering*, Vol 10, No. 5, May, 277-280.

Todd, D.K., 1979, *Ground-water hydrology (Second Edition)*: John Wiley and Sons, New York, 535 p.

U.S. Geological Survey Circular 1186, 1999 W.M. Alley, T.E. Reilly, and O.L. Franke *Sustainability of Ground-Water Resources*. Denver, Colorado.

White, W. B. 1969. Conceptual models for carbonate aquifers. *Ground Water* 7, no. 3:15-22.

APPENDIX A The list of wells for the long term data monitoring.

Location & Name of Wells	Second Name	Situation	Monitoring	Q (m ³ /h)	Last water Level (m)	Last Monitoring Date	First water level (m)	First Monitoring Date	dh (m)	dt (years)	dh/dt (m)
Karşıyaka											
MTA-14	Karşıyaka MTA-14 well	working	valid data	52.0	152	2009	224	2002	72	7	10.28
B-35	-	Replaced by MTA-14	invalid data	0	188	1999	-	-	-	-	-
MTA-15	-	working	valid data	18	280	2009	308	1999	28	10	2.80
Lapta											
MTA-8	-	working	valid data	4	255	2002	258	1998	19	6	3.17
MTA-12	Lapta well MTA-12	working	valid data	32.0	260	2010	267	2003	25	7	3.75
MTA-9	-	working-irrigation	invalid data	2	-	-	-	-	-	-	-
53/68	-	working	invalid data	28.0	-	-	-	-	-	-	-
9/74	-	working	valid data	35	241	2001	272	1981	115	20	5.75
Alsancak Region											
48/69	-	working	valid data	4	150.5	2009	200.5	1996	63	13	4.85
1991/55	Goçeri well 1	working	valid data	45	261	2009	310	1993	49	16	3.06
2005/20	Goçeri well 2	working	valid data	30	297	2009	309	2005	12	4	3.00
Karaman											
43/34	Karaman-Ilgaz Arasi Well	working	invalid data	3	147	-	-	-	-	-	-
26A	-	working	valid data	20	205	2009	261	1981	13	5	2.60
26B	-	working	valid data	5	218	2008	231	2004	35	4	3.25
2004/8	New well 1	working	invalid data	60	229	2005	234.5	2004	5.5	1	5.50
2006/17	New well 2	working	invalid data	60	225	-	-	-	-	-	-
MTA-11	-	working	valid data	40	214	2007	227	1998	13	3	4.33
MTA-1	-	working	valid data	27	238	2009	244	1996	8	13	0.61
63/54	-	not working	invalid data	-	362	-	-	-	-	-	-

Location & Name of Wells	Second Name	Situation	Monitoring	Q (m ³ /h)	Last water Level (m)	Last Monitoring Date	First water level (m)	First Monitoring Date	dh (m)	dt (years)	dh/dt (m)
Dikmen Region											
1/74	Dikmen Dego Well	working	valid data	30	275	2009	277	1997	15	12	1.25
22/74C	-	working	valid data	10	269	2009	280	2004	15	5	3.00
45/79	-	not working	valid data	-	266	1994	277.5	1979	12	16	0.75
23/46	-	not working	valid data	-	263	2003	275	1981	12	22	0.55
173/62	-	observation well	valid data	-	271	2009	330	2004	32	5	6.40
36/76	-	not working	invalid data	-	-	-	-	-	-	-	-
38/87	Belediye Yukari Dikmen well	working	valid data	32	235	2009	278.5	1984	59	25	2.36
1994/25	-	not working	valid data	0	236	2009	250.7	2004	30	5	6.00
Çatalköy and Beylerbeyi Region											
MTA-13	-	working	valid data	30	170	2008	183	2004	13	4	3.22
B/20	-	working	valid data	16	259	2000	262	1997	3	3	1.00
14/70	-	working	valid data	3	351	1998	366	1981	15	17	0.88
B-30	Egri well	working(inclined well)	valid data	20	263	2001	263	1981	0	20	0.00
MTA-2	Tirmen well	working	valid data	20	246	2009	256	1997	14	14	1.00
MTA-4	-	working	valid data	100	295	2009	313	1998	18	11	1.64
EB-10	Pademili well	working	valid data	15	225	2009	241	2003	22	6	3.66
Değirmenlik Region											
20/74A	Arapköy well	working	valid data	40	254	2009	265	1999	25	11	2.27
20/74 B	Arapköy well	working	valid data	40	242	2008	264.7	1981	22.7	27	0.84
13-A	-	closed	valid data	3	342	1999	354	1964	12	35	0.34
19/74	-	working	invalid data	10	-	-	-	-	-	-	-
75/37	Ercan well	working	valid data	75	239	2009	258.5	1976	19.5	33	0.59
21/89	Ercan Yedek well	working	valid data	30	242	2009	280	1989	44	22	1.90
18-B	Alefkaya well	working	valid data	50	229	2009	252	1998	23	11	2.09

Location & Name of Wells	Second Name	Situation	Monitoring	Q (m ³ /h)	Last water Level (m)	Last Monitoring Date	First water level (m)	First Monitoring Date	dh (m)	dt (years)	dh/dt (m)
Karaağaç Alevkayasi Region											
44/67	-	working	valid data	12	280	2009	317	1981	37	28	1.32
MTA-19	-	working	valid data	20	313	2006	322	1998	9	8	1.12
Tirmen Region											
16A	Old well	working	invalid data	10	319	-	-	-	-	-	-
68/6	-	working	valid data	5	83	2008	164.6	1968	81	44	1.84
17/74	-	working	valid data	36	204	2009	280	1974	76	35	2.17
MTA-3	-	working	valid data	36	140	2009	153	1998	47	11	4.27
19/66	-	not working	valid data	-	323	2004	383	1966	60	38	1.58
37/76	-	not working	valid data	-	333	2003	362	1976	29	27	1.07
Kantara Region											
116/65	-	working	valid data	25	190.5	2004	221	1987	36	17	2.12
B-3	Tatlısu Old well	working	invalid data	15	208	2001	263	1981	55	20	2.75
MTA-21		not working	valid data	25	186	2009	Sea water (204)	1998			
MTA-5		not working	valid data	0	292	2009	Sea water (290)	1998			
1993/34		not working	invalid data	0	579	2003	607	1995	28	8	3.50
MTA-17		working	invalid data	10	583	1999					
MTA-7		working	invalid data	4	395	1998					
B-1		working	valid data	6	347.6	2003	375.6	1998	28	5	5.60
Boğaz Region											
MTA-10		working	valid data	30	252	2009	269	2003	21	6	3.5
61/50	DHM-1	working	valid data	60	240	2001	268.6	1981	28.6	20	1.43
40/71	DHM-2	working	invalid data	70	240						
1/65	BOZDAG WELL	working	valid data	45	259	2009	277.5	1981	38	1.9	2.00
13/74	CIKLOS WELL	working	valid data	15	298.6	2009	298	1996	-0.6	13	-0.05

APPENDIX B: The Penman Monteith Formula

B.1.1: The Penman Monteith Formula

The main reference for computing evapotranspiration is the report by Allen et al. (1981), in which the Penman-Monteith method, based on the formula:

$$ET_o = \frac{0.408\Delta(R_n - G) + \gamma \frac{900u_2(e_s - e_a)}{T + 273}}{\Delta + \gamma(1 + 0.34u_2)} \quad (\text{B.1})$$

To make feasible the computation of this formula, a feasible approach is presented here:

In the formula (4.9) involved variables are:

ET_o : reference evapotranspiration [mm day^{-1}];

G : soil heat flux density [$\text{MJ m}^{-2} \text{day}^{-1}$];

T : mean daily air temperature at 2 m height [$^{\circ}\text{C}$];

u_2 : wind speed at 2 m height [m s^{-1}];

e_s : mean saturation vapour pressure [kPa];

e_a : actual vapour pressure [kPa];

$e_s - e_a$: saturation vapour pressure deficit [kPa];

Δ : slope of the vapour pressure curve [$\text{kPa } ^{\circ}\text{C}^{-1}$]; and

γ : psychrometric constant [$\text{kPa } ^{\circ}\text{C}^{-1}$].

The sections in the following will quickly describe the approaches to the evaluation of all those variables.

B.1.2 The psychrometric constant (γ)

The psychrometric constant, γ , expressed in [kPa °C⁻¹], is given by:

$$\gamma = \frac{c_p P}{\varepsilon \lambda} = 0.665 \times 10^{-3} P \quad (\text{B.2})$$

Where P: atmospheric pressure [kPa], λ : latent heat of vaporization, 2.45 [MJ kg⁻¹], c_p : specific heat at constant pressure, 1.013×10^{-3} [MJ kg⁻¹ °C⁻¹], and ε : ratio molecular weight of water vapour/dry air = 0.622.

The atmospheric pressure, P, is the pressure exerted by the weight of the earth's atmosphere, given by.

$$P = 101.3 \left(\frac{293 - 0.0065z}{293} \right)^{5.26} \quad (\text{B.3})$$

Where z: elevation above sea level [m], for Lapta z = 200 m.

From equation (B.1.3)

$$P = 98.96 \text{ kPa,}$$

Solved by equation (B.1.2)

$$\gamma = 0.066 \text{ kPa } ^\circ\text{C}^{-1}$$

B.1.3 Saturation Vapour Pressure e° (T)

The higher the air temperature, the higher the storage capacity and the higher its saturation vapour pressure (Figure B.1.1) It is expressed as follow:

$$e^\circ(T) = 0.6108 \exp\left(\frac{17.27T}{T + 237.3}\right) \quad (\text{B.1.4})$$

Where e° (T): saturation vapour pressure at the air temperature T [kPa] and T: air temperature [° C],

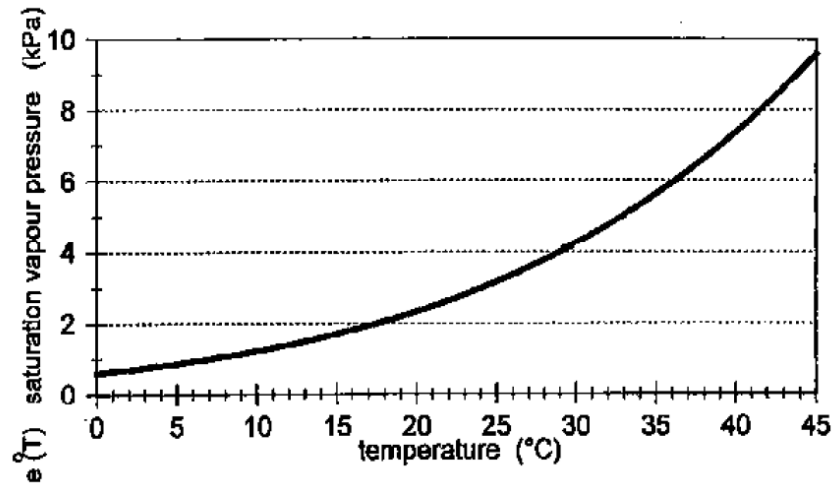


Figure B.1.1: Saturation vapour pressure shown as a function of temperature: $e^{\circ}(T)$ curve (Allen et al. 1998).

B.1.4 Mean saturation vapour pressure (e_s)

The mean saturation vapour pressure (e_s) for a day, week, decade or month should be computed as the mean between the saturation vapour pressure at the mean daily maximum and minimum air temperatures for that period:

$$e_s = \frac{e^{\circ}(T_{\max}) + e^{\circ}(T_{\min})}{2} \quad (\text{B.1.5})$$

$$e_s = 2.629 \text{ kPa.}$$

T_{\max} : maximum air temperature and T_{\min} : minimum air temperature

$e^{\circ}(T)$ For Lapta region by taken $T_{\max} = 26.5^{\circ} \text{C}$, and $T_{\min} = 15.8^{\circ} \text{C}$, by metrology department. As shown in tables 4.2 and 4.3.

$$e^{\circ}(T_{\max}) = 3.462 \quad \text{kPa}$$

$$e^{\circ}(T_{\min}) = 1.795 \quad \text{kPa}$$

B.1.5 Actual vapour pressure (e_a)

The actual vapour pressure (e_a) is the vapour pressure exerted by the water in the air. When the air is not saturated, the actual vapour pressure will be lower than the saturation vapour pressure.

B.1.5.1 Derived from dewpoint temperature

The actual vapour pressure (e_a) is the saturation vapour pressure at the dewpoint temperature (T_{dew} [$^{\circ}\text{C}$]), it is given by:

$$e_a = e^{\circ}(T_{\text{dew}}) = 0.6108 \exp\left(\frac{17.27T_{\text{dew}}}{T_{\text{dew}} + 237.3}\right) \quad (\text{B.1.6})$$

The T_{dew} : is the temperature, to which the air needs to be cooled to make the air saturated,

B.1.5.2 Derivation of e_a from relative humidity data

The actual vapour pressure (e_a) is also related to the Relative Humidity (RH)

For RH_{max} and RH_{min} :

$$e_a = \frac{e^{\circ}(T_{\text{min}}) \frac{\text{RH}_{\text{max}}}{100} + e^{\circ}(T_{\text{max}}) \frac{\text{RH}_{\text{min}}}{100}}{2} \quad (\text{B.1.7})$$

Where e_a : actual vapour pressure [kPa]; $e^{\circ}(T_{\text{min}})$: saturation vapour pressure at daily minimum temperature [kPa]; $e^{\circ}(T_{\text{max}})$: saturation vapour pressure at daily maximum temperature [kPa]; RH_{max} : maximum relative humidity [%]; and RH_{min} : minimum relative humidity [%].

When using equipment where errors in estimating RH_{min} can be large, or when RH data integrity is in doubt, one should use only RH_{max} :

$$e_a = e^{\circ}(T_{\text{min}}) \frac{\text{RH}_{\text{max}}}{100} \quad (\text{B.1.8})$$

For RH_{mean} :

In the absence of RH_{max} and RH_{min} , another equation can be used to estimate e_a :

$$e_a = \frac{\text{RH}_{\text{max}}}{100} \left[\frac{e^{\circ}(T_{\text{max}}) + e^{\circ}(T_{\text{min}})}{2} \right] \quad (\text{B.1.9})$$

where,

$$\text{RH}_{\text{mean}} = \frac{\text{RH}_{\text{min}} + \text{RH}_{\text{max}}}{2} \quad (\text{B.1.10})$$

However, Equation B.1.10 is less desirable than are Equation B.1.8 and B.1.9.

If RH data is not available, e_a can be estimated by assuming that the dewpoint temperature is quasi equal to the minimum daily temperature, thus:

$$e_a = e(T_{\text{dew}} \approx T_{\text{min}}) = 0.611 \exp \left[\frac{17.27 T_{\text{min}}}{T_{\text{min}} + 237.3} \right] \quad (\text{B.1.11})$$

Where T_{min} is in °C, then:

$$e_a = 1.796 \text{ kPa.}$$

In Arid zones the air can be saturated at a temperature different from the minimum one, therefore it should be taken into account that $T_{\text{dew}} < T_{\text{min}}$ (Allen et al. 1998).

B.1.6 Slope of the vapour pressure curve (Δ)

The slope of the vapour pressure curve (Figure 4.8) at a given temperature is given by.

$$\Delta = \frac{4098 \left[0.6108 \exp \left(\frac{17.27 T}{T + 237.3} \right) \right]}{(T + 237.3)^2} \quad (\text{B.1.12})$$

Where Δ : slope of saturation vapour pressure curve at air temperature T [kPa °C⁻¹], and T : the mean air temperature [°C] then,

$$\Delta = 0.153 \text{ kPa } ^\circ\text{C}^{-1}$$

B.1.7 The soil heat flux (G)

The soil heat flux, G , is the energy that is utilized in heating the soil. It is presented here for a long time steps (monthly), based on the idea that the soil temperature follows air temperature:

$$G = c_s \frac{T_j + T_{j-1}}{\Delta t} \Delta z \quad (\text{B.1.13})$$

Where G : soil heat flux [MJ m⁻² day⁻¹], c_s : soil heat capacity [MJ m⁻³ °C⁻¹], T_j : air temperature at time j [°C], T_{j-1} : air temperature at time $j - 1$ [°C], Δt : length of time interval [day], and Δz : effective soil depth [m].

- For day and ten-day periods:
 - For the period of a day and ten-day periods it can be assumed that: $G_{\text{day}} = 0$
- For monthly period:
 - The soil heat capacity c_s assumed to be constant equal to $2.1 \text{ MJ m}^{-3} \text{ }^\circ\text{C}^{-1}$
 - The effective soil depth might be 2 m or more.

So The G is expressed as:

$$G_{\text{month},j} = 0.14 \left(T_{\text{month},j} - T_{\text{month},j-1} \right) \quad (\text{B.1.14})$$

where $T_{\text{month}, j}$ mean air temperature of month j [$^\circ\text{C}$], and $T_{\text{month}, j-1}$ mean air temperature of previous month [$^\circ\text{C}$], $G = 0.042 \text{ MJ m}^{-2} \text{ day}^{-1}$

B.1.8 Wind speed u_2

To adjust wind speed data obtained from instruments placed at elevations other than the standard height of 2 m, a logarithmic wind speed profile may be used for measurements above a short grassed surface:

$$u_2 = u_z \frac{4.87}{\ln(67.8z - 5.42)} \quad (\text{B.1.15})$$

Where u_2 : wind speed at 2 m above ground surface [m s^{-1}], u_z : measured wind speed at z m above ground surface [m s^{-1}], and z : height of measurement above ground surface [m].

$$u_2 = 2.0 \text{ m s}^{-1}$$

B.1.9 Calculation Procedure of the Net Radiation (R_n)

B.1.9.1 Extraterrestrial radiation for daily periods (R_a)

$R_a = f$ (Latitude, solar declination, time of the year)

$$R_a = \frac{24 \times 60}{\pi} G_{sc} d_r \left(\omega_s \sin \varphi \sin \delta + \cos \varphi \cos \delta \sin \omega_s \right) \quad (\text{B.1.16})$$

where R_a :extraterrestrial radiation [$\text{MJ m}^{-2} \text{ day}^{-1}$], G_{sc} :solar constant = $0.0820 \text{ MJ m}^{-2} \text{ min}^{-1}$, d_r :inverse relative distance Earth-Sun, ω_s : sunset hour angle [rad], φ : latitude [rad], and δ : solar declination [rad].

$$R_a = 1.966 \text{ MJ m}^{-2} \text{ day}^{-1}$$

The inverse relative distance Earth-Sun, d_r , and the solar declination, δ , is given by:

$$d_r = 1 + 0.033 \cdot \cos\left(\frac{2\pi}{365} J\right) = 1 + 0.033 \cdot \cos(0.0172J) \quad (\text{B.1.17})$$

$$d_r = 1.033.$$

$$\delta = 0.409 \cdot \sin\left(\frac{2\pi}{365} J - 1.39\right) = 0.409 \cdot \sin(0.0172J - 1.39) \quad (\text{B.1.18})$$

$$\delta = -0.0403.$$

Where J is the number of the day in the year between 1 (1 January) and 365 or 366 (31 December), it can be estimated by:

$$J = \text{int}(30.42M - 15.23) \quad (\text{B.1.19})$$

J: average day of the month and M: month of the year

The sunset hour angle, ω_s , is given by:

$$\omega_s = \arccos(-\tan\varphi \cdot \tan\delta) \quad (\text{B.1.20})$$

$$\omega_s = 1.751$$

B.1.9.2 Solar radiation (R_s)

B.1.9.2.1 Clear-sky solar radiation (R_{so})

The calculation of the clear-sky radiation, R_{so} , when $n = N$, is required for computing net long wave radiation.

For near sea level or when calibrated values for a_s and b_s are available

$$R_{so} = (a_s + b_s) R_a \quad (\text{B.1.21})$$

where R_{so} : clear-sky solar radiation [$\text{MJ m}^{-2} \text{ day}^{-1}$]; and $a_s + b_s$: fraction of extraterrestrial radiation reaching the earth on clear-sky days ($n = N$).

When calibrated values for a_s and b_s are not available

$$R_{so} = (0.75 + 210^{-5} z) R_a \quad (\text{B.1.22})$$

where z station elevation above sea level [m].

In alternative one may use simply the FAO recommended values, $a_s = 0.25$ and $b_s = 0.50$, obtaining:

$$R_{so} = 0.75.R_a \quad (\text{B.1.23})$$

Then,

$$R_{so} = 1.475 \text{ MJ m}^{-2} \text{ day}^{-1}$$

If the solar radiation, R_s , is not measured, it can be calculated with the Angstrom formula which relates solar radiation to extraterrestrial radiation and relative sunshine duration:

$$R_s = \left(a_s + b_s \frac{n}{N} \right) R_a \quad (\text{B.1.24})$$

where R_s : solar or shortwave radiation [$\text{MJ m}^{-2} \text{ day}^{-1}$]; n : actual duration of sunshine [hour]; N : maximum possible duration of sunshine or daylight hours [hour], estimated from the sunset hour angle, ω_s , it is given as:

$$N = \frac{24}{\pi} \omega_s \quad (\text{B.1.25})$$

$\frac{n}{N}$: Relative sunshine duration [-], R_a : extraterrestrial radiation [$\text{MJ m}^{-2} \text{ day}^{-1}$], a_s : regression constant, expressing the fraction of extraterrestrial radiation reaching the earth on overcast days ($n = 0$), and $a_s + b_s$: fraction of extraterrestrial radiation reaching the earth on clear days ($n = N$).

If n is not available, $\frac{n}{N}$ can be replaced by, m_c , which is the fractional cloud cover:

$$\frac{n}{N} = 1 - m_c \quad (\text{B.1.26})$$

m_c : represents the fractional average number of the eight part of the sky covered with clouds (Okta).

If that information is not available R_s can be estimated with the Hargreaves –Samani formula:

$$R_s = k_{Rs} (T_{\max} + T_{\min})^{1/2} R_a \quad (\text{B.1.27})$$

Where $k_{Rs} = 0.16 - 0.19$ depends on the considered zone (internal or costal) T_{\max} and T_{\min} are expressed in °C.

$$R_s = 2.43 \text{ MJ m}^{-2} \text{ day}^{-1}$$

B.1.9.2.2 Net solar or net shortwave radiation (R_{ns})

The net shortwave radiation resulting from the balance between incoming and reflected solar radiation is given by:

$$R_{ns} = (1 - \alpha) \cdot R_s \quad (\text{B.1.28})$$

where R_{ns} : net solar or shortwave radiation [$\text{MJ m}^{-2} \text{ day}^{-1}$], α : albedo or canopy reflection coefficient, which is 0.23 for the hypothetical grass reference crop [dimensionless] table B.1.1, R_s : the incoming solar radiation [$\text{MJ m}^{-2} \text{ day}^{-1}$] and R_{ns} : is expressed in the above equation in $\text{MJ m}^{-2} \text{ day}^{-1}$.

$$R_{ns} = 1.871 \text{ MJ m}^{-2} \text{ day}^{-1}$$

Table B.1.1 Some values of the albedo values

Surface	Mean	Min	Max
Water	0,20	0,02	1,00
snow	0,63	0,29	0,95
clouds	0,32	0,05	0,84
city	0,16	0,12	0,21
roads	0,19	0,10	0,28
forest	0,18	0,10	0,24
grass	0,25	0,14	0,45
cereals	0,18	0,16	0,23
coton	0,21	0,20	0,22
tomato	0,19		

B.1.9.2.3 Net longwave radiation (R_{nl})

The rate of longwave energy emission is expressed by the Stefan-Boltzmann law.

$$R_{nl} = f \cdot \varepsilon' \cdot \sigma \cdot \frac{(T_{\max}^4 + T_{\min}^4)}{2} \quad (\text{B.1.29})$$

where R_{nl} : net outgoing longwave radiation [$\text{MJ m}^{-2} \text{ day}^{-1}$], σ : Stefan-Boltzmann constant [$4.903 \cdot 10^{-9} \text{ MJ K}^{-4} \text{ m}^{-2} \text{ day}^{-1}$], T_{\max} : maximum absolute temperature during the 24-hour period [$\text{K} = ^\circ\text{C} + 273.16$], T_{\min} : minimum absolute temperature during the 24-hour period [$\text{K} = ^\circ\text{C} + 273.16$], f : Cloudiness adjustment factor expresses the effect of cloudiness, and ε' : Net emissivity expressing a correction for air humidity.

When solar radiation data is available, f is given by:

$$f = \left(a_c \frac{R_s}{R_{so}} + b_c \right) \quad (\text{B.1.30})$$

Where a_c and b_c : are cloudiness factors; R_s : Solar radiation for measured short wave [$\text{MJ m}^{-2} \text{ day}^{-1}$], R_{so} : Clear-sky shortwave Solar radiation [$\text{MJ m}^{-2} \text{ day}^{-1}$]. $a_c = 1.35$ and $b_c = -0.35$ for arid areas $a_c = 1$ and $b_c = 0$ for humid areas. Those values are recommended by FAO (1977).

The net emissivity is expressed by:

$$\varepsilon' = (a_1 + b_1 \sqrt{e_a}) \quad (\text{B.1.31})$$

e_a = actual vapour pressure [kPa], a_1 = calibration coefficient [0.34;0.44]; b_1 = calibration coefficient [-0.25;-0.14]; $a_1 = 0.34$ and $b_1 = -0.14$ are the recommended values by FAO (1977).

$$R_{nl} = 0.00039 \text{ MJ m}^{-2} \text{ day}^{-1}$$

4.5.9.3 Net radiation (R_n)

The net radiation (R_n) is the difference between the incoming net shortwave radiation (R_{ns}) and the outgoing net long wave radiation (R_{nl}), Figure B.1.2:

$$R_n = R_{ns} - R_{nl} \quad (\text{B.1.32})$$

$$R_n = 1.871 - 0.00039 = 1.871$$

Figure B.1.2 Various Components of the Solar Radiation

